

T-3253

An experimental study of solubility differences between  
phenol and m-cresol in supercritical carbon dioxide

by

Luis A. Chu

ARTHUR LAKES LIBRARY  
COLORADO SCHOOL of MINES  
GOLDEN, COLORADO 80401

ProQuest Number: 10782831

All rights reserved

INFORMATION TO ALL USERS

The quality of this reproduction is dependent upon the quality of the copy submitted.

In the unlikely event that the author did not send a complete manuscript and there are missing pages, these will be noted. Also, if material had to be removed, a note will indicate the deletion.



ProQuest 10782831

Published by ProQuest LLC (2018). Copyright of the Dissertation is held by the Author.

All rights reserved.

This work is protected against unauthorized copying under Title 17, United States Code  
Microform Edition © ProQuest LLC.


ProQuest LLC.  
789 East Eisenhower Parkway  
P.O. Box 1346  
Ann Arbor, MI 48106 – 1346

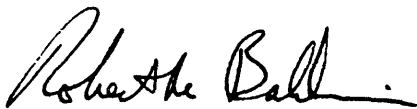
T-3253


A thesis submitted to the Faculty and the Board of Trustees of the Colorado School of Mines in partial fulfillment of the requirements for the degree of Master of Science (Chemical and Petroleum-Refining Engineering)

Golden, Colorado

Date August 27, 1986

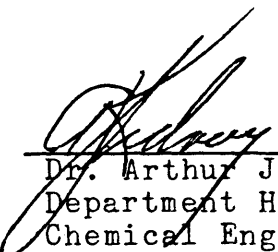
Signed:   
Luis A. Chu

Approved:   
Dr. Robert M. Baldwin  
Thesis Co-advisor

  
Dr. James F. Ely  
Thesis Co-advisor

Golden, Colorado

Date 9/1/86

  
Dr. Arthur J. Kidnay  
Department Head  
Chemical Engineering  
and Petroleum-Refining

## ABSTRACT

An experimental apparatus was designed and built to study the solubilities of pure organic compounds and mixtures in supercritical fluids, for a pressure range of 1 to 200 atm and for a temperature range of 308.0 to 433.0 K.

Solubility data in supercritical carbon dioxide were measured for phenol, m-cresol and their mixtures at 309 and 318 K over a pressure range of 60 to 200 atm. The results showed that the solubility of phenol in supercritical carbon dioxide is enhanced with respect to the pure phenol-carbon dioxide system by the addition of m-cresol at condensed phase compositions of 50 to 70 mole % phenol. No significant effect was observed by adding either water or acetone (entrainers) to an equimolar condensed phase mixture of phenol and m-cresol in supercritical carbon dioxide at 309 K.

## TABLE OF CONTENTS

<u>Section</u>	<u>Page</u>
ABSTRACT .....	iii
LIST OF FIGURES .....	vi
LIST OF TABLES .....	x
ACKNOWLEDGEMENTS .....	xii
INTRODUCTION .....	1
THESIS OBJECTIVES .....	4
LITERATURE SURVEY .....	5
Solubility of aromatic isomers .....	11
Entrainers and mixed solvents in SCE .....	13
Experimental methods to measure solubility in SCF	16
Equilibration systems .....	16
Analytical systems .....	23
EXPERIMENTAL APPARATUS .....	31
Equilibration system .....	31
Analytical system .....	37
EQUIPMENT CALIBRATION .....	40
Chemicals .....	40
Pressure transducer and transducer indicator ....	40
Thermocouple probe and digital thermocouple indicator .....	40
Flowsensor and digital flow meter .....	41
Thermal conductivity detector .....	41

<u>Section</u>	<u>Page</u>
EQUIPMENT PRETESTS .....	48
EXPERIMENTAL PROCEDURE .....	56
Apparatus preparation .....	56
Loading the sample .....	58
Sampling the dense gas .....	60
Making another run .....	62
EXPERIMENTAL RESULTS AND DISCUSSION .....	63
Effect of condensed phase composition .....	66
Effect of entrainers .....	86
Effect of system temperature .....	86
CONCLUSIONS .....	91
RECOMMENDATIONS .....	93
REFERENCES CITED .....	95
APPENDIX A - GAS CHROMATOGRAPH CALIBRATION DATA .....	99
APPENDIX B - EXPERIMENTAL DATA .....	109
APPENDIX C - PRESSURE DEPENDENCE OF ENHANCEMENT FACTOR .....	121
APPENDIX D - UNCERTAINTY ANALYSIS .....	126

## LIST OF FIGURES

Figure		Page
1	Extraction of tar with ethylene at 4500 psia and 25 °C (Wise 1970) .....	10
2	Schematic diagram of a static apparatus used to obtain solid solubilities in a supercritical fluid (Tsekhanskaya, et al., 1962) .....	18
3	Schematic diagram of a static equilibrium column used to obtain solid solubilities in a supercritical fluid (Tsekhanskaya, et al., 1962) .....	19
4	Schematic diagram of a flow apparatus used to obtain liquid or solid solubilities in a supercritical fluid (Kurnik and Reid, 1982) .....	21
5	Schematic diagram of a recirculating flow apparatus used to obtain solid or liquid solubilities in a supercritical fluid (Morris, 1984) .....	22
6	Direct gas chromatographic sampling technique to measure the composition of the dense gas mixture (Monge and Prausnitz, 1983) .....	25
7	Schematic diagram of an apparatus for direct coupling of fluid extraction with thin-layer chromatography (Stahl, et al., 1978) .....	27
8	Schematic diagram of a NIR spectroscopic apparatus used to obtain solid or liquid solubilities in a supercritical fluid (Swaid, et al., 1985) .....	28
9	Schematic diagram of an apparatus for direct mass spectrometric analysis of supercritical fluid processes (Smith and Udseth, 1983) .....	30

Figure		Page
10	Schematic diagram of the experimental apparatus used in this study to obtain solubilities in supercritical carbon dioxide .....	32
11	Schematic diagram of the equilibrium cell used in this study (Autoclave Engineers) .	34
12	Calibration curve for naphthalene at a TCD range of 3 .....	45
13	Calibration curve for carbon dioxide at a TCD range of 3 .....	46
14	Experimental solubilities for naphthalene in supercritical carbon dioxide at 313.3 K	49
15	Experimental solubilities of naphthalene in supercritical carbon dioxide at 318.2 K	50
16	Experimental solubilities of phenol in supercritical carbon dioxide at 309.3 K ..	54
17	Typical gas chromatogram and integrator output .....	61
18	Comparison of experimental solubilities of phenol and m-cresol in supercritical carbon dioxide at 309 K .....	65
19	Experimental solubilities of phenol and m-cresol in supercritical carbon dioxide at 309.4 K. Condensed phase: 25 mole % phenol and 75 mole % m-cresol, excluding carbon dioxide. ....	68
20	Experimental solubilities of phenol and m-cresol in supercritical carbon dioxide at 309.3 K. Condensed phase: 50 mole % phenol and 50 mole % m-cresol, excluding carbon dioxide. ....	69



Figure		Page
21	Experimental solubilities of phenol and m-cresol in supercritical carbon dioxide at 309.3 K. Condensed phase: 75 mole % phenol and 25 mole % m-cresol, excluding carbon dioxide. ....	70
22	Comparison of solubilities of m-cresol in supercritical carbon dioxide at 309.3 K, for various condensed phase compositions of phenol and m-cresol .....	72
23	Comparison of solubilities of phenol in supercritical carbon dioxide at 309.3 K, for various condensed phase compositions of phenol and m-cresol .....	73
24	Comparison of enhancement factors of m-cresol in supercritical carbon dioxide for various condensed phase compositions of phenol and m-cresol .....	76
25	Comparison of enhancement factors of phenol in supercritical carbon dioxide for various condensed phase compositions of phenol and m-cresol .....	77
26	Experimental partial molar volumes of naphthalene and fluorene at infinite dilution in supercritical carbon dioxide (Van Wasen and Schneider, 1980) .....	81
27	Effect of condensed phase composition and pressure on selectivity in the phenol, m-cresol and carbon dioxide system at 309.3 K .....	83
28	Experimental solubilities for phenol and m-cresol mixture in supercritical carbon dioxide at 309.3 K and 105 atm .....	84

Figure		Page
29	Comparison of experimental solubilities of phenol and m-cresol in supercritical carbon dioxide at 309.3 K, with acetone and water as entrainers. Condensed phase: 50 mole % phenol and 50 mole % m-cresol, excluding carbon dioxide. ....	87
30	Comparison of experimental solubilities of phenol and m-cresol in supercritical carbon dioxide at 309.1 and 318.4 K. Condensed phase: 50 mole % phenol and 50 mole % m-cresol, excluding carbon dioxide. ....	88
31	Schematic diagram of an apparatus for fractional distraction. A : variable temperature finger (Zosel, 1978). ....	90
A-1	Calibration curve for carbon dioxide, TCD Range 3 .....	101
A-2	Calibration curves for phenol, m-cresol and naphthalene, TCD Range 3 .....	102
A-3	Calibration curve for carbon dioxide, TCD Range 5 .....	103
A-4	Calibration curves for phenol, m-cresol and naphthalene, TCD Range 5 .....	104
A-5	Calibration curve for carbon dioxide, TCD Range 7 .....	105
A-6	Calibration curve for phenol, TCD Range 7 .....	106
A-7	Calibration curve for m-cresol, TCD Range 7 .....	107
A-8	Calibration curve for naphthalene, TCD Range 7 .....	108

## LIST OF TABLES

Table		Page
1	Solubility data for ternary systems .....	6
2	Description of notation in Figure 10a .....	33
3	Gas chromatograph operating conditions .....	43
4	Summary of experimental runs for the phenol and m-cresol system in supercritical carbon dioxide .....	64
5	Vapor pressures of phenol, m-cresol and naphthalene (Perry and Chilton, 1973) .....	67
6	Predicted vapor pressures of phenol, m-cresol and naphthalene .....	67
A-1	Pure component calibration equations .....	100
B-1	Experimental solubilities of naphthalene (peak area %) in supercritical carbon dioxide at 313.3 K. Condensed phase (solid): 100 % naphthalene .....	110
B-2	Experimental mole fractions of naphthalene in supercritical carbon dioxide at 318.2 K. Condensed phase (solid): 100 % naphthalene ....	111
B-3	Mole fractions of naphthalene in supercritical carbon dioxide at 318 K measured by other measured by other researchers .....	112
B-4	Experimental mole fractions of phenol in supercritical carbon dioxide at 309.3 K. Condensed phase (solid): 100 % phenol .....	113
B-5	Mole fractions of phenol in supercritical carbon dioxide at 309 K (Van Leer and Paulaitis) .....	114
B-6	Experimental mole fractions of m-cresol in supercritical carbon dioxide at 309.2 K. Condensed phase (liquid): 100 % m-cresol .....	115

Table		Page
B-7	Experimental mole fractions of phenol and m-cresol mixtures in supercritical carbon dioxide at 309.4 K. Condensed phase (liquid): 25 mole % phenol and 75 mole % m-cresol .....	116
B-8	Experimental mole fractions of phenol and m-cresol mixtures in supercritical carbon dioxide at 309.3 K. Condensed phase (liquid): 50 mole % phenol and 50 mole % m-cresol .....	117
B-9	Experimental mole fractions of phenol and m-cresol mixtures in supercritical carbon dioxide at 309.3 K. Condensed phase (liquid): 75 mole % phenol and 25 mole % m-cresol .....	118
B-10	Effect of entrainers on the experimental mole fractions of phenol and m-cresol mixtures in supercritical carbon dioxide at 309.3 K. Condensed phase (liquid; 150 g): 50 mole % phenol and 50 mole % m-cresol .....	119
B-11	Experimental mole fractions of phenol and m-cresol mixtures in supercritical carbon dioxide at 318 K. Condensed phase (liquid): 50 mole % phenol and 50 mole % m-cresol .....	120
D-1	Tabulated uncertainties .....	128

ACKNOWLEDGEMENTS

I wish to thank Dr. Robert M. Baldwin for his patience, counsel and support throughout the course of this study. Dr. James Ely's assistance was invaluable to the completion of this thesis. Finally, the financial assistance provided by Resource Technology Associates, Boulder, Colorado is gratefully acknowledged.

## INTRODUCTION

Supercritical fluid extraction (SCE) has attracted significant interest in the chemical and food industries over the past few years. The basic principle involves contact of a condensed phase (liquid or solid) with a fluid that is at a temperature above its vapor-liquid critical point (Ely and Baker, 1983). This separation process offers the following attractive features (King and Bott, 1982):

- Extraction of high boiling and/or thermally labile compounds may be accomplished at relatively low temperatures.
- Selective extraction of one or more compounds from a mixture in one continuous process.
- Relatively small changes in temperature and/or pressure in the supercritical or near critical region produce large changes in density and solvent power, facilitating the recovery of solvent.
- The available number of supercritical fluids provide the choice of less toxic solvents (e.g. carbon dioxide) as alternatives to hazardous organic industrial solvents.
- The properties of a supercritical fluid (SCF) are between those of a gas (low viscosity and high diffusivity) and a liquid (solvent power and density).

A research program was initiated at Colorado School of Mines with the overall objective of investigating the application of supercritical fluids to the separation of polar species from coal tar distillates. The separation of phenol and the isomers of cresol from coal tar, and subsequent isomer purification are of particular interest, since they are extensively employed in the manufacture of resins, plasticizers, disinfectants, antioxidants, and agricultural chemicals.

Cresols used in industry are mainly derived from petroleum or coal tar. Crude coal tar is produced as a result of the manufacture of coke in by-product coke ovens. The coal tar typically contains 2 to 3 % cresylic acid or tar acid, which is made up of phenol, cresols, xylenols and higher phenolics. Generally, the term cresylic acid is used to designate mixtures containing significant amounts of two or more of the cresol isomers. The separation of coal tar distillates into commercially acceptable fractions of phenol, o-cresol, cresylic acid and xylenols is described by MacNeil (1965) and Clonts and McKetta (1981). High efficiency distillation of the tar acids yields pure o-cresol (99+ %), but the similarity in boiling points of the meta and para isomers result in their appearance as cresylic acid (96+ % m,p-cresol). Synthetic processes are

employed to yield high purity (99+ %) m-cresol and p-cresol. The commercial synthesis of cresols involves the use of phenol or toluene, which have higher market values relative to the finished cresol prices (Clonts and McKetta, 1981). Supercritical fluid extraction provides potential advantages in energy cost over distillation and commercial synthesis.



## THESIS OBJECTIVES

In order to provide a basis for the potential application of SCE in the separation of coal tar and tar acids, an experimental system was constructed to measure the equilibrium solubility of pure compounds or complex mixtures in various supercritical fluids. The experimental method may be used to provide precise, quantitative results to be used in predictions and theoretical modeling. However, the system may also be applied for quick qualitative analysis of a large number of complex natural mixtures.

The experimental system was tested with mixtures of phenol and m-cresol in supercritical carbon dioxide. Three reasons prompted the choice of this system: (1) provide data for the verification of solubility differences between phenol and cresol isomers (DeBeer, 1985); (2) the results will help evaluate the potential separation of m-cresol from p-cresol; and (3) carbon dioxide is a cheap, environmentally acceptable solvent, and a large amount of data with carbon dioxide as the SCF is available in the literature.

## LITERATURE SURVEY

One area of major interest to researchers is the application of supercritical fluids to extraction processes. Yet, in order to evaluate the selectivity of SCE, solubility data for multicomponent systems are needed. Most experimental data to date have been reported for pure compounds in contact with a supercritical fluid. DeBeer (1985) compiled a list of published experimental work, which included mainly binary systems. Table 1 lists data for ternary systems available in the literature. Brunner and Peter (1982) have compiled a list of process designs in the field of supercritical fluid extraction as applied to crude oil, oil shale, coal and natural food products.

Wise (1970) investigated the extraction of coal tar with supercritical ethylene. The experiments consisted of exposing a sample of coal tar to successive aliquots of compressed ethylene at 25 °C and 306 atm (i.e. a process analogous to differential distillation). The amount of "volatiles" in the gas phase and the extent of tar stripping were measured at each equilibration. The experiments were meant to provide a qualitative evaluation, and the results shown in Figure 1. The vapor concentrations at 150 °C corresponding to differential distillation were included for

Table 1. Solubility data for ternary systems

Solute 1	Solute 2	T/Tc	P/Pc	Reference
SCF: CARBON DIOXIDE				
naphthalene	phenanthrene	1.01 - 1.05	1.04 - 3.80	Gopal (1985)
naphthalene	phenol	1.01 - 1.05	0.73 - 3.76	Gopal (1985)
naphthalene	biphenyl	1.01 - 1.05	0.77 - 3.77	Gopal (1985)
naphthalene	phenanthrene	1.01	1.63 - 3.80	Kurnik (1982)
benzoic acid	phenanthrene	1.01	1.63 - 3.80	Kurnik (1982)
2,3-dimethyl-naphthalene	phenanthrene	1.01 - 1.05	1.63 - 3.80	Kurnik (1982)
2,6-dimethyl-naphthalene	phenanthrene	1.01	1.63 - 3.80	Kurnik (1982)
naphthalene	benzoic acid	1.01 - 1.05	1.63 - 3.80	Kurnik (1982)
2,3-dimethyl-naphthalene	naphthalene	1.01	1.63 - 3.80	Kurnik (1982)
2,3-dimethyl-naphthalene	2,6-dimethyl-naphthalene	1.01 - 1.05	1.63 - 3.80	Kurnik (1982)

Table 1. (continued)

Solute 1	Solute 2	T/Tc	P/Pc	Reference
SCF: CARBON DIOXIDE				
6-methoxy-1-tetralone	7-methoxy-1-tetralone	1.01	1.49	Chang (1985)
5-methoxy-1-tetralone	7-methoxy-1-tetralone	1.01	1.49	Chang (1985)
methyl-o-nitrobenzoate	methyl-m-nitrobenzoate	1.01	1.49	Chang (1985)
methyl-o-nitrobenzoate	methyl-p-nitrobenzoate	1.01	1.49	Chang (1985)
1-methyl-naphthalene	toluene	1.16 - 1.36	0.03 - 1.96	Morris (1984)
acetone	water	1.03 - 1.10	0.14 - 1.29	Panagio. (1985)
isopropanol	water	1.10	1.42 - 1.65	Radosz (1984)
trans-decalin	n-eicosane	0.95 - 1.01	0.70 - 1.06	Tiffin (1978)
trans-decalin	2-methyl-naphthalene	0.86 - 1.04	0.34 - 1.18	Tiffin (1978)

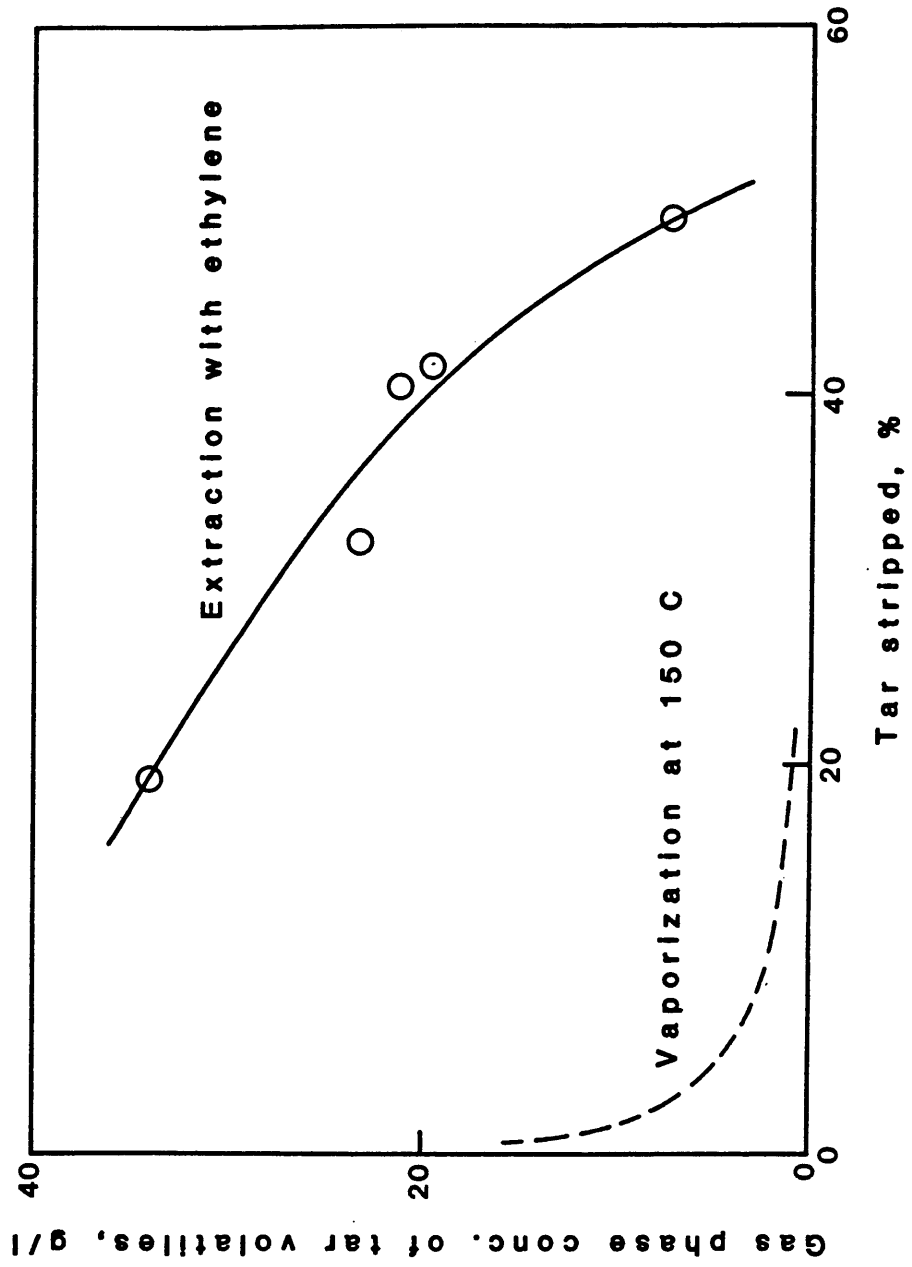
Table 1. (continued)

Solute 1	Solute 2	T/Tc	P/Pc	Reference
SCF: CARBON DIOXIDE				
tridecane	hexadecane	1.39	1.09 - 4.75	Konrad (1983)
tridecane	1-hexadecanol	1.39	1.09 - 4.75	Konrad (1983)

comparison. Figure 1 demonstrates the potential application of supercritical fluids to the extraction of coal tar.

A few studies also focus on the use of entrainers and mixed solvents in SCE. The experimental study of multicomponent systems and the use of mixed supercritical solvents have led to refinements in the designs of equilibration and analytical methods used for "simple" binary systems.

Figure 1., Extraction of tar with ethylene at 4500 psia and 25 °C (Wise 1970)



Solubility of aromatic isomers

Krukonis and Kurnik (1985) measured the solubility of two families of disubstituted aromatic isomers, the hydroxybenzoic acids and the dihydroxybenzenes, in supercritical carbon dioxide. The measurements were limited to binary systems. The results showed an inverse relationship between the solubility within an isomer family and their melting points. Two orders of magnitude difference in solubility between the ortho and para isomers were observed. Krukonis and Kurnik suggested the possibility of using SCE to separate the mixture of ortho and para isomers, based on the results obtained from binary systems.

Chang and Morrell (1985) measured the solubilities of methoxy-1-tetralone and methyl nitrobenzoate isomers and their mixtures. Both families are also disubstituted aromatic isomers. Results from the binary systems showed that the closer the functional groups of an isomer, the higher the solubility of the isomer in supercritical carbon dioxide. They also noted that the closer the functional groups of an isomer, the lower the melting of the isomer, in agreement with the melting point effect observed by Krukonis and Kurnik (1985).

Chang and Morrell (1985) also observed strong



influences by the phase(s) and composition of the condensed mixture on the solubility of the individual components. The authors concluded that: (1) if the condensed mixture is liquid, the solubility of an individual component decreases with the addition of a second solute, and (2) if the solid phase of a component is also present in the liquid mixture, the solubility of this component is enhanced.

The effect of condensed phase composition was also studied by Kurnik and Reid (1982), who reported that the solubility of a solid component in a ternary system can be enhanced as much as 300 % over the solubility of the pure solid system at the same operating conditions.

Entrainers and Mixed Solvents in SCE

Most studies related to solubility in supercritical fluids have been restricted to pure solvent systems. However, it has been suggested that the use of mixed supercritical fluids have certain advantages (Joshi and Prausnitz, 1984). In SCE it is desirable to operate at as high a temperature as possible, thereby increasing the vapor pressure of the condensed components. It is also recommended to use the fluid near its critical state in order to take advantage of the sensitivity of the fluid density to small temperature and pressure changes. However, to satisfy both conditions it might require the use of a mixture of solvents that has an effective critical temperature between the critical temperatures of the pure fluids. Joshi and Prausnitz (1984) illustrated the advantages of mixed solvents by presenting some calculated results based on mixtures of propane and carbon dioxide at different compositions.

The only experimental study with mixed solvents was presented by Smith and Udseth (1983), who extracted samples of bituminous coal using a mixture of 95 % pentane and 5 % isopropanol (estimated critical temperature of 199 °C for the mixture) at 280 °C and 5 to 100 bar. The extraction was performed to test the direct mass spectrometric analysis of

the products of SCE processes (See ANALYTICAL METHODS below). Unfortunately, the experimental results were not compared to solubilities in the pure solvents.

The properties of the SCF may also be modified by the use of entrainers. Ely and Baker (1983) defined an entrainer as "a substance added to the supercritical solvent which has a volatility intermediate between the substances to be separated and the supercritical gas". Entrainers differ from mixed solvents in that the former is characterized by being in the subcritical state and its concentration is small compared to the primary solvent. The advantages in using entrainers are the enhancement in solubility and/or selectivity, and the regeneration of the solvent by temperature alone. These advantages have been illustrated by the separation of glycerides (Brunner and Peter, 1982), the extraction of coal (Sunol, 1982) and the decaffeination of green coffee beans (Zosel, 1978). More recently, Van Alsten and Eckert (1985) observed a 500 % increase in the solubility of acridine in doped supercritical carbon dioxide (5 % methanol as the entrainer). Brunner (1983) studied the effect of various supercritical fluids and entrainers on the solubility of the hexadecanol-octadecane system.

Sunol, et al. (1985) suggested some guidelines in the

selection of entrainers in SCE based on thermodynamic considerations.

### Experimental methods to measure solubility in SCF

The need for more data, especially from multicomponent systems, have led to improvements in the design of experimental equipment to generate accurate data quicker. Although the equipment and analytical methods do not constitute technological breakthroughs, the study of phase equilibrium at high pressures presents a few challenges both in equipment construction and analytical methods. The research work involves high pressure processes and sometimes corrosive and flammable materials, thereby requiring a careful hazard analysis.

This review applies only to bench scale research equipment used in the study of solubility in supercritical fluids or high pressure vapor-liquid equilibria. The feedstock is either a solid or a liquid and may range from a pure compound to a complex natural product. The feedstock is generally loaded in batches at the start of the experiment. All experimental equipment presented in the literature consists of two parts: (1) an equilibration system and (2) an analytical system.

### Equilibration systems

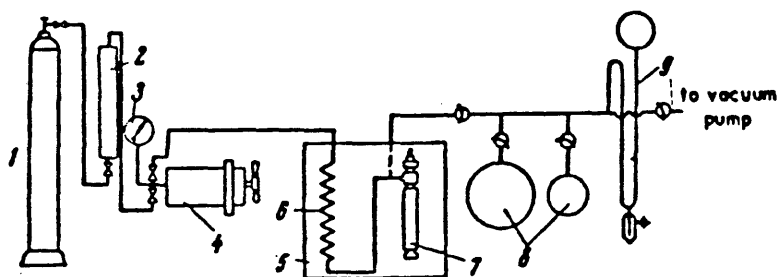
The equilibration system includes a pressurization unit and an equilibration cell. The pressurization unit can

be (1) a gas cylinder with a two stage regulator; (2) a gas cylinder connected to a compressor; (3) a liquefied gas cylinder, with a syphon for liquid withdrawal, connected to a pump; or (4) a cylinder and hydraulic press. The choice of pressurization system depends on the type of fluid used as the supercritical solvent.

The equilibration cell or extractor is a high pressure vessel that contains the condensed phase. The design might range from a custom built autoclave to a thick walled pipe with high pressure fittings at the ends. High pressure sapphire windows are sometimes included in order to observe phase behavior directly. Some researchers use a Jerguson gage as the equilibration cell. The equilibration system may be classified as static or dynamic.

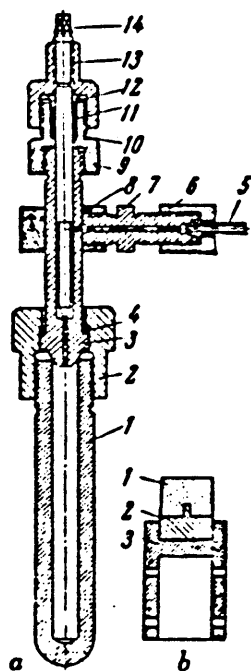
Tsekhanskaya, et al. (1962) used a static method to measure the solubility of pure solids in SCF's. The apparatus is depicted in Figure 2, and a schematic of the equilibrium cell is shown in Figure 3. The method consists of placing a tablet of compressed solid in the calibrated high pressure column and metering in the required amount of solvent. After equilibration, the fluid is expanded into a calibrated glass apparatus, and the amount of solid dissolved in the SCF at a set temperature and pressure is determined by the weight loss of the tablet.

Figure 2. Schematic diagram of a static apparatus used to obtain solid solubilities in a supercritical fluid (Tsekhanskaya, et al., 1962)



Apparatus for the measurement of the solubility of solids in compressed gases: 1) cylinder with purified carbon dioxide; 2) drying column; 3) manometer; 4) hydraulic press; 5) thermostat; 6) coil; 7) column for the measurement of the solubilities; 8) glass calibration flasks; 9) closed glass mercury manometer.

Figure 3. Schematic diagram of a static equilibrium column used to obtain solid solubilities in a supercritical fluid (Tsekhanskaya, et al., 1962)



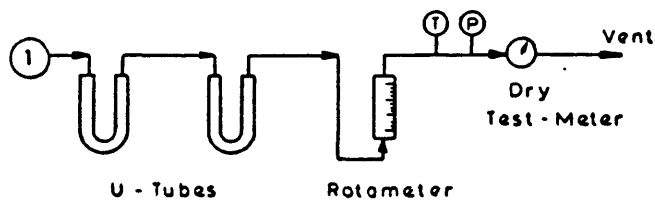
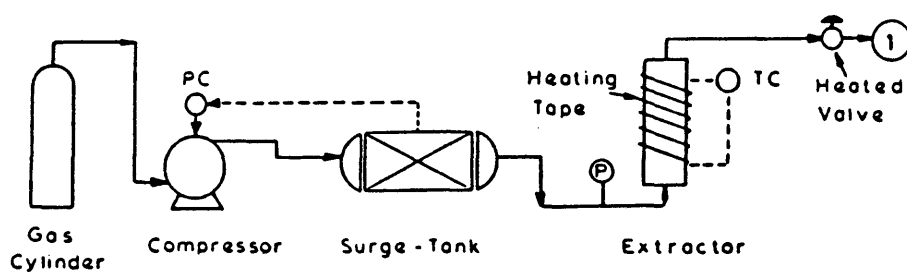
- a)** Column for the measurement of the solubility of solids in compressed gases;  
**b)** stirrer with compressed tablet; **a)**: 1) shell; 2) nut; 3) head; 4) ring; 5) cone; 6) lock nut; 7) nipple; 8) sleeve; 9) shell of stuffing box; 10) ring; 11) stuffing box; 12) main bush; 13) lid of stuffing box; 14) needle valve;  
**b)**: 1) compressed tablet; 2) iron support; 3) iron stirrer with slots.



A more common method is to saturate the SCF by using a flow system. The flow system in turn may employ a single pass or recirculation to achieve saturation. Figure 4 shows a schematic diagram for a typical single pass flow apparatus (Kurnik, et al., 1981; Kurnik and Reid, 1982; Krukonis and Kurnik, 1985). A saturated solution out of the extractor was assured by pumping the solvent at low flowrates ranging from 60 to 300 standard  $\text{cm}^3/\text{min}$  (Van Leer and Paulaitis, 1980). The on-line surge tank was used to dampen pressure fluctuations. The stability of temperature can be improved by using a preheater and placing the equilibration system in a thermostatic oven (McHugh and Paulaitis, 1980; Schmitt and Reid, 1984; Chang and Morrell, 1985). However, pressure fluctuations average  $\pm 1\%$  over the entire pressure range. This type of apparatus is used mainly to study solubilities at pressures higher than the critical region, where fluid density (i.e. solubility behavior) is very sensitive to pressure and temperature fluctuations.

The use of a recirculating flow stream in a high pressure system was favored by Dorau et al., 1983; Morris, 1984; and Radosz, 1984. The experimental apparatus is shown schematically in Figure 5 (Morris, 1984). The equipment was designed to study vapor-liquid equilibria. Both the vapor and the liquid are circulated by a "custom-made

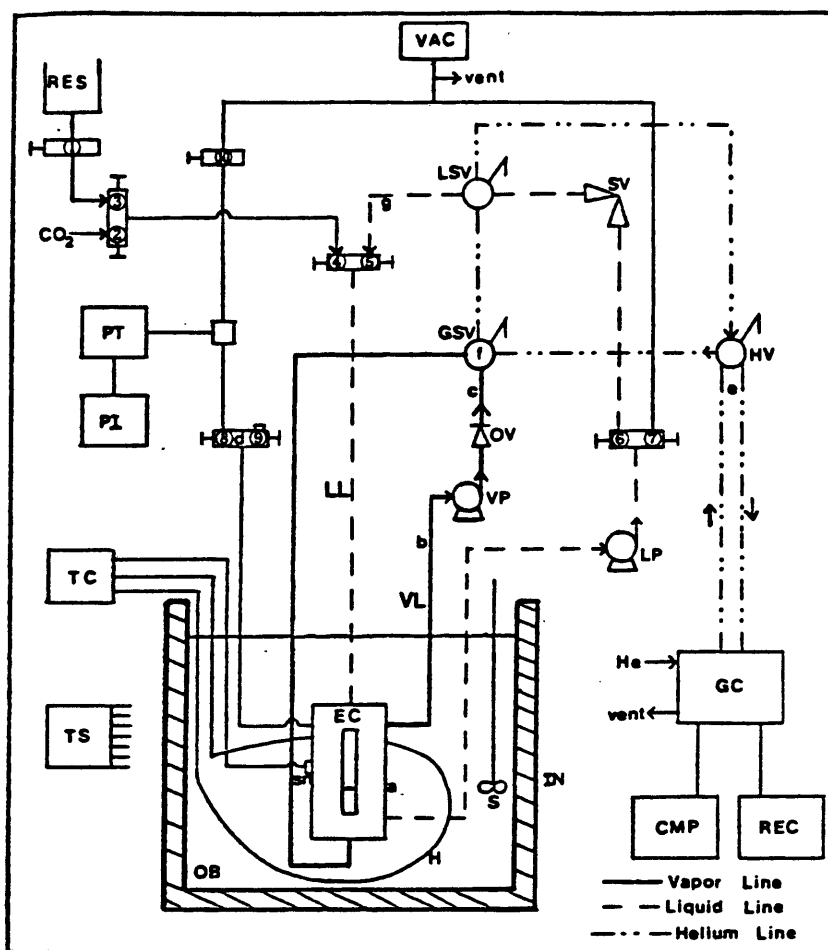
Figure 4. Schematic diagram of a flow apparatus used to obtain liquid or solid solubilities in a supercritical fluid (Kurnik and Reid, 1982)



- Key
- TC - Temperature Controller
  - PC - Pressure Controller
  - P - Pressure Gauge
  - T - Thermocouple

Equipment Flow - Chart

Figure 5. Schematic diagram of a recirculating flow apparatus used to obtain solid or liquid solubilities in a supercritical fluid (Morris, 1984)



CMP=computer; EC=equilibrium cell; GC=gas chromatograph; GSV=gas sampling valve; H=heater; He=helium; HV=helium valve; IN=insulation; LL=liquid line; LP=liquid pump; LSV=liquid sampling valve; OB=oil bath; OV=one-way valve; PI=pressure indicator; PT=pressure transducer; REC=chart recorder; RES=liquid reservoir; S=stirrer; sn=temperature sensor; SV=safety valve; TC=temperature controller; TS=thermocouple switch; VAC=vacuum pump; VL=vapor line; VP=vapor pump; ① to ⑥ valve numbers; a to g thermocouples.

electromagnet-driven piston-type pump" and a Milton Roy minipump, respectively. While temperature fluctuations of  $\pm 0.1$  °C were reported, values for pressure fluctuations were not mentioned. Since low circulating flow rates were used, significant pressure fluctuations would only be found near the pumps, which are located downstream from the sampling valves. The pressure and temperature stabilities allowed Morris (1984) to obtain experimental vapor-liquid equilibrium compositions at a pressure range of 2.5 to 130 atm.

#### Analytical systems

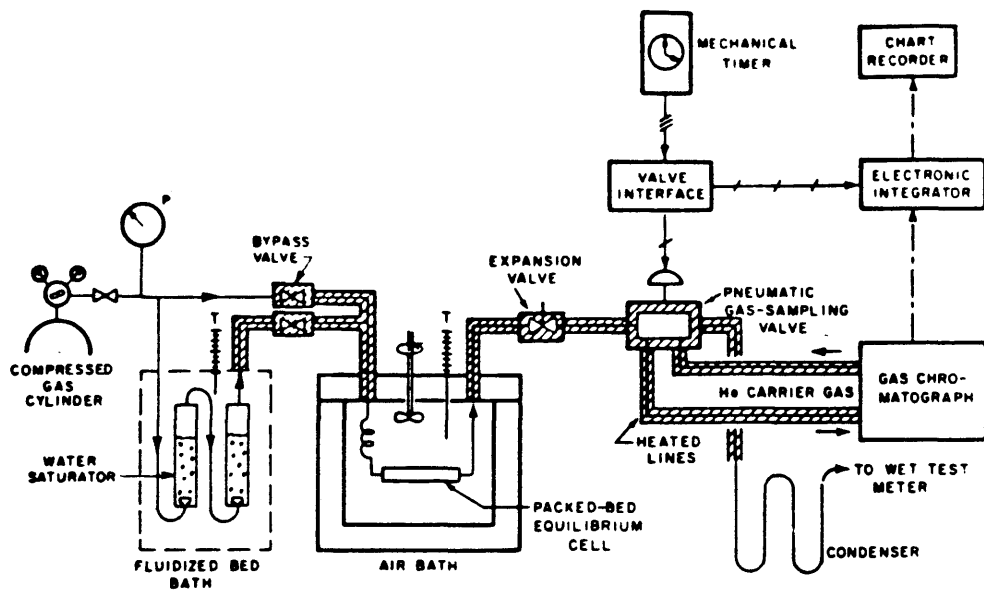
The most common method used to determine the solubility of a pure compound is gravimetical analysis. A schematic diagram of the typical equipment needed is shown in Figure 4. The saturated effluent from the extractor is expanded to atmospheric pressure through a heated metering valve. The solutes accumulate in tared U-tubes packed with glass wool and immersed in cold baths. The corresponding amount of solute free gas is monitored by a dry test meter. The calculation of pure component solubilities is straightforward. For mixtures, a liquid solvent is used to extract the solutes from the U-tubes and the composition determined chromatographically (Kurnik and Reid, 1982; Chang

and Morrell, 1985; Gopal, et al., 1985).

Another analytical method is the direct chromatographic sampling of the saturated SCF by a high pressure chromatographic valve. Figure 6 shows a schematic diagram of the apparatus used by Monge and Prausnitz (1983) in which the expanded fluid is sampled (Radosz, 1984). Panagiotopoulos and Reid (1985) and Morris (1984) favored a direct depressurization of the saturated SCF into the carrier gas stream of the gas chromatograph (See Figure 5). Morris (1984) used a 6-port sampling valve (loops of 20  $\mu\text{l}$  or 250  $\mu\text{l}$ ) and a 4-port internal sampling loop (0.5  $\mu\text{l}$ ) to sample the vapor and liquid phases, respectively. Panagiotopoulos and Reid (1985) used two high pressure switching valves of internal volume 0.5  $\mu\text{l}$  and 0.2  $\mu\text{l}$  for the vapor and liquid phases, respectively. Morris (1984) required larger gas sample volumes because the study was at higher temperatures (i.e. lower fluid densities). The small samples withdrawn would not affect the conditions in the cell significantly.

Stahl, et al. (1978) coupled the extraction system directly to a thin-layer chromatograph to investigate the solubility behavior of natural products. Thin-layer chromatography (TLC) allows the study of many substances that can not be eluted under normal conditions of gas

Figure 6. Direct gas chromatographic sampling technique to measure the composition of the dense gas mixture (Monge and Prausnitz, 1983)

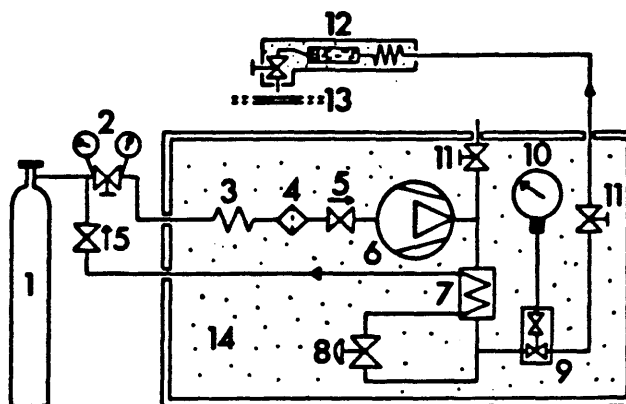


chromatography (GC). The schematic layout of the apparatus is shown in Figure 7. The emerging stream from the microautoclave is expanded onto a TLC plate. Direct coupling of GC or TLC methods to extraction systems provide relative compositions of multicomponent systems (qualitative results from the chromatograms) and quantitative results by means of calibration standards. This flexibility allows the screening of a large number of substances and solvents, or the production of experimental data for modeling and technical application of SCE.

Konrad, et al. (1983) and Swaid, et al. (1985) used near infrared spectroscopy (NIR) to study the high pressure vapor-liquid equilibrium of the system hexane and carbon dioxide. The schematic diagram of the spectroscopic apparatus is presented in Figure 8 (Swaid, et al., 1985). The cell was designed to operate at temperatures between 300 to 450 K and at pressures up to 2000 bar. The system is calibrated by introducing into the cell known amounts of the mixture constituents. The composition is determined as a function of the integrated molar absorptivity. NIR is well suited for the quantitative determination of compounds that contain O-H, N-H or C-H groups (Konrad, et al., 1983).

Smith and Udseth (1983) developed a method for direct mass spectroscopic analysis of the products from

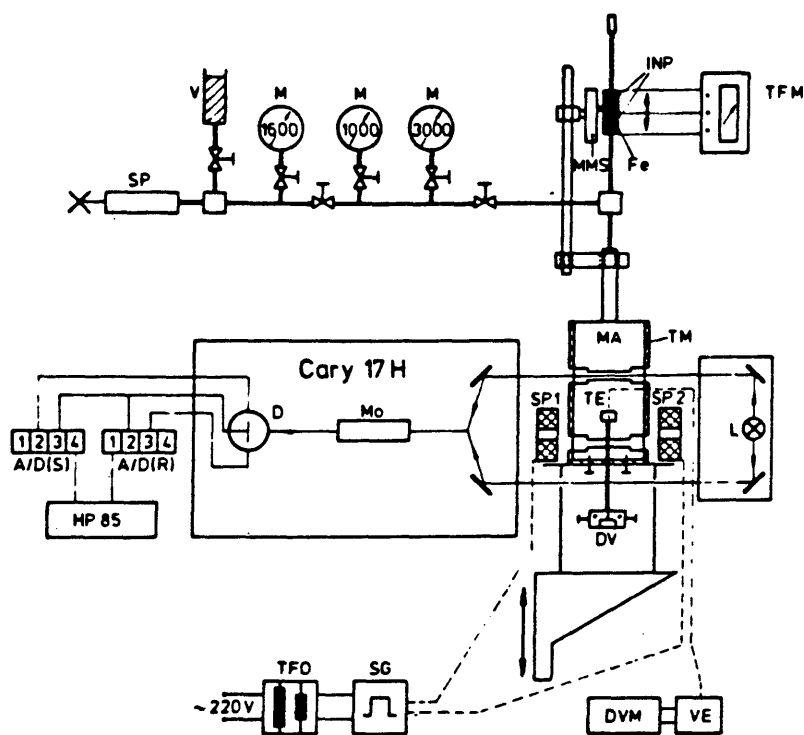
Figure 7. Schematic diagram of an apparatus for direct coupling of fluid extraction with thin-layer chromatography (Stahl, et al., 1978)



: 1) gas cylinder, 2) pressure-reducing valve, 3) preheating column, 4) filter, 5) check valve, 6) diaphragm compressor, 7) heat exchanger, 8) back-pressure regulator, 9) attenuators, 10) precision pressure gauge, 11) shut-off valve, 12) microautoclave for extraction, 13) TLC plate, 14) thermostatically-controlled container.



Figure 8. Schematic diagram of a NIR spectroscopic apparatus used to obtain solid or liquid solubilities in a supercritical fluid (Swaid, et al., 1985)



A/D (S) analog-digital convertor for sample signal

A/D (R) analog-digital convertor for reference signal

Cary 17H spectrophotometer

D detector, DV inlet valve, DVM digital voltmeter, Fe ferrite tip, HP 85 micro-

computer, INP thermostatically controlled solenoids for volume measurement,

L lamp, M pressure gauges, MA high-pressure cell, MMS micrometer screw, Mo mono-

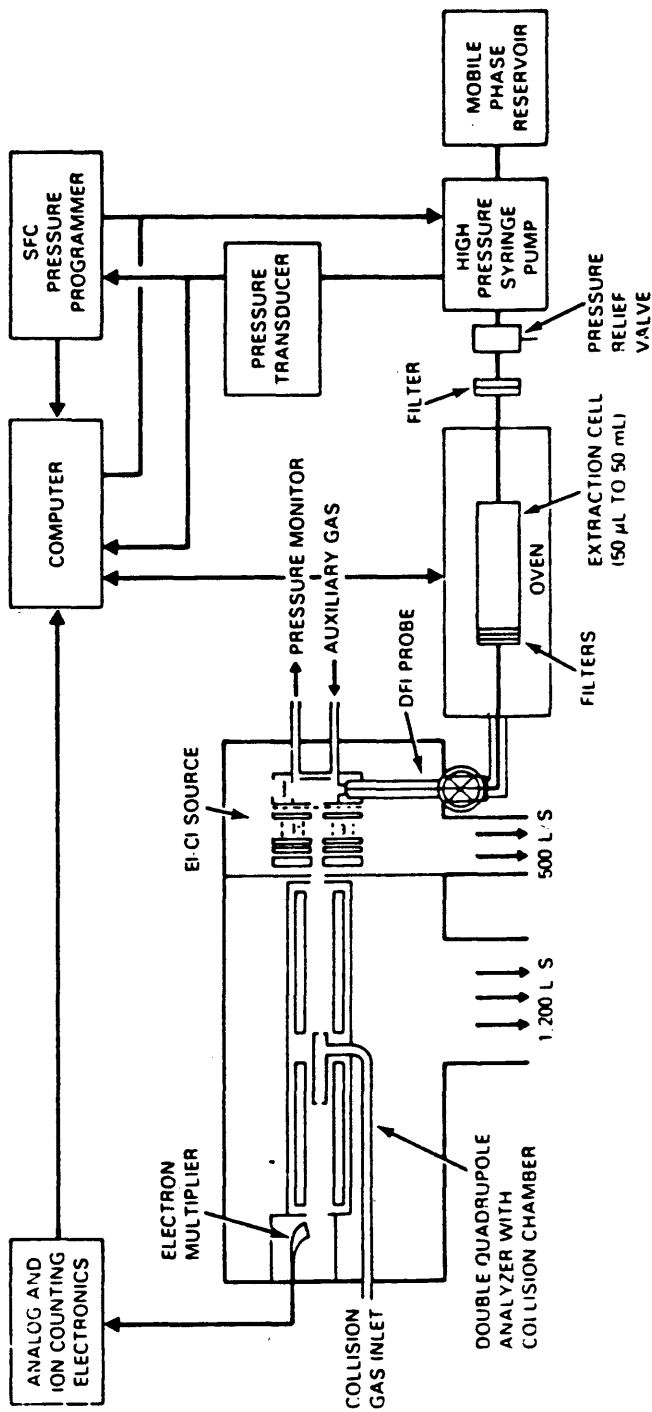
chromator, SG signal generator, SP screw press, (SP<sub>1</sub>, SP<sub>2</sub>) solenoids, TE thermo-

couple, TFM carrier wave amplifier, TFO transformer, TM thermostating jacket,

V hydraulic oil reservoir, VE reference junction.

supercritical extraction processes. A schematic representation of the supercritical fluid extraction-mass spectrometer is shown in Figure 9. The system was tested with bituminous coal at 280 °C and 5 to 100 bar. Continuous mass spectrometric sampling allows the study of the extent of supercritical fluid reaction or extraction over a period of time. The loss of sample due to sampling can be made insignificant for reaction times up to several hours (Smith and Udseth, 1983). This method is very well suited for kinetic studies of SCE processes.

Figure 9. Schematic diagram of an apparatus for direct mass spectrometric analysis of supercritical fluid processes (Smith and Udseth, 1983)



## EXPERIMENTAL APPARATUS

The experimental apparatus used to determine the dense gas composition is shown schematically in Figure 10. It consists of two parts: (1) the equilibration system and (2) an analytical system.

Equilibration system

The equilibration system was designed for a maximum working pressure of 3000 psig and a working temperature range of 35 to 55 °C. The main component is the 300 cm<sup>3</sup> equilibrium cell, which is a 316 stainless steel pressure vessel designed by Autoclave Engineers (See Figure 11). It has a rated maximum working pressure of 5400 psia at 360 °C. There are five ports machined into the cell. A 3/4 in. fractional tube to 3/4 in. male NPT Swagelok connector is bolted onto the top central port of the cell. This opening is used to load condensed samples into the cell at the start of the experiment and also to remove the condensed samples at the end of the experimental runs (See Experimental Procedure section). One of the ports is used to attach a pressure transducer to the cell. Another one is connected an externally adjustable relief valve, which is set to vent at a pressure in excess of 3200 psig.

The remaining two ports are used to recirculate the

Figure 10. Schematic diagram of the experimental apparatus used in this study to obtain solubilities in supercritical carbon dioxide

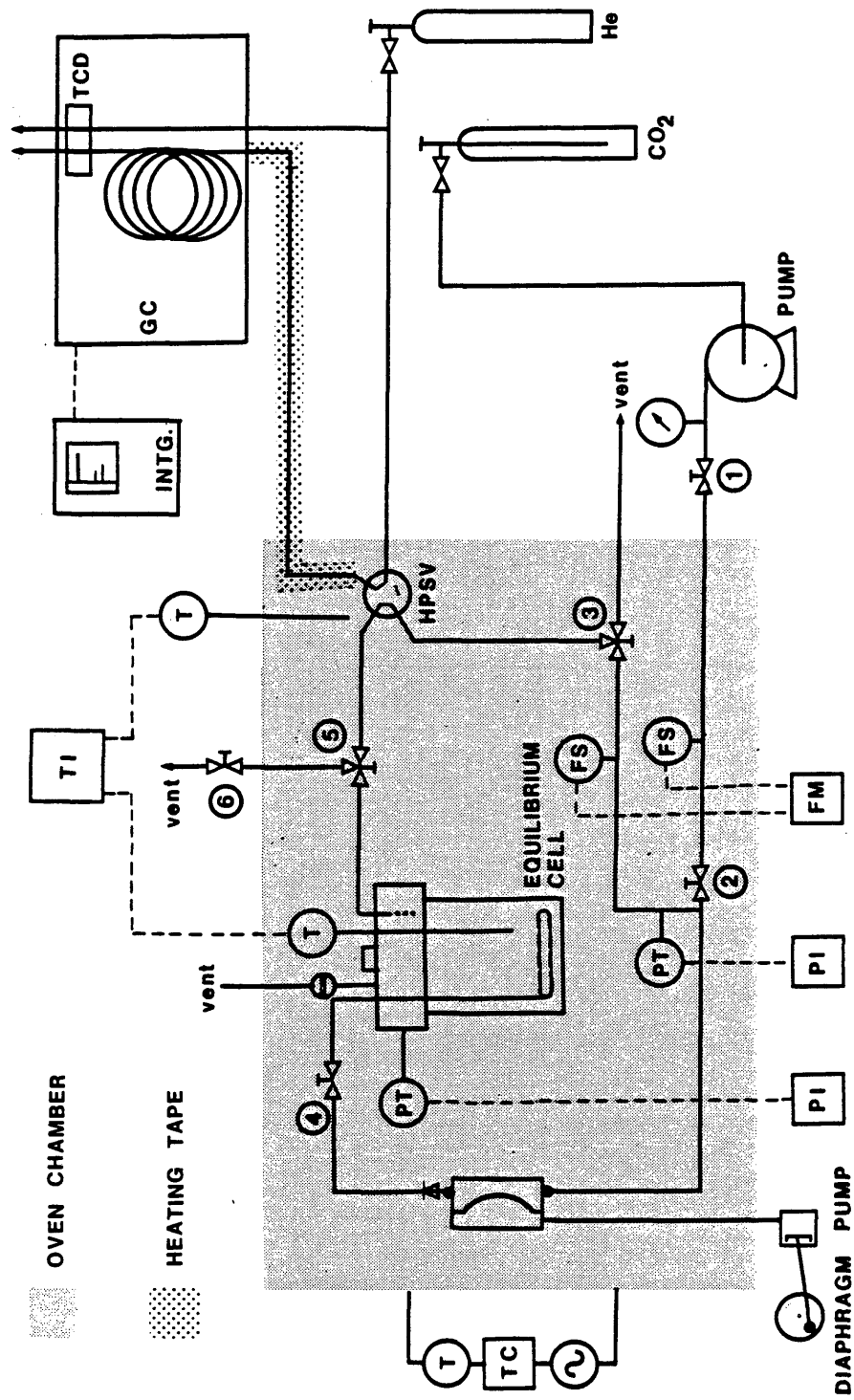
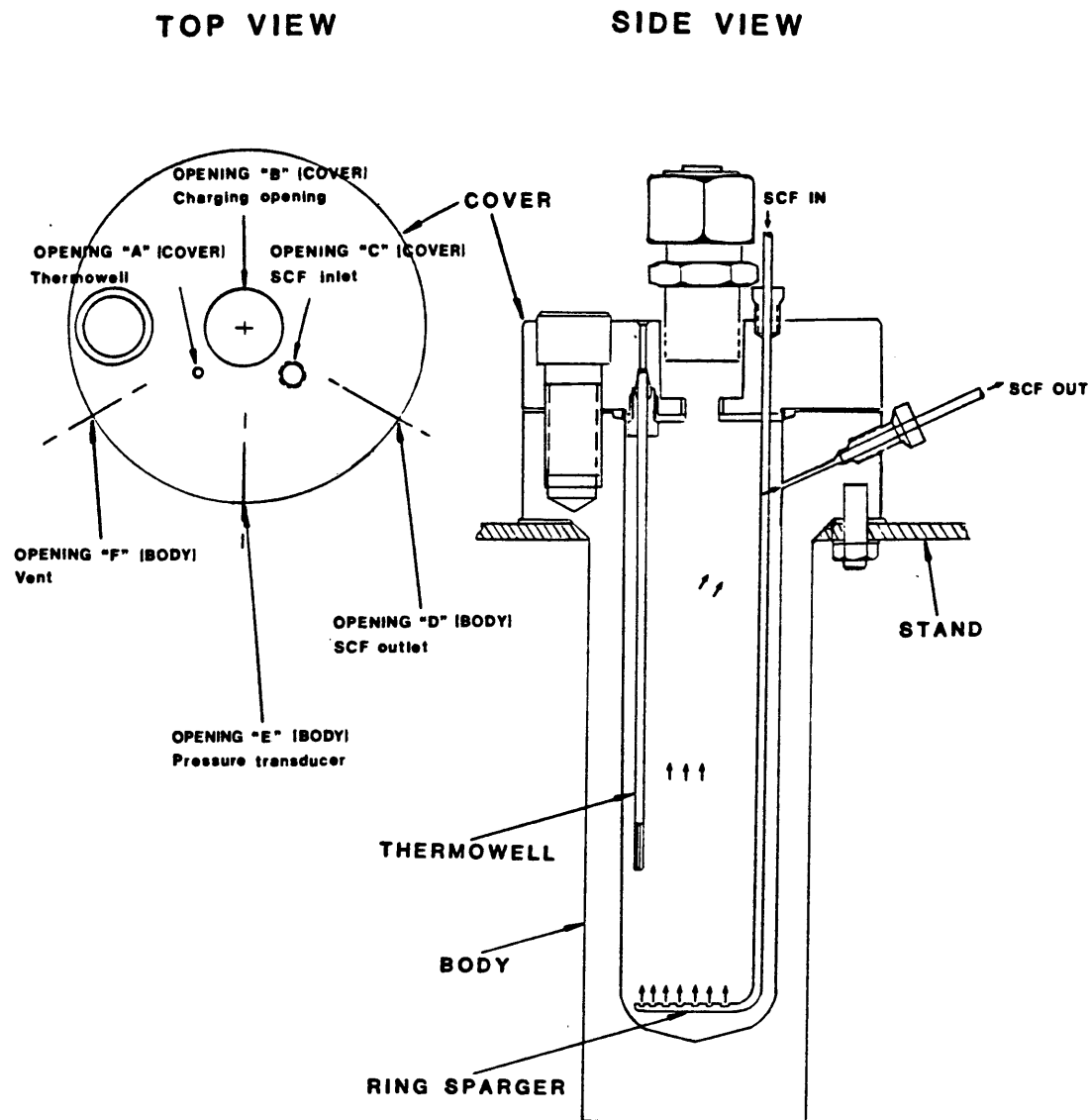


Table 2. Description of notation in Figure 10

FS:	Flowsensor
FM:	Flowmeter
PT:	Pressure transducer
PI:	Pressure indicator
T:	Thermocouple
TI:	Temperature indicator
TC:	Temperature controller
HPSV:	High pressure sampling valve
GC:	Gas chromatograph
INTG:	Integrator
TCD:	Thermal conductivity detector

Figure 11. Schematic diagram of the equilibrium cell used in this study (Autoclave Engineers, Inc.)



dense gas mixture in and out of the equilibrium cell. The recirculation is made possible by a diaphragm metering pump (Pulsafeeder Products Model 680-S-E). The pump consists of a remote head, which houses the stainless steel diaphragm, and is linked by a hydraulic line (1/4 in. O.D. stainless steel tubing) to the mechanical pump unit. The remote head isolates the recirculating fluid in a controlled environment that is separate from the pumping mechanism. The remote head has a rated working pressure of 3000 psig and working temperature of 60 °C. The estimated maximum flow capacity is 0.155 GPH (about 10 cm<sup>3</sup>/min), based on liquid flow. Although the diaphragm pump was designed to pump liquids, it works very well for simple recirculation of dense gases. The pumping rate is controlled by micrometer dial located on the pumping unit. The recirculation rate is monitored by a thermal mass flow sensor (Linde, Part No. 13M-202-4180) and a multiple channel mass flowmeter and flow controller (Linde, Model No. FM-4570-13M-13M), which displays the flowrate in terms of sccm (standard cubic centimeters per minute). The operating temperature range for the flow sensor is from -18 to +65 °C and the operating pressure range is from vacuum to 3000 psig.

The system pressure is measured by two pressure transducers (Omega Engineering, Model No. Px-301-5KGV), and



the corresponding pressures are displayed on digital transducer indicators (Omega Engineering, Model No. DP420). The operating pressure for the pressure transducer is from 0 to 5000 psig, and the operable temperature is from -45 to 107 °C. The compensated temperature range is from 0 to 55 °C. The transducer indicators have a resolution of 1 part in 10000 (the display is in psig). The pressure transducers and their matched digital transducer indicators were calibrated with a dead-weight tester to a pressure range of 0 to 3000 psig, for the desired working temperature (See CALIBRATION section).

The valves were manufactured by Whitey Company. Swagelok fittings are used in all the connections, except for the Autoclave fittings used in the equilibrium cell. The Whitey valves and Swagelok fittings (316 stainless steel was the choice of material) were supplied by Denver Valve and Fitting. The interconnecting piping system consists of 1/8-in. O.D. 316 stainless steel tubing with a wall thickness of 0.03 inch.

The equilibration system is housed inside a mechanical convection oven (Thermolyne, Model OV35245). It has a chamber capacity of 148 liters (48 cm x 63 cm x 48 cm). The stability of the oven allows control of the system temperature to  $\pm 0.1$  °C of the desired setting. The

equilibration system is supported inside the chamber by a rectangular cage constructed from UNISTRUT metal framing and is bolted into the oven walls.

The temperatures of the equilibrium cell and the mechanical oven are monitored separately by two thermocouple probes (Calalloy, Part No. C03J80-R8-MPJ). One of the probes is placed inside a thermowell, which penetrates  $3/4$  of the way into the equilibrium cell. The other probe is placed inside the oven chamber and it measures the temperature of the circulating air. The probes are connected to a digital thermocouple indicator (Omega Engineering, Digicator model 412b-J-C). This indicator has a resolution of 0.1 degree and a five point selector switch. The thermocouple probes and the digital indicator were calibrated to a temperature range of 30 to 60 °C (See CALIBRATION section).

A peripheral unit to the equilibration system is the metering pump (Milton Roy Co., Part No 92014803) used to pressurize the liquified carbon dioxide syphoned out of the reservoir tank. The pump was designed for a maximum working pressure of 6000 psig and has a flowrate range of 45 to 460  $\text{cm}^3/\text{hr}$ . Liquified carbon dioxide is required for the pump to work. Therefore, the carbon dioxide coming out of the tank is kept liquified by cold water flowing through a coil

of 1/8-in O.D. copper tubing that is wrapped around the stainless steel tubing connecting the carbon dioxide tank to the metering pump. The cold water is obtained from tap water flowing through a coil of copper tubing, which is submerged in a dewar containing ice and water.

#### Analytical system

Sampling of the equilibrium dense gas mixture is done with a high pressure sample injection valve (Valco Instruments Co., Part No. RCI4PX1H1), which has a calibrated internal volume of 1.2 microliters. The valve was preset by the manufacturer to operate at 3000 psig and 60 °C.

The sampling valve is located in the oven chamber, so that the dense gas mixture is allowed to equilibrate at a constant temperature. The valve is actuated manually using a 6 inch extension shaft (Valco Instruments, Part No. 6S0), which protrudes through a hole in the side wall of the oven. The lever is located outside the oven, which allows the sampling to be done without opening the oven door and disturbing temperature in the oven chamber. The samples are expanded directly into a helium gas stream and the composition of the mixtures is determined by gas chromatographic methods. The sampling valve and gas chromatograph are connected by 1/16-in. O.D. stainless steel

tubing, which is wrapped by heating tape kept at 100 °C.

The gas chromatograph (Hewlett Packard, model HP5890A) has a "HP Series 530 $\mu$ " packed column (5 m. long; stationary phase: methyl silicone) and utilizes a thermal conductivity (TC) detector. The effluent out of the TC detector is routed to a flame ionization detector (TCD-to-FID jumper tube, HP Part No. 19302-80600). In addition to the sampling valve, the gas chromatograph also has a syringe injection port. The gas chromatograph is connected to a Hewlett Packard integrator, model HP3390A.

## EQUIPMENT CALIBRATION

Chemicals

Sigma Chemical Co. supplied the m-cresol (Cat No. C5015, 99%) and the phenol (Cat No. P3653, 99%). Aldrich Chemical Co. supplied the naphthalene (Cat. No. 18450-0, Gold Label, 99+%). General Air Service & Supply provided the liquified carbon dioxide tanks (99.9+%, syphon for liquid withdrawal). All the chemicals were used without further purification.

Pressure transducer and transducer indicator

Each pressure transducer is matched to an indicator, and the pairs were calibrated separately with a dead weight gauge tester (Aschcroft Gauge Division, Type 1313A) for a pressure range of 0 to 3000 psig. The transducers were wrapped with a heating tape during the calibrations, in order to reduce the effects due to ambient temperature changes. The calibration instructions from the dead weight tester and digital indicator manufacturers were followed.

Thermocouple probe and digital thermocouple indicator

Both thermocouple probes are connected to a digital indicator, which has a five position switch selector. Each

probe is connected to a different channel, and calibrated using a constant temperature ( $\pm 0.1$  °C stability) water bath. The temperature of the water bath was also checked with calorimetric mercury thermometers (0.05 °C per division). The thermocouple probes were calibrated for a temperature range of 0.0 (ice-water mixture) to 55.0 °C. The instructions from the manufacturer were followed in the calibration of the digital indicator.

#### Flowsensor and digital flowmeter

The flowsensor and flowmeter were used without checking the manufacturer's calibration. The exact recirculation flowrate was not considered critical to the experiment.

#### Thermal conductivity detector

The detector sensitivity increases as the temperature difference between the detector filament (automatically set) and the surrounding detector body (chosen detector zone temperature) increases. The filament temperature is maintained at a relatively constant difference (preset by Hewlett Packard) above the detector operating temperature. The preset difference (i.e. sensitivity) decreases with increasing detector body temperature. Therefore, the choice of detector temperature is limited by the highest boiling

component that might condense inside the detector. A temperature of 250 °C was used for all runs (the highest boiling component was naphthalene, b.p. 218 °C).

The detector sensitivity is also influenced by the flowrate ratio between the carrier effluent and the reference gas streams. The carrier gas flowrate through the column in turn influences the elution time and peak resolution, but the effects may be compensated by temperature programming. Test analysis showed that a column flowrate of 20 cm<sup>3</sup>/min and reference gas flowrate of 30 cm<sup>3</sup>/min provided high sensitivity and good peak resolution. These flowrates were used throughout the experimental work. Table 3 summarizes the operating conditions for the gas chromatograph.

The thermal conductivity detector of the gas chromatograph was calibrated by injecting samples of known composition and obtaining calibration curves for each component (amount versus peak area).

The equilibration system and the calibrated high-pressure sampling valve were used to prepare calibration curves for carbon dioxide. Carbon dioxide samples of known pressure, temperature and volume were injected into the gas chromatograph, and the respective peak area responses were correlated. Data source for supercritical carbon dioxide

Table 3. Gas chromatograph operating conditions

---

Detector type	Thermal conductivity
Temperature	250 °C
Inlet type	Packed
Temperature	250 °C
Oven	Temperature programmed
Initial Temp	40 °C
Initial Time	4.0 min.
Rate	60 °C per min.
Final Temp	150 °C
Final Time	0.5 min.
Column:	
Part No.	19095S (#100)
Dimensions	530 µm ID; 5 m
Stationary phase	Methyl silicone
Flowrates:	
Carrier (Helium)	20 cm <sup>3</sup> /min
Reference (Helium)	30 cm <sup>3</sup> /min

---



(IUPAC, 1973) was used to calculate the density at the system temperature and pressure.

Syringe injections of standard solutions were used to prepare calibration curves for phenol, m-cresol and naphthalene. The standards were prepared by weighing the compounds with an analytical balance (Cenco Scientific; sensitivity: 0.1 mg) and dissolving them in a known weight of methyl ethyl ketone. The density of the standards were determined with the use of pipets and the Cenco balance. Microliter syringes (Hamilton) were used to inject accurate volumes of standard through the injection port of the gas chromatograph.

Figures 12 and 13 show the calibration curves for naphthalene and carbon dioxide, respectively, at a detector sensitivity of range 3. The response factor (mole of sample divided by the integrated area response) for naphthalene at range 3 is constant due to the small sample sizes encountered. The calibration curves become nonlinear for larger sample sizes. However, the response factor of carbon dioxide at range 3 is constant despite the larger sample size with respect to naphthalene. This is due to the narrow sample size region that was plotted.

The calibration curves for each component and for three different detector sensitivity ranges are presented in

Figure 12. Calibration curve for naphthalene at a TCD range of 3

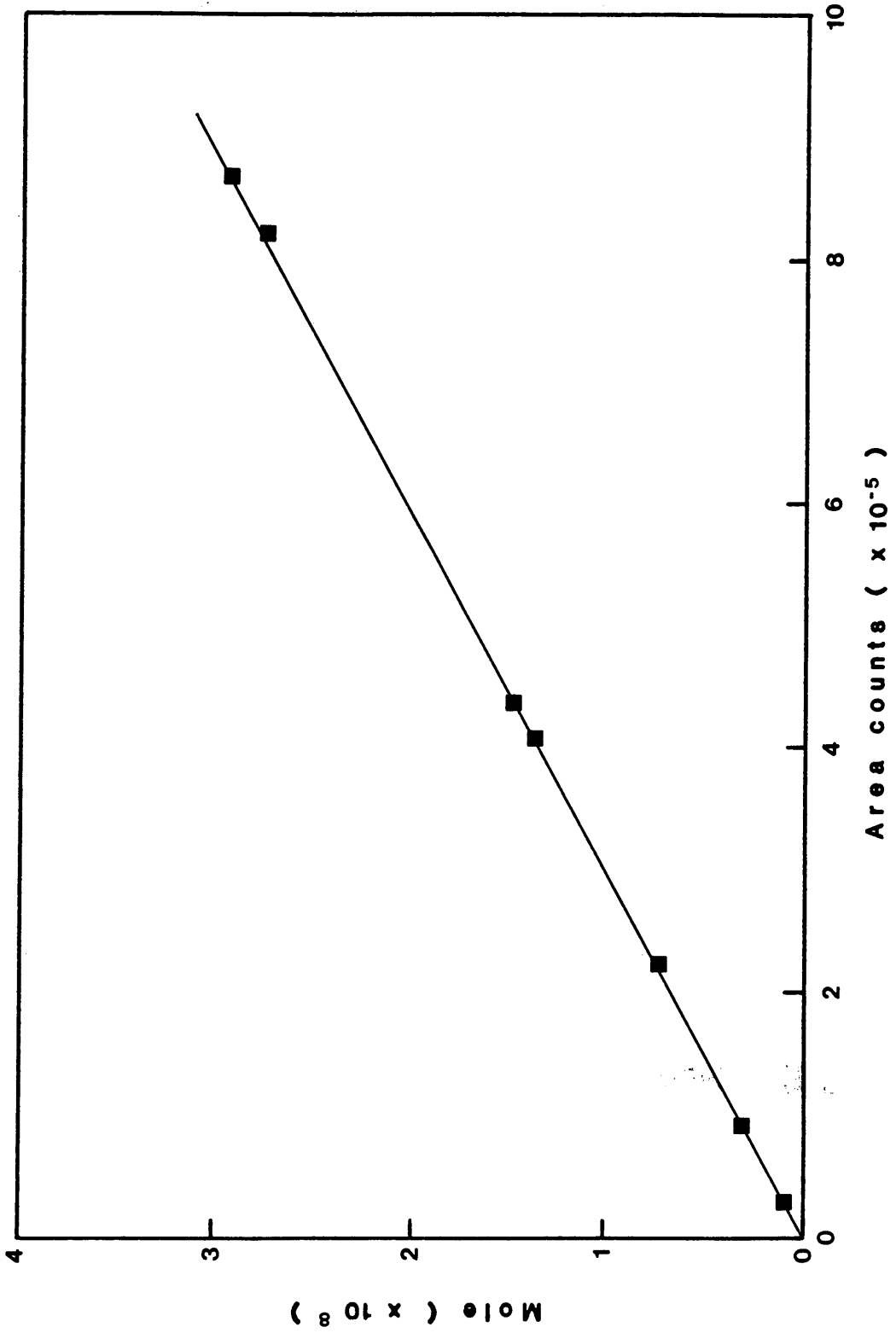
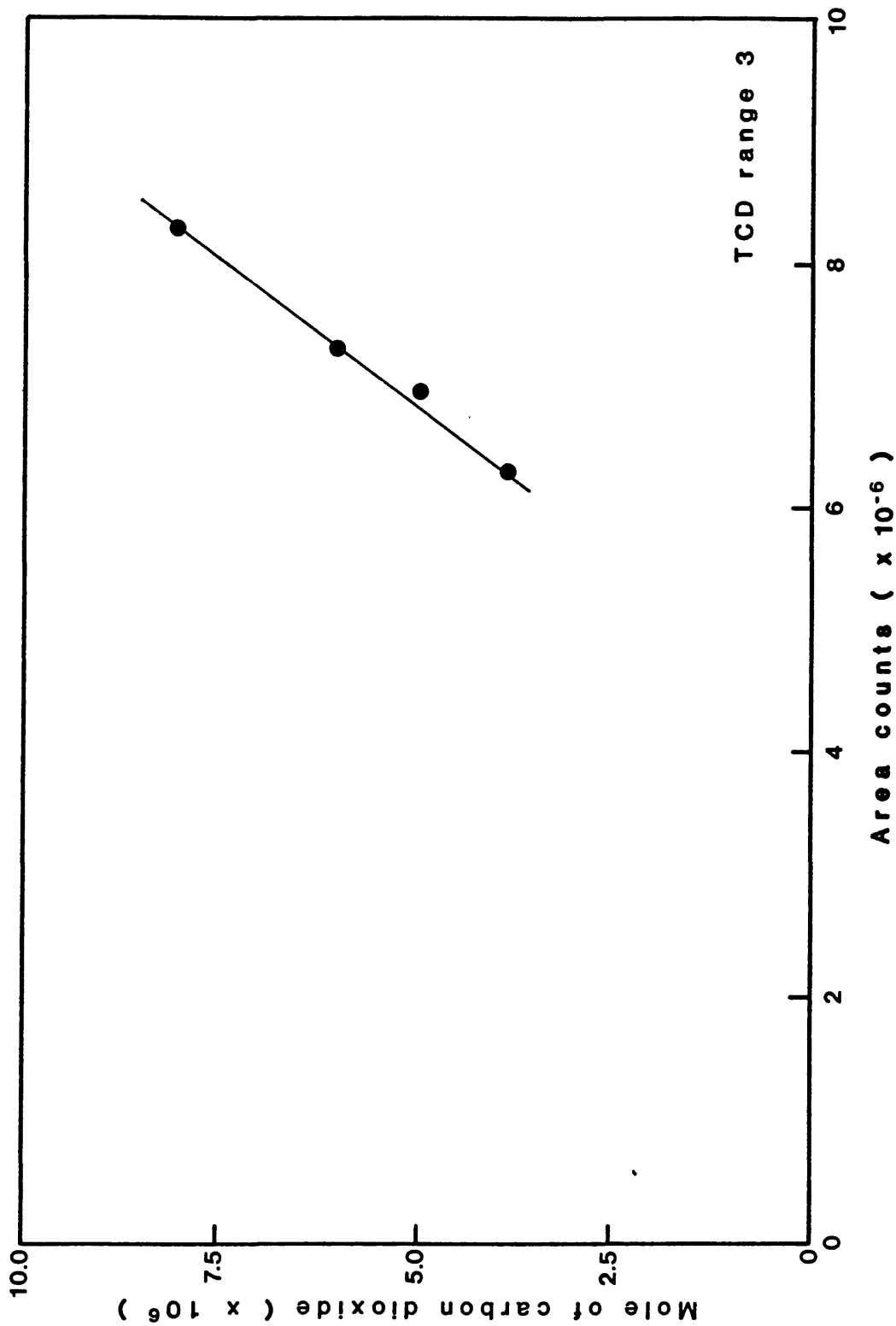


Figure 13. Calibration curve for carbon dioxide at a TCD range of 3



Appendix A. Each calibration curve was fitted to a linear equation (Ranges 3 and 5) or to a quadratic or cubic equation (Range 7). Note that the linear equations have an y-intercept other than zero. The attempt was only to fit the equations to a given range of experimental data.

## EQUIPMENT PRETESTS

A number of preliminary experiments were conducted to assure that the experimental equipment would provide reliable data. The naphthalene-carbon dioxide system at 313.3 K was chosen to check the reproducibility of the experimental data. The results from two different runs are presented in Table B-1 in Appendix B and plotted in Figure 14. The solubility units are in terms of the reported results from the integrator, i.e. the ratio of the naphthalene peak area to the total peak area (naphthalene + carbon dioxide). The area of each peak is proportional to the mass of each component in the mixture injected into the gas chromatograph. Therefore, the area % is proportional to the mole fraction of each component. Each experimental datum is an average of at least three different chromatographic analyses that are reproducible within 5 % of the absolute value. Comparison of the data set of both runs shows that the results agree to better than 3 %.

Two other experiments were conducted on the naphthalene-carbon dioxide system at 318.2 K. The results from this study are presented in Table B-2 and shown in Figure 15 and compared with data reported in the literature (Tsekhanskakya, et al., 1964; Chang and Morrell, 1985). The results obtained in this study agree with the reported data

Figure 14. Experimental solubilities of naphthalene in supercritical carbon dioxide at 313.3 K

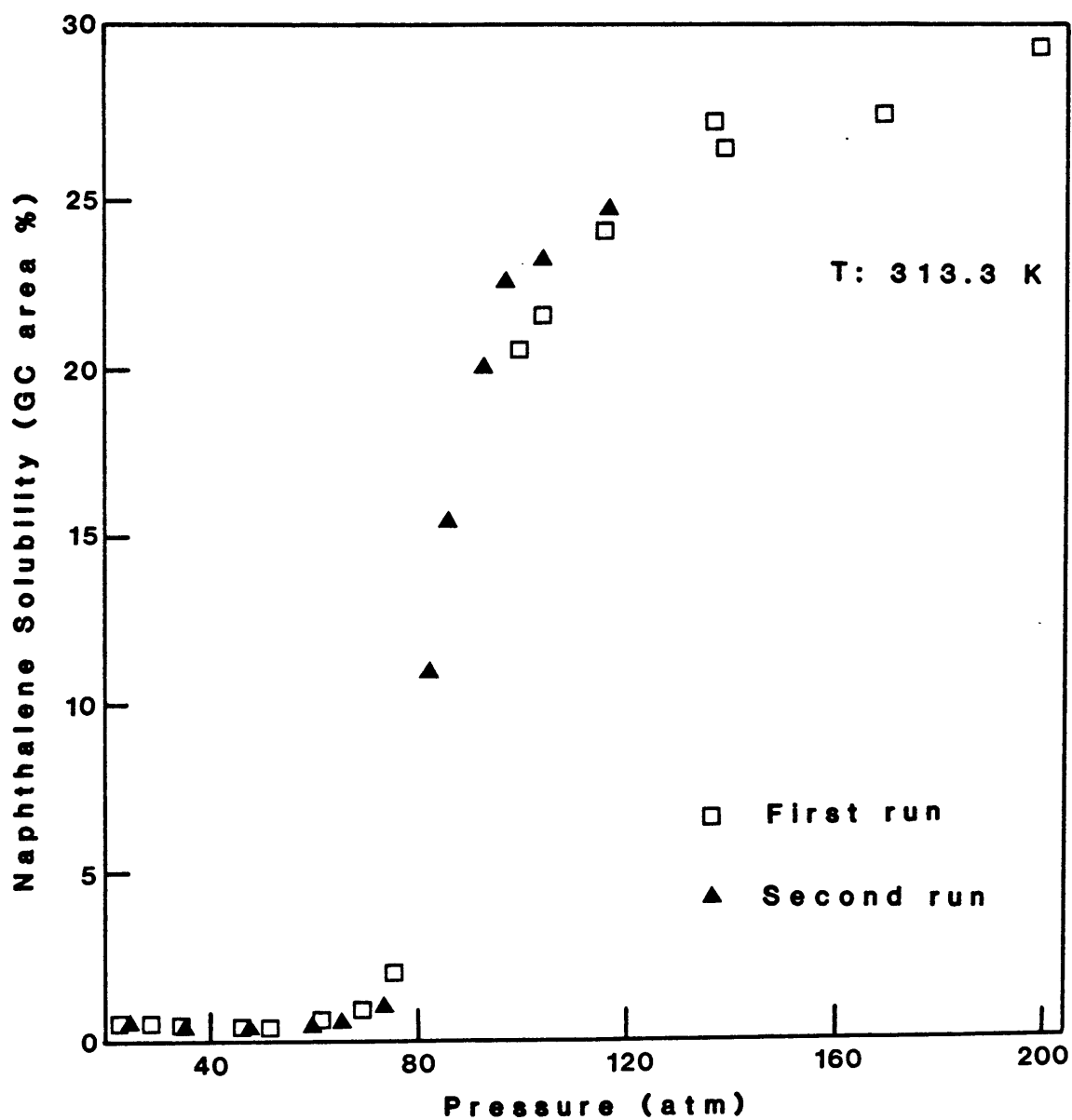
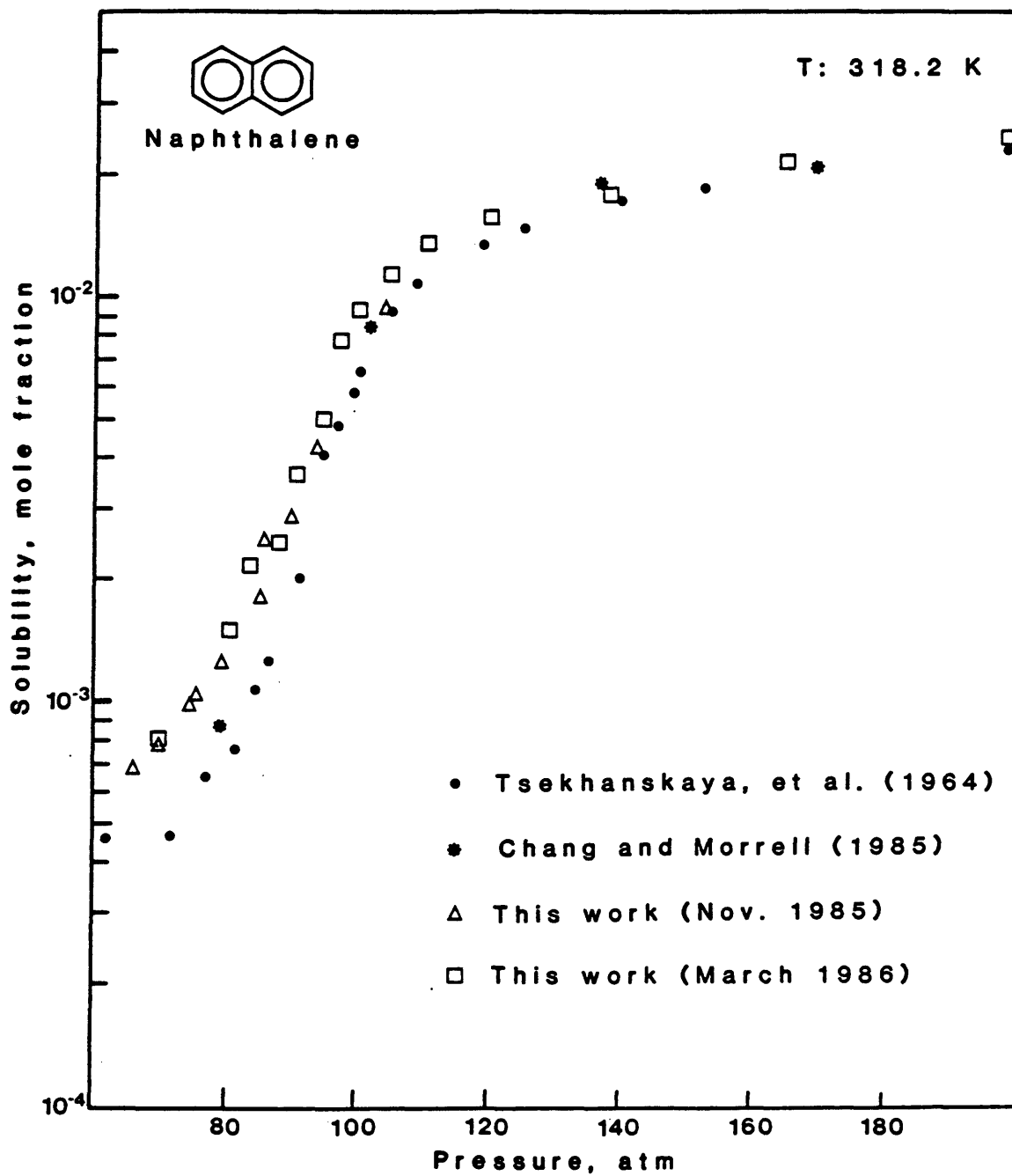


Figure 15. Experimental solubilities of naphthalene in supercritical carbon dioxide at 318.2 K



to better than 5 %, at pressures between 120 to 200 atm. But the solubilities differ by as much as 100 % within the pressure range of 60 to 120 atm. Chang and Morrell (1985) reported only one solubility value below 100 atm, and it differed by 20 % from the result obtained by Tsekhanskaya, et al. The values reported by Tsekhanskaya, et al. and by Chang and Morrell are presented on Table B-3 in Appendix B.

The solubility of naphthalene in carbon dioxide undergoes a dramatic increase within the pressure range of 80 to 120 atm. The density of carbon dioxide is also very sensitive to pressure and temperature changes in this region. Chang and Morrell (1985) used a flow type apparatus and reported that "fluctuations in pressure due to pumping are less than 1 % of the operation pressure over the entire pressure range". This translates to a fluctuation of 1 atm at an operation pressure of 100 atm. The pressure fluctuations encountered might explain why Chang and Morrell did not report any solubility measurements between 80 and 100 atm. Kurnik, et al. (1981) also compared their test data for naphthalene-carbon dioxide at 328 K to those of Tsekhanskaya, et al. (1964), but only at pressures between 150 to 250 atm.

Tsekhanskaya, et al. (1964) made their measurements by the static gravimetric method described previously.



The solubility was determined by measuring the weight loss of a pelleted solid naphthalene (about 1 g) in a 24 cm<sup>3</sup> equilibration cell. The mole fraction of naphthalene in carbon dioxide is about 0.0005 at 70 atm and 318 K. This is equivalent to a weight loss of 0.006 g from the 1 g naphthalene tablet. Tsekhanskaya, et al. (1963) reported that "after reduction of pressure, crystals of naphthalene settled on the surface of the tablet, but could be readily removed with a soft hair brush". Even though an analytical balance was used to weigh the tablets to within 0.2 mg, the above technique would be questionable at low solubilities. From reading the article, it is unclear how accurate or reproducible are their results, or even if there were any replicate experiments.

The possible errors in the experimental data from this study may be due to:

- entrainment in the dense gas phase,
- pressure and temperature calibrations, and
- calibration of the detector.

Entrainment of naphthalene solid in the gas phase may be ruled out, since it is rarely reproducible and the results from two different set of experiments show good agreement. The pressure and temperature calibrations were checked after each experiment and the results were within

2 psia and 0.1 K, respectively, of the expected values. A new set of calibration curves were prepared to calculate the solubility values of the second run (March 1986). The results for both set of experiments in this study agree within experimental error.

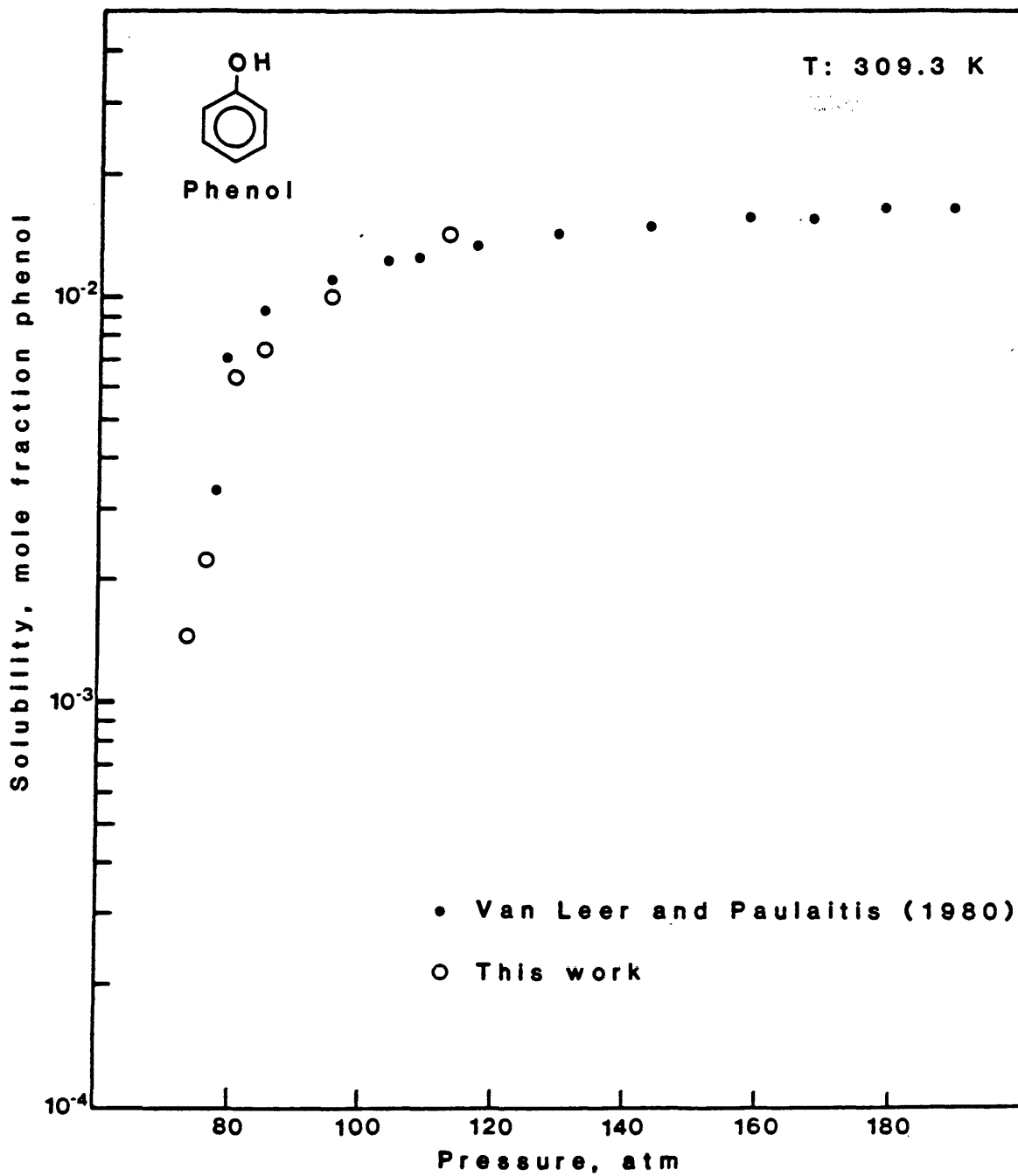
Furthermore, it was estimated that the uncertainty in the experimental solubilities from this study is  $\pm 10\%$  of the absolute value. The uncertainty analysis was based on a propagation of errors and the estimates are presented in Appendix D. The  $\pm 10\%$  uncertainty does not explain the difference between the solubilities calculated in this study and those from Tsekhanskaya, et al. (1964).

Figure 16 compares phenol solubility data from this study (See Table B-4) with those reported by Van Leer and Paulaitis (1980), and are in agreement to better than 10% (See Table B-5). No data were obtained beyond 115 atm in this study, because of a leak in the hydraulic line of the recirculation pump.

It was concluded that the experimental equipment and procedure would provide reliable data that would meet the thesis objectives because:

- there is good reproducibility in the results from the naphthalene-carbon dioxide system, and in the results from the m-cresol-phenol-carbon dioxide system (See

Figure 16. Experimental solubilities of phenol in supercritical carbon dioxide at 309.3 K



EXPERIMENTAL RESULTS section) obtained in this study,  
- Tsekhanskaya, et al. did not report the precision of  
their experimental results, and  
- results from the naphthalene-carbon dioxide system  
obtained in this study correctly described the  
expected behavior reported by Tsekhanskaya, et al.,  
and the data agree to within 5 % at pressures between  
120 and 200 atm.

## EXPERIMENTAL PROCEDURE

A complete experiment is comprised of a series of isothermal runs performed within a pressure range of 750 to 3000 psig, for a fixed condensed phase composition. For each choice of pressure, the composition of the dense gas mixture is determined using the gas chromatograph. The purpose of the experiments is to generate data for equilibrium solubility (mole fraction of solute in the dense gas phase) as a function of pressure at constant temperature. This section describes in detail the procedure followed for a typical experiment.

Apparatus preparation

It is necessary to purge the equilibration system before a new condensed mixture is loaded. The system will be at a pressure of up to 3000 psig at the end of each experimental run. The carbon dioxide is carefully vented through the regulating valve #6 (See Figure 10), which is wrapped with a heating tape to prevent it from freezing.

A vacuum pump and a filtering flask are used to remove a liquid sample from the equilibrium cell. The 3/4-in Swagelock fitting located at the top of the cell is used as the loading and exhaust port. If the condensed phase is a solid, a quantity of solvent is added to the cell in order

to facilitate the clean-up procedure.

After removing the bulk of the condensed sample, the equilibration system is charged with acetone or any other organic solvent. The diaphragm pump is used to recirculate the solvent through the cell, valves and tubing system. The solvent dissolves any organic material that condensed on the walls of the cell and tubing when the system was depressurized. The solvent is allowed to recirculate for about 15 minutes before a vacuum pump, cold trap and filtering flask are used to remove the solvent from the system. This procedure is repeated two or three more times, depending on whether a sample of different composition or nature from the previous run is to be added to the cell. Normally, no more than two flushings are required.

The equilibration system is then isolated and the oven chamber is sealed and heated to 50 °C. Once the oven is up to temperature, a vacuum pump and cold trap system is attached to valve #6 and the remaining solvent is purged from the equilibration system.

The system is left purging for about an hour, then valve #6 is closed once again and the equilibration system is pressurized with carbon dioxide to 800 psig. The equilibration system is isolated and the oven is heated to the desired temperature for the next experiment. The

diaphragm metering pump is turned on. This step has a two-fold purpose. One, it brings the whole system to temperature; nearly all the equipment is made up of stainless steel, which takes time to heat up. Second, once the system is allowed to equilibrate, a sample is injected into the gas chromatograph to check if the equilibration system is sufficiently purged.

#### Loading of the sample

The sample is prepared for loading while the system is depressurized. Pure liquid and solid samples are weighed prior to loading into the cell. In the case of mixtures, the weighted pure components are mixed prior to loading. The experiments performed in this work did not require the handling of solid mixtures. Although phenol is a solid at room temperature, the mixtures of phenol and m-cresol were in the liquid phase at room temperature for all compositions studied in this work. For solid mixtures, Chang (1985) suggested that the solutes be "melted, mixed, cooled to room temperature, and then pulverized before packing into the extractor".

The condensed sample of known composition is quickly loaded into the system through the 3/4-in Swagelok fitting located at the top of the cell. The Swagelok cap is then

tightened into position. The air introduced into the system while loading is evacuated with the vacuum pump through valve #6. After evacuation of the equipment, valve #6 is closed. Ball valve #1 is opened to pressurize the equilibration system with carbon dioxide. Regulating valve #2 is used to adjust the rate of carbon dioxide flow into the system. Regulating valve #4 and three-way valves #3 and #5 are left open to the equilibrium cell, so that it may be pressurized through the ring sparger and through the top of the cell. This step minimizes the risk of entraining small amounts of condensed sample in the tubing system and sampling valve.

The oven chamber is sealed and allowed to reach the desired set temperature. After the system is charged with carbon dioxide to the desired initial pressure, ball valve #1 is closed. The diaphragm pump is started and adjusted for a recirculation flow of about 5 cm<sup>3</sup>/min. Although the digital flowmeter displays in units of standard cm<sup>3</sup>/min, the volumetric flow (at the system pressure and temperature) may be quickly estimated from a temperature-entropy diagram for carbon dioxide. The approach to equilibrium is monitored by the stability of the pressure and temperature of the cell. It normally takes 15 to 30 minutes for the system to stabilize, but during the initial pressurization, the



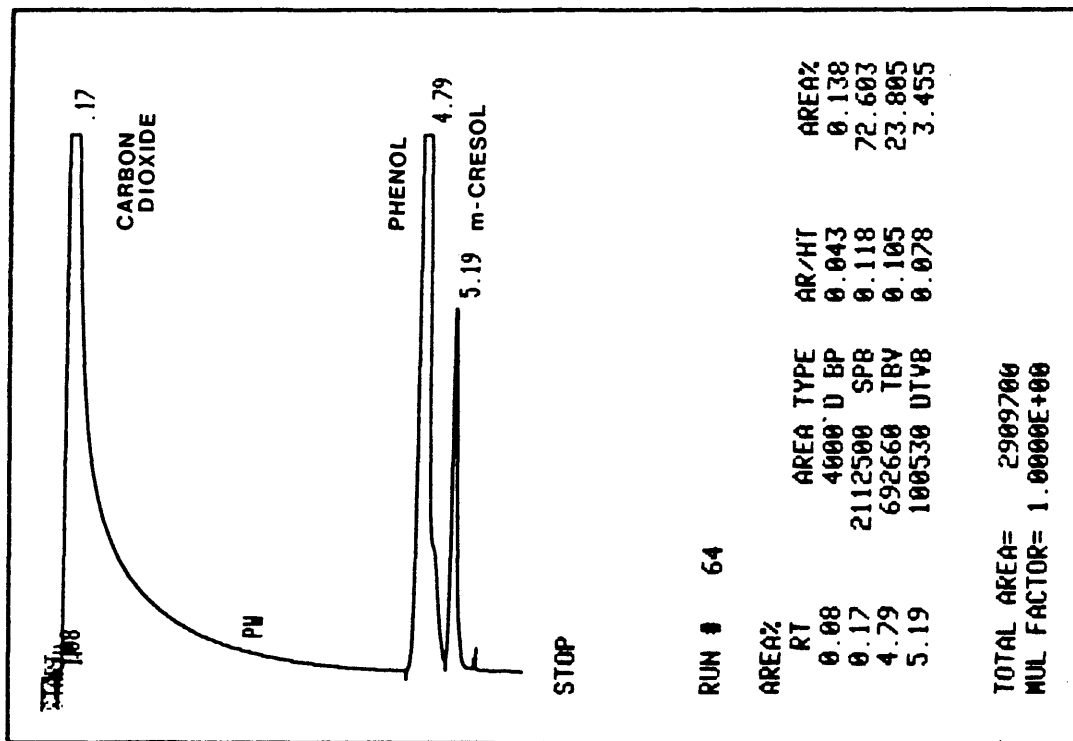
subsequent equilibration period takes about one hour.

#### Sampling of the dense gas

The high pressure sampling valve is normally kept in the inject position (the internal sample volume of the valve in-line with the helium flow), while the recirculating pump is on. The recirculation pump is turned-off prior to sampling. The sample valve lever is then rotated 90 degrees (load position) to allow the dense gas to fill the internal sample volume. The small amount of helium that is introduced into the equilibration system is negligible compared to the total volume of the system. The valve is left in the load position for 30 seconds, before injection into the gas chromatograph. The recirculation pump is restarted while the chromatographic analysis is taking place.

A typical chromatogram is shown in Figure 17. The carbon dioxide is eluted out of the column about 8 seconds after injection. The tailing is characteristic of solvent peaks. The elution time for the solutes depends on the temperature program. The oven temperature program for the gas chromatograph is also shown in the figure. The temperature program was chosen with the following consideration: peak resolution, peak shape, and duration of

Figure 17. Typical gas chromatogram and integrator output



DETECTOR: Thermal conductivity

COLUMN: Methyl silicone (530µm x 5 m)

GC OVEN TEMPERATURE PROGRAM:

Initial Temperature: 40 °C  
 Initial Time : 4.0 min.  
 Rate : 60 °C per min.  
 Final Temperature : 150 °C  
 Final Time : 0.5 min.

the analysis. The HP3390A integrator reports the elution time for each component, the peak area and the area percent (based on the sum of the areas of all the detected peaks).

The chromatographic analysis and subsequent cool-down period takes about 12 minutes. A new sample injection is easily done every 15 minutes. Injections are made until three runs (two of which are consecutive) are reproducible to within 5%.

#### Making another run

After the analysis of the dense gas composition is completed at one pressure, the equilibration system is pressurized with carbon dioxide to the next desired setting. The above procedure is repeated for as many times as required, up to a pressure of 3000 psig.

## EXPERIMENTAL RESULTS AND DISCUSSION

The phenol and m-cresol system in carbon dioxide was chosen as the case study. The experimental runs are summarized in Table 4. Five of the runs were performed at 309 K to study the effect of condensed phase composition on the equilibrium solubility. Two additional runs were performed in the presence of entrainers: acetone and water. The final experimental run was conducted at 318 K. The experimental solubility data are reported in Appendix B.

The reported physical state of the condensed phase was determined by placing an equivalent mixture composition in a sealed flask and heating it to the temperature of interest. The condensed phase compositions exclude the amount of carbon dioxide dissolved in the liquid phase. Sufficient amounts of substrate were added initially to insure that the final condensed phase composition changed by less than 2 %. Therefore, the condensed phases are characterized quantitatively by the ratio of the mole fraction of the substrates, and qualitatively by the phases present in the equilibrium cell.

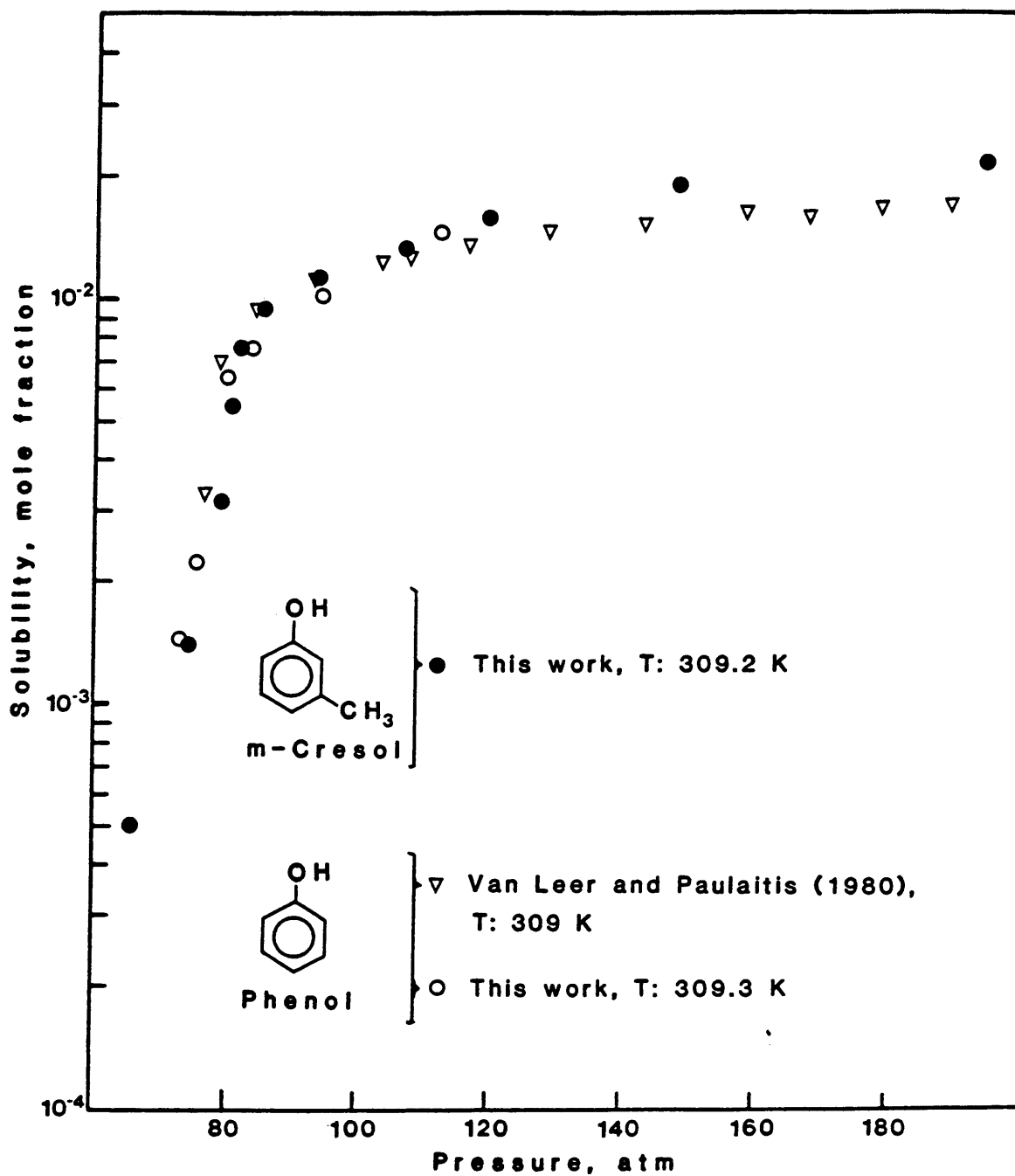
The experimental equilibrium solubility data for pure phenol and pure m-cresol in carbon dioxide at 309 K are shown in Figure 18. Phenol is a solid at 309 K, while m-cresol is a liquid. The contrast in solubility can be

Table 4. Summary of experimental runs for the phenol and m-cresol system in supercritical carbon dioxide

CONDENSED PHASE phenol:m-cresol	phases present	ENTRAINER	T (K)	Figure #	Table #
0 : 100	L - F		309.2	17	B-6
25 : 75	L - F		309.4	18	B-7
50 : 50	L - F		309.3	19	B-8
75 : 25	L - F		309.3	20	B-9
100 : 0	S - F		309.3	17	B-4
50 : 50	L - F	acetone	309.3	28	B-10
50 : 50	L - F	water	309.3	28	B-10
50 : 50	L - F		318.4	29	B-11

Note: 1. The condensed phase composition excludes dissolved carbon dioxide.  
 2. S = solid ; L = liquid ; F = dense gas.

Figure 18. Comparison of experimental solubilities of phenol and m-cresol in supercritical carbon dioxide at 309 K



explained qualitatively by the melting point effect and the volatility of the pure substrate. Phenol melts at a higher temperature than m-cresol, 314.1 and 285.1 K, respectively. Dissolution, like melting, involves overcoming intermolecular forces of a crystal (Krukonis and Kurnik, 1985). Therefore, a higher solubility of m-cresol would be expected. In supercritical extraction, however, the solubility is a strong function of vapor pressure of the solute, i.e. the system temperature (Schmitt and Reid, 1984). The lowest available vapor pressures found in the literature (Perry and Chilton, 1973) are shown in Table 5. These values were fitted to the Antoine equation in order to generate the constants for the equation (Table 5). The predicted vapor pressures for phenol and m-cresol at 309 K are 0.3 and 0.7 torr, respectively. The higher vapor pressure of phenol compensates for its higher melting point, resulting in phenol solubilities approaching those of m-cresol.

#### Effect of condensed phase composition

The experimental solubility of mixtures of m-cresol and phenol in carbon dioxide at 309 K are plotted in Figures 19 to 21. Duplicate runs were performed on the equimolar compositions of phenol and m-cresol (Figure 20). The runs

Table 5. Vapor pressures of phenol, m-cresol and naphthalene (Perry and Chilton, 1973)

COMPOUND	Pressure, torr			A	B	C
	1	5	10			
	Temperature, °C					
phenol	40.1	62.5	73.8	15.7421	3096.41	156.60
m-cresol	52.0	76.0	87.8	18.5621	4692.47	200.80
naphthalene	52.6	74.2	85.8	11.6262	1562.96	81.834

Note:  $\log P = A - B/(t + C)$ , where P is in torr and t is in °C

Table 6. Predicted vapor pressures of phenol, m-cresol and naphthalene

COMPOUND	Temperature, K	
	309	318
	Pressure, torr	
phenol	0.7	1.5
m-cresol	0.3	0.6
naphthalene	0.2	0.5



Figure 19. Experimental solubilities of phenol and m-cresol in supercritical carbon dioxide at 309.4 K. Condensed phase: 25 mole % phenol and 75 mole % m-cresol, excluding dissolved carbon dioxide

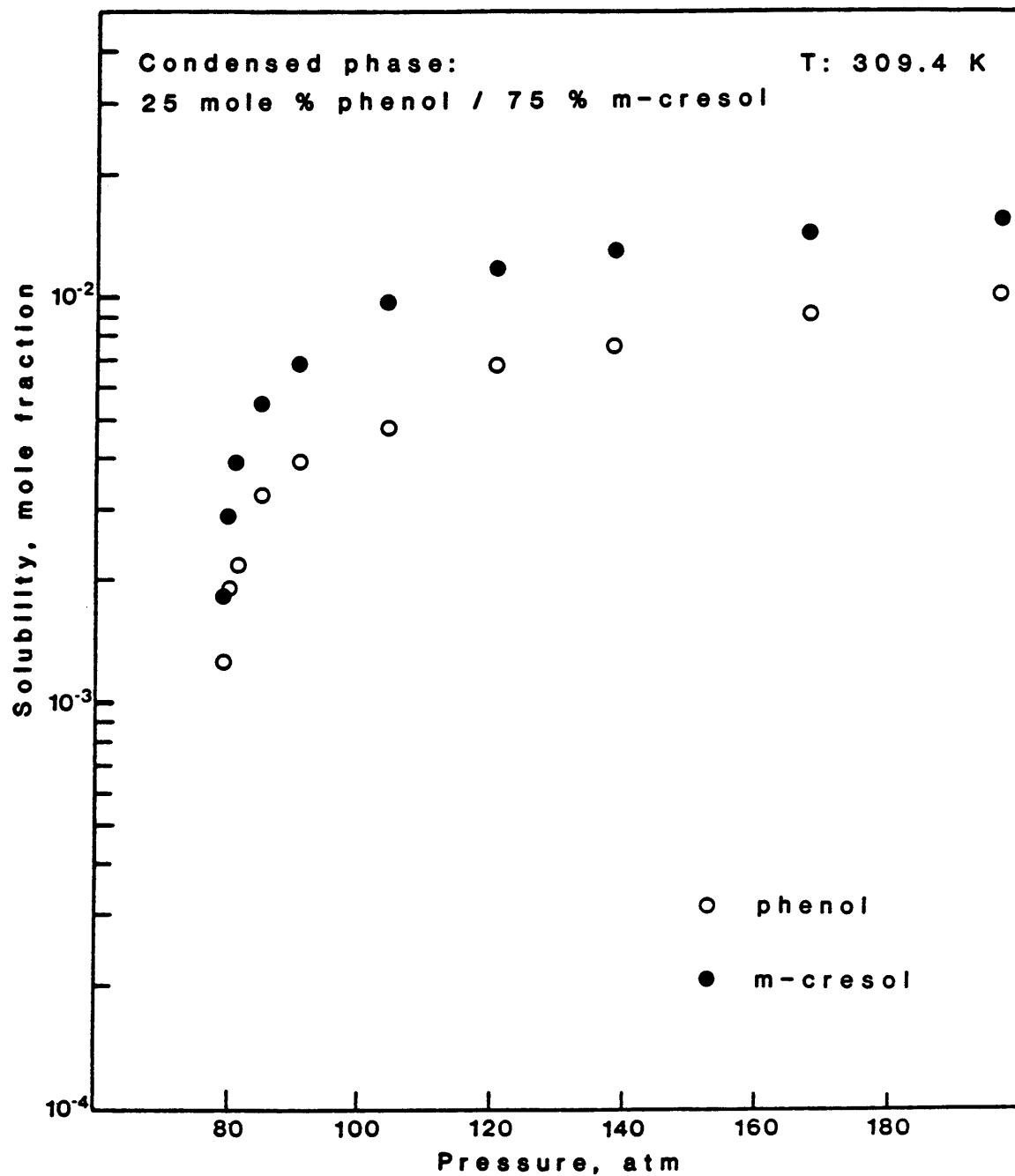


Figure 20. Experimental solubilities of phenol and m-cresol in supercritical carbon dioxide at 309.3 K. Condensed phase: 50 mole % phenol and 50 mole % m-cresol, excluding dissolved carbon dioxide

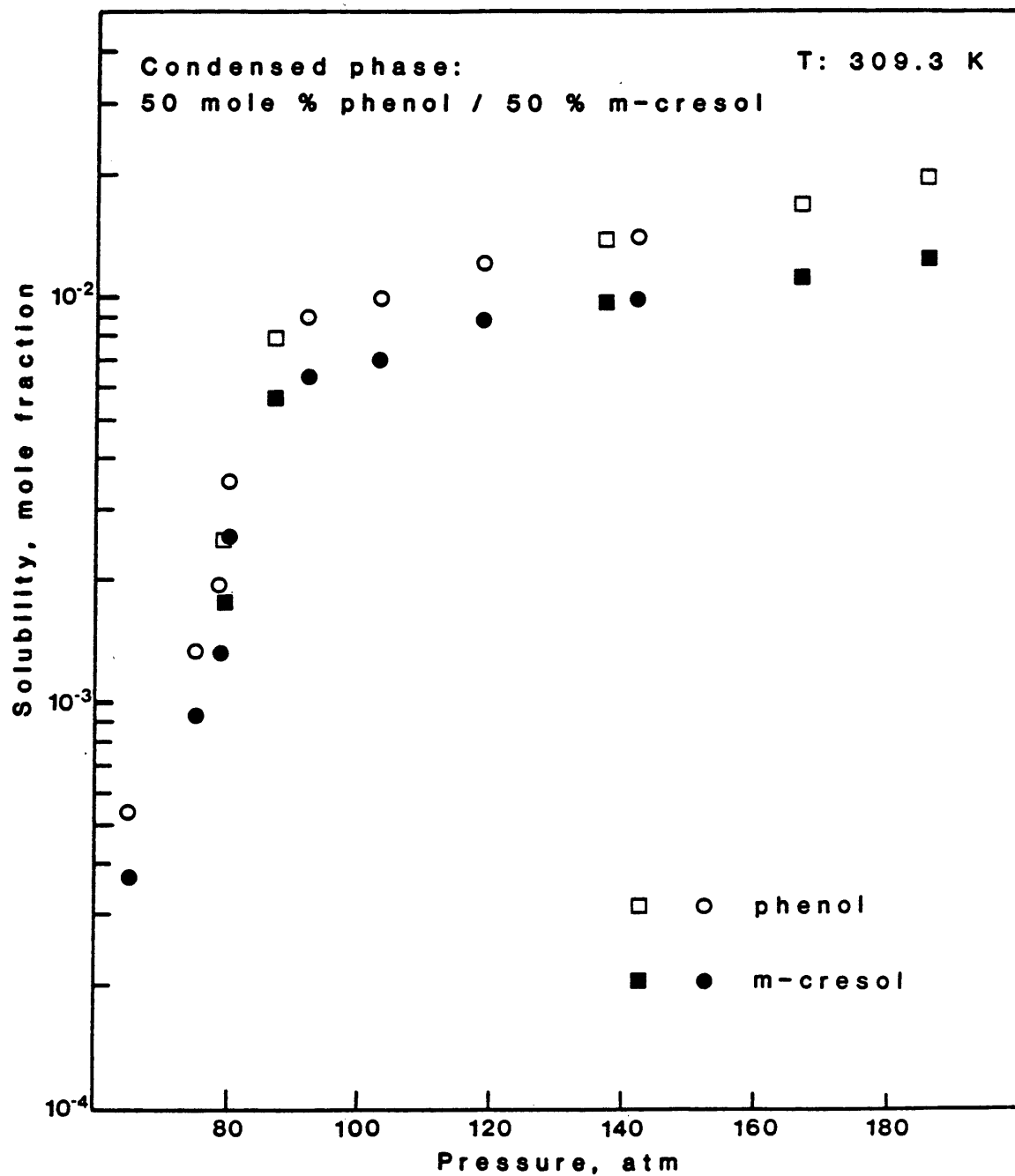
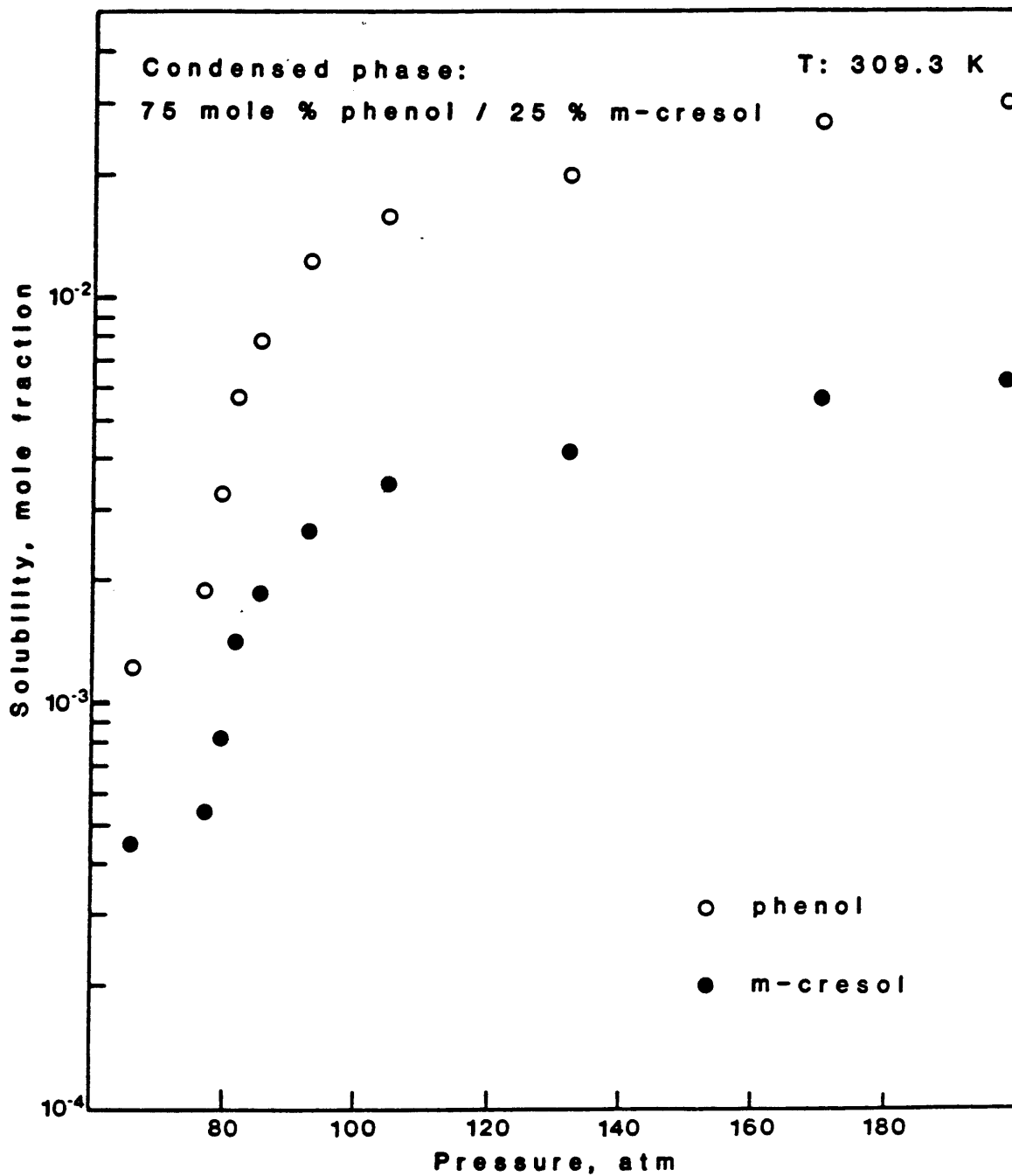


Figure 21. Experimental solubilities of phenol and m-cresol in supercritical carbon dioxide at 309.3 K. Condensed phase: 75 mole % phenol and 25 mole % m-cresol, excluding dissolved carbon dioxide



were conducted one day apart, and a fresh condensed phase mixture was prepared for the second run. The results show good reproducibility, even in the critical region.

The solubilities of m-cresol and phenol are presented separately in Figures 22 and 23, respectively, in order to compare the effects of condensed phase composition. The experimental data were not plotted so that the presentation may be simplified. Figure 22 shows that the solubility of m-cresol in the ternary system decreases as its composition in the condensed phase decreases from the pure component (binary system). On the other hand, Figure 23 shows that the solubility of phenol is enhanced with respect to the phenol-carbon dioxide system, by the addition of m-cresol in amounts exceeding the equimolar concentration. This may be attributed to an entrainer effect. The presence of m-cresol in the condensed phase may be disrupting the crystal lattice of phenol by decreasing hydrogen bonding. In addition, m-cresol may hydrogen bond with phenol in the dense gas phase thereby increasing the solubility. Note that the mixture of 75 mole % phenol and 25 % m-cresol is in the liquid state at 309 K. It has been noted by other researchers (Gopal, et al., 1985; Brunner, 1983; Brunner and Peter, 1982) that the solubility in the dense gas phase is enhanced with an increase in solubility of the dense gas in

Figure 22. Comparison of solubilities of m-cresol in supercritical carbon dioxide at 309.3 K, for various condensed phase compositions of phenol and m-cresol

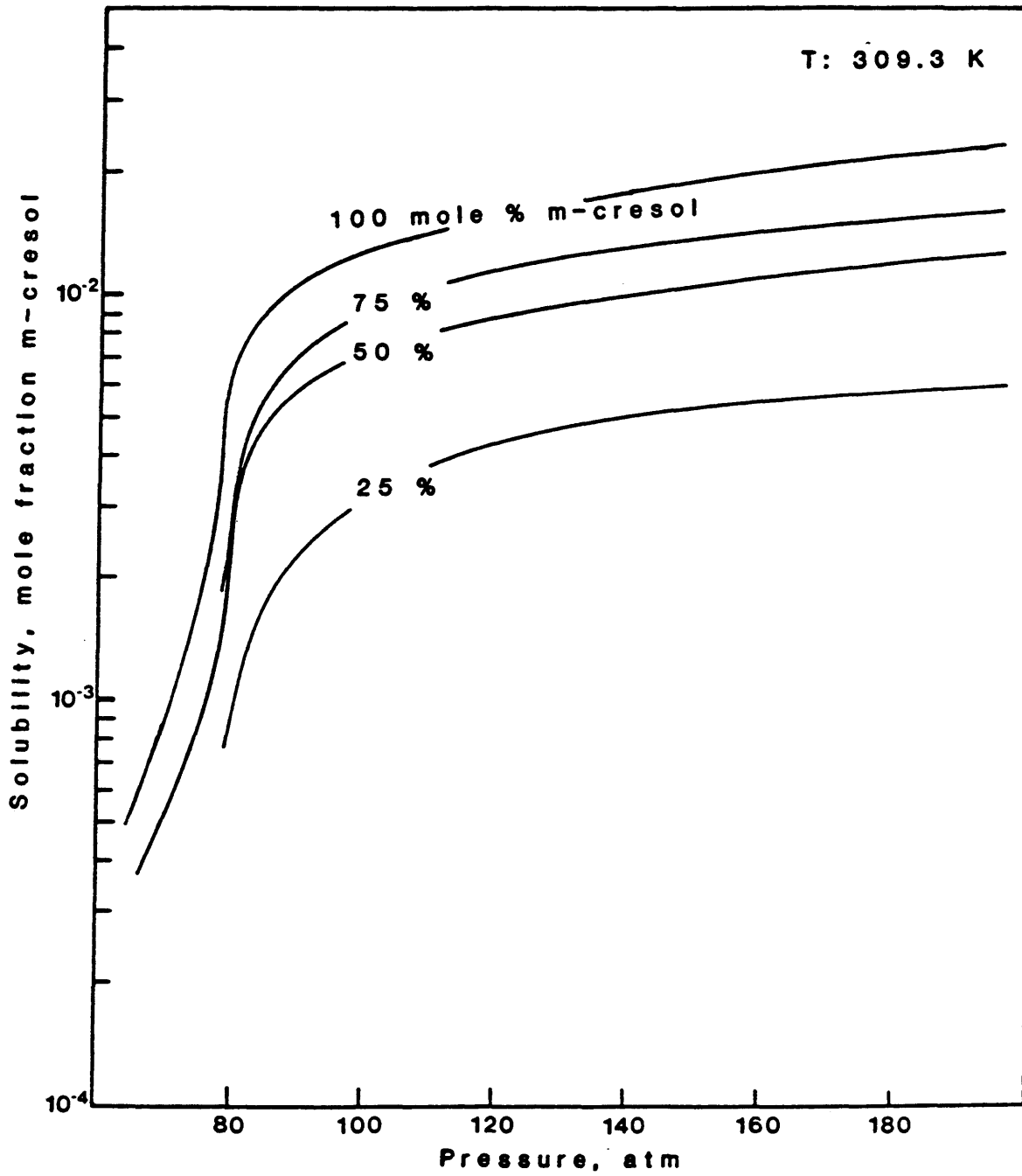
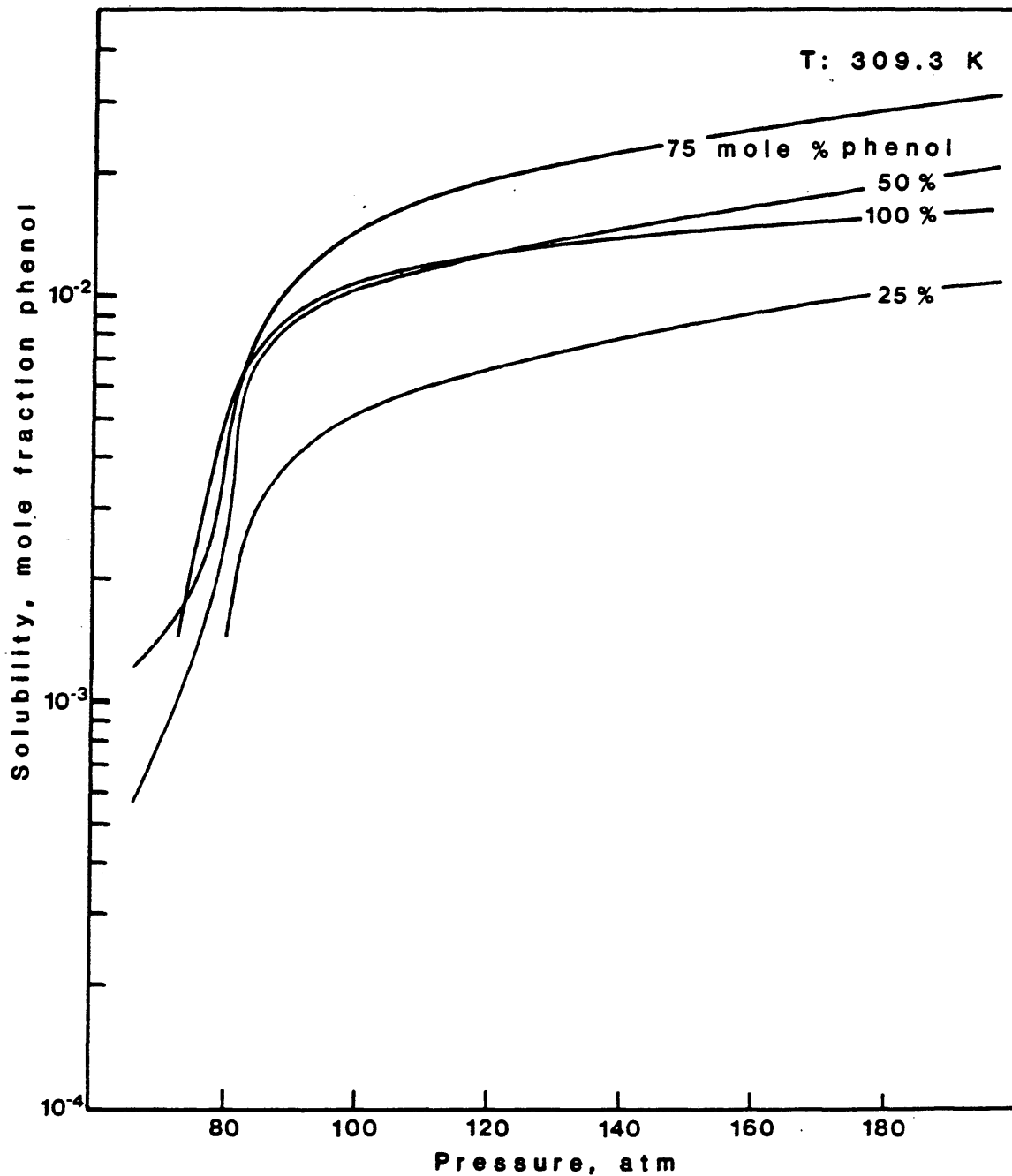


Figure 23. Comparison of solubilities of phenol in supercritical carbon dioxide at 309.3 K, for various condensed phase compositions of phenol and m-cresol



the liquid phase.

The solubility enhancement by the addition of a second solute at low concentration has been observed in isomer and solid mixtures (Chang and Morrell, 1985; Kurnik and Reid, 1982), and in the presence of entrainers (Van Alsten and Eckert, 1985; Brunner and Peter, 1982).

The above results may be better illustrated by presenting the solubilities as a function of reduced solvent density (Johnston and Eckert, 1981; Schmitt and Reid, 1984). The reduced density is based on the density of pure carbon dioxide at the system pressure and temperature, and the critical density of carbon dioxide ( 0.01063 gmole/ml ). This is a good approximation for dilute systems. Tsekhanskaya, et al. (1964) measured the molar volumes of saturated solutions of naphthalene in ethylene and carbon dioxide, and found them to differ by 1 to 5 % from those of pure ethylene and carbon dioxide, respectively.

Schmitt and Reid (1984) suggested the modification of the solubility parameter, i.e. mole fraction of solute in the SCF, with an enhancement factor, E, defined as:

$$E = y/(P_{\text{vap}}/P) \quad (1)$$

where  $y$  is the equilibrium mole fraction of the solute,  $P_{\text{vap}}$  is the vapor pressure of the pure solute at the system

temperature, and  $P$  is the system pressure. The enhancement factor represents the ratio of the actual mole fraction of the solute in the supercritical fluid to the ideal solubility, i.e. a correction factor.

The calculated enhancement factors for each solute at different condensed phase compositions are presented in Appendix B. The vapor pressures of the pure solute at system temperature were extrapolated from values found in the literature (Table 6). The accuracy of these vapor pressures is not important since they are used only to compare systems at the same temperature. The results are presented in graphical form in Figures 24 and 25. The calculated enhancement factors were omitted in order to simplify the figures. The plots are more linear than for the case where pressure coordinates are used, and the curves intersect less frequently.

The dashed lines in Figures 24 and 25 represent regions where no experimental data were obtained. The plots show a linear behavior away from the critical region. However, inflection points were observed at the critical region. This behavior may be explained in terms of the fugacity coefficient in the high pressure gas mixture and the partial molar volume of the solute in the supercritical fluid as follows. The fundamental equations relating the solubility



Figure 24. Comparison of enhancement factors of m-cresol in supercritical carbon dioxide for various condensed phase compositions of phenol and m-cresol

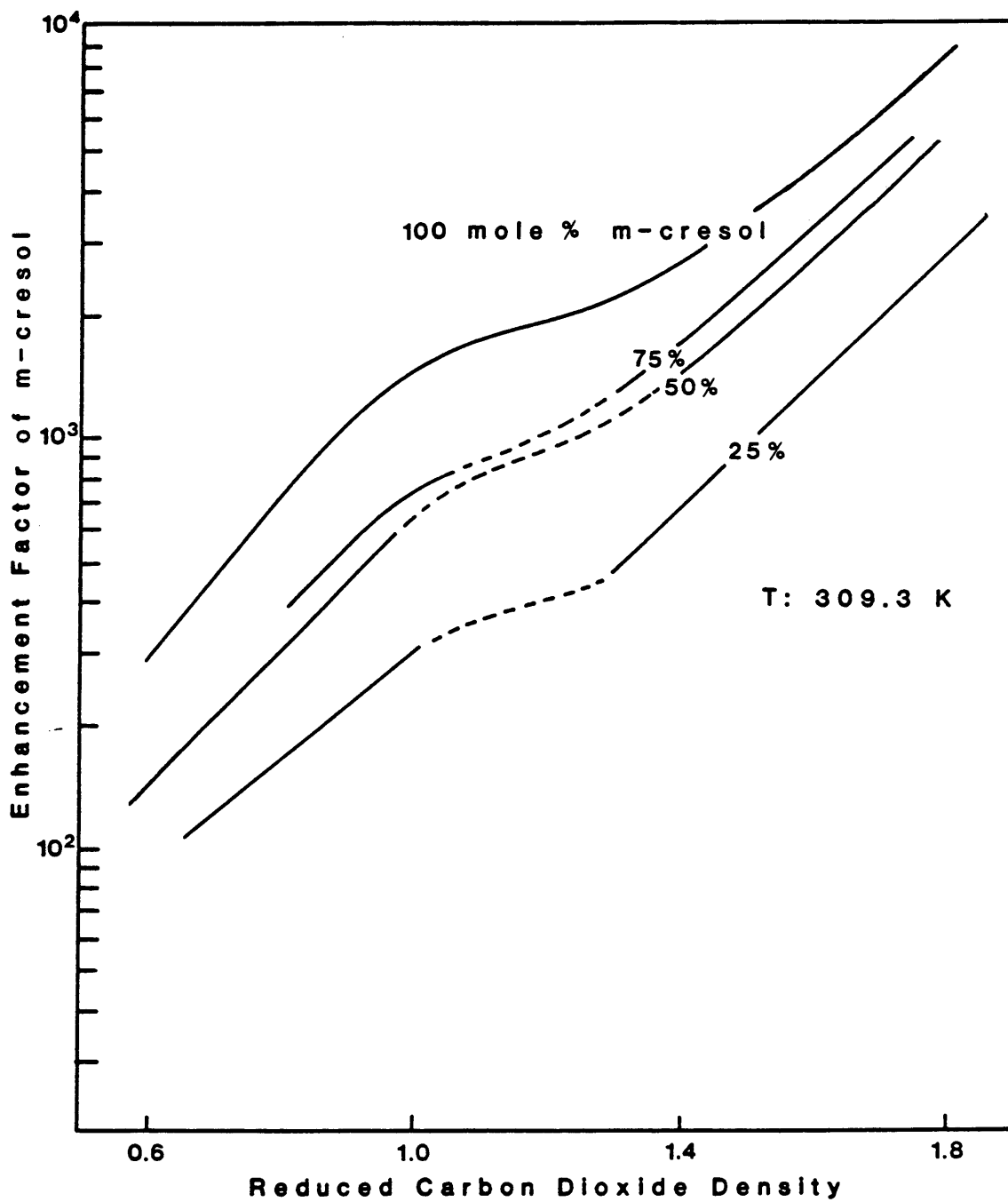
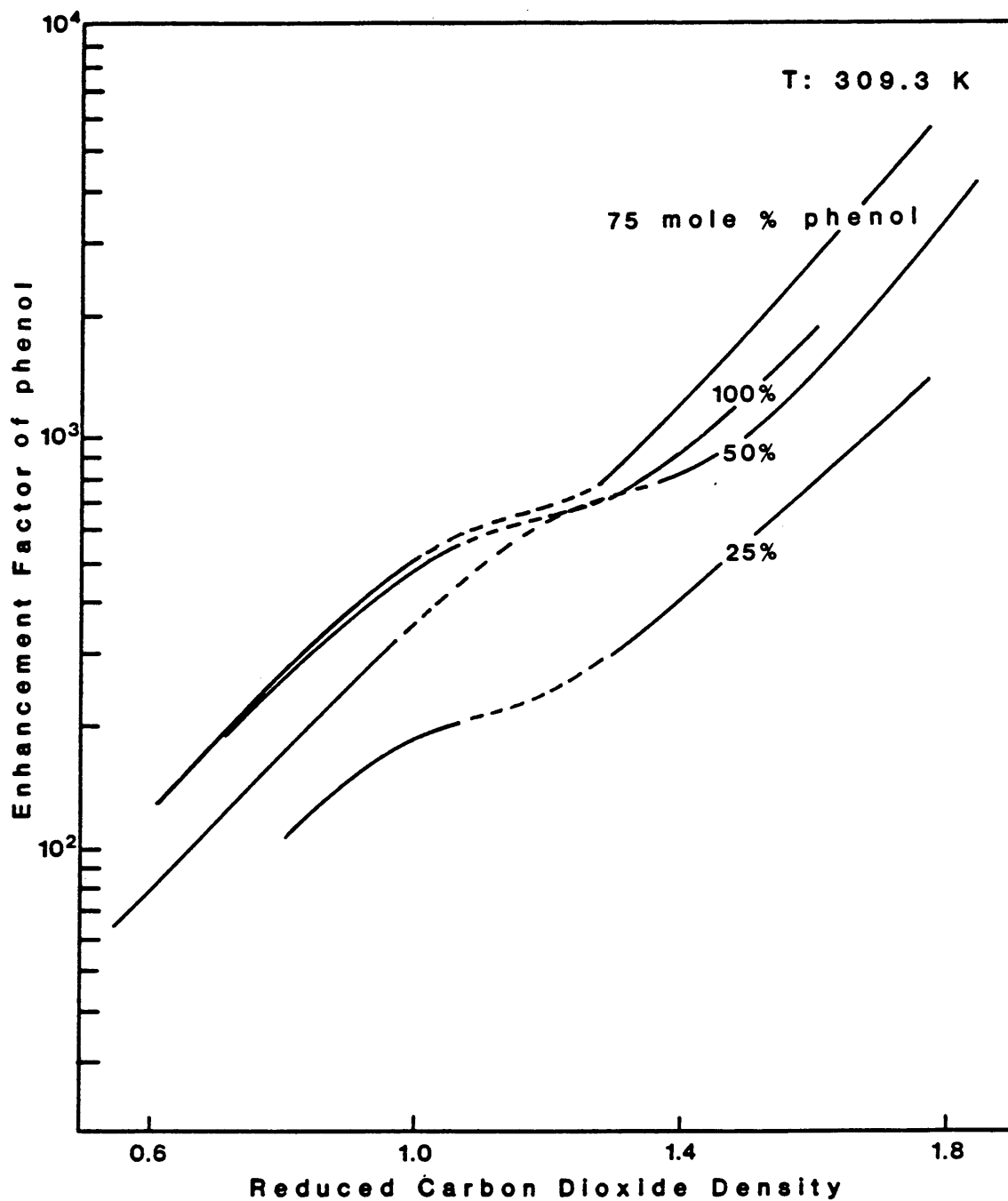


Figure 25. Comparison of enhancement factors of phenol in supercritical carbon dioxide for various condensed phase compositions of phenol and m-cresol



of a pure solid or a pure liquid in a compressed gas were derived by Prausnitz (1969). Let 1 stand for the gaseous solvent (SCF) and 2 for the heavy solute in the gas phase:

$$\text{For a solid: } y_2 = \left( \frac{P_2^S}{P} \right) \left( \frac{\phi_2^S}{\phi_2} \right) \exp \int_{P_2^S}^P \frac{v_2^S dP}{RT} \quad (2)$$

where  $\phi_2^S$  is the fugacity coefficient at saturation pressure  $P_2^S$ ,  $v_2^S$  is the solid molar volume at temperature  $T$ , and  $\phi_2$  is the vapor-phase fugacity coefficient.

$$\text{For a liquid: } y_2 = \left( \frac{P_2^S}{P} \right) \left( \frac{\phi_2^S}{\phi_2} \right) (1-x_1) \exp \int_{P_2^S}^P \frac{v_2^L dP}{RT} \quad (3)$$

where  $x_1$  is the mole fraction of the gaseous solvent in the liquid phase,  $\phi_2^S$  is the fugacity coefficient at saturation pressure  $P_2^S$ ,  $v_2^L$  is the liquid molar volume at temperature  $T$ , and  $\phi_2$  is the vapor-phase fugacity coefficient of component 2 in the gaseous phase.

Substitution of equation (1) into equations (2) and (3) and solving for the enhancement factor, yield the following expressions:

$$\text{For a solid: } E = \frac{\phi_2^S}{\phi_2} \exp \int_{P_2^S}^P \frac{v_2^S dP}{RT} \quad (4)$$

$$\text{For a liquid: } E = (1-x_1) \frac{\phi_2^S}{\phi_2} \exp \int_{P_2^S}^P \frac{v_2^L dP}{RT} \quad (5)$$

The enhancement factor for a pure solid in compressed gases contains three correction terms (Prausnitz, 1969): (1)  $\phi_2^S$ , which represents the nonideality of the pure saturated vapor; (2) the Poynting correction, which accounts for the effect of pressure on the fugacity of the pure solid; and (3)  $\phi_2$ , which accounts for the nonideality of the solute in the compressed gas mixture. The enhancement factor for a pure liquid in compressed gases has an additional term,  $(1-x_1)$ , which takes into account the solubility of the SCF in the liquid phase.

Of the correction terms mentioned above, the vapor-phase fugacity coefficient in the SCF is by far the most significant (Prausnitz, 1969). Consequently, the enhancement factor may be described as being inversely proportional to the vapor-phase fugacity coefficient:

$$E \propto \frac{1}{\phi_2} \quad (6)$$

The vapor-phase fugacity coefficient may be calculated using volumetric data (e.g. equation of state) and the following expression (provided that the volumetric data is in volume-explicit form):

$$\ln \phi_2 = \frac{1}{RT} \int_0^P \left( \bar{v}_2 - \frac{RT}{P} \right) dP \quad (7)$$

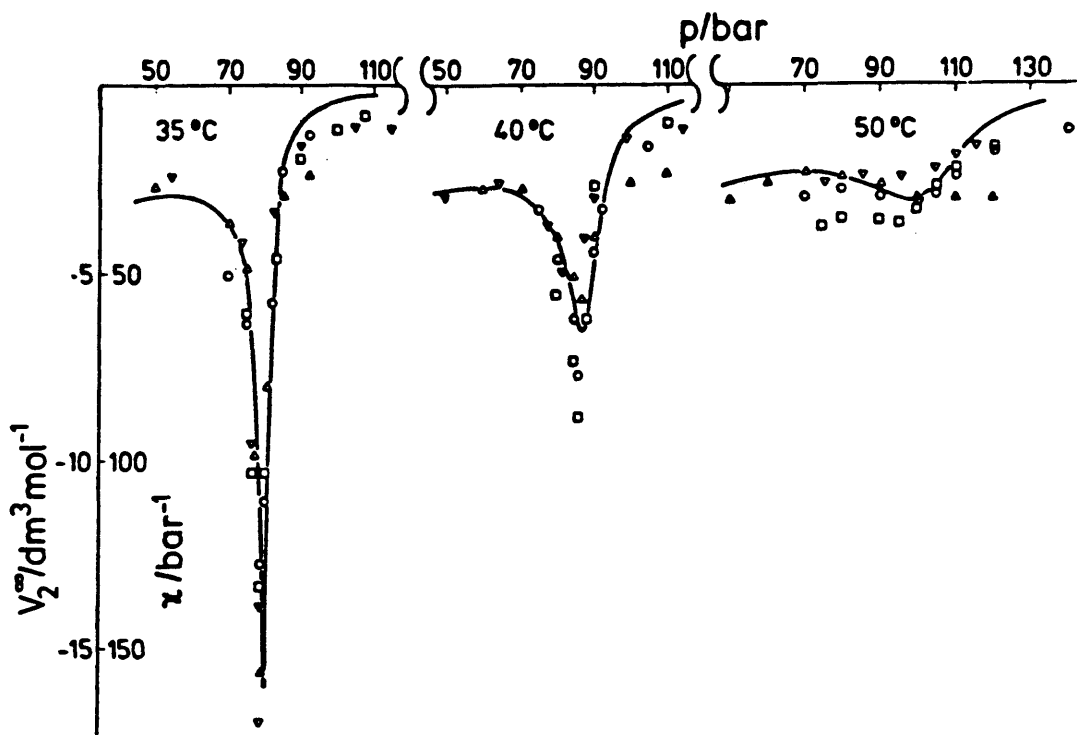
where  $\bar{v}_2$  is the partial molar volume of solute 2 in the SCF.

Van Wasen and Schneider (1980) showed that the partial molar volume of naphthalene and fluorene at infinite dilution in supercritical carbon dioxide tends to negative infinity when approaching the critical point of the solvent (See Figure 25).

In order to explain the inflection points observed in Figures 23 and 24, the following assumptions were made: (1) the enhancement factors for each solute in a ternary system are inversely proportional to their respective vapor-phase fugacity coefficients; and (2) the partial molar volume of each solute in a ternary system tends to negative infinity when approaching the critical point of the SCF. It is shown in Appendix C that the second order partial derivative of the enhancement factor with respect to the system pressure (at constant temperature) does not exist at the critical point of the SCF. Furthermore, at constant temperature and volume, the density of the dense gas mixture is proportional to the system pressure. These results indicate the existence of a point of inflection in a plot of

Figure 26. Experimental partial molar volumes of naphthalene and fluorene at infinite dilution in supercritical carbon dioxide (Van Wasen and Schneider, 1980)

Partial molar volumes  $V_2^\infty$  of naphthalene and fluorene at infinite dilution in supercritical carbon dioxide [( $\nabla$ ) naphthalene, stationary phase Perisorb A; ( $\Delta$ ) naphthalene, stationary phase Perisorb RP 8; ( $\square$ ) fluorene, stationary phase Perisorb A; ( $\circ$ ) fluorene, stationary phase Perisorb RP 8; (—) isothermal compressibility  $\kappa$  of pure  $\text{CO}_2$  (from ref 4)].



enhancement factor as a function of reduced density. Such an inflection point would be located at the critical point of the dense gas mixture, which may vary from the critical point of the pure solvent.

Figure 27 shows the selectivity of the supercritical extraction as a function of pressure for different condensed phase compositions. The selectivity for the dense gas phase is defined as the ratio of the solubility of phenol with respect to the solubility of m-cresol. On the other hand, the selectivity in the condensed phase is just the ratio of the mole fraction of phenol with respect to m-cresol. The selectivities in the condensed phase were constant throughout the experimental pressure range of each run, and are denoted by the solid lines. Each run suggests that the dense gas phase was richer in phenol with respect to the condensed phase at system pressures higher than 75 atm. This may be illustrated by a plot of solubility in carbon dioxide as function of condensed phase composition at 105 atm and 309 K (Figure 28). The result of interest is the higher solubility of phenol at a condensed phase composition of 75 mole % phenol, with respect to pure phenol in carbon dioxide. The results suggest a maximum solubility of phenol in the ternary system at 309 K for a pressure range of 75 to 200 atm.

Figure 27. Effect of condensed phase composition and pressure on selectivity in the phenol, m-cresol and carbon dioxide system at 309.3 K

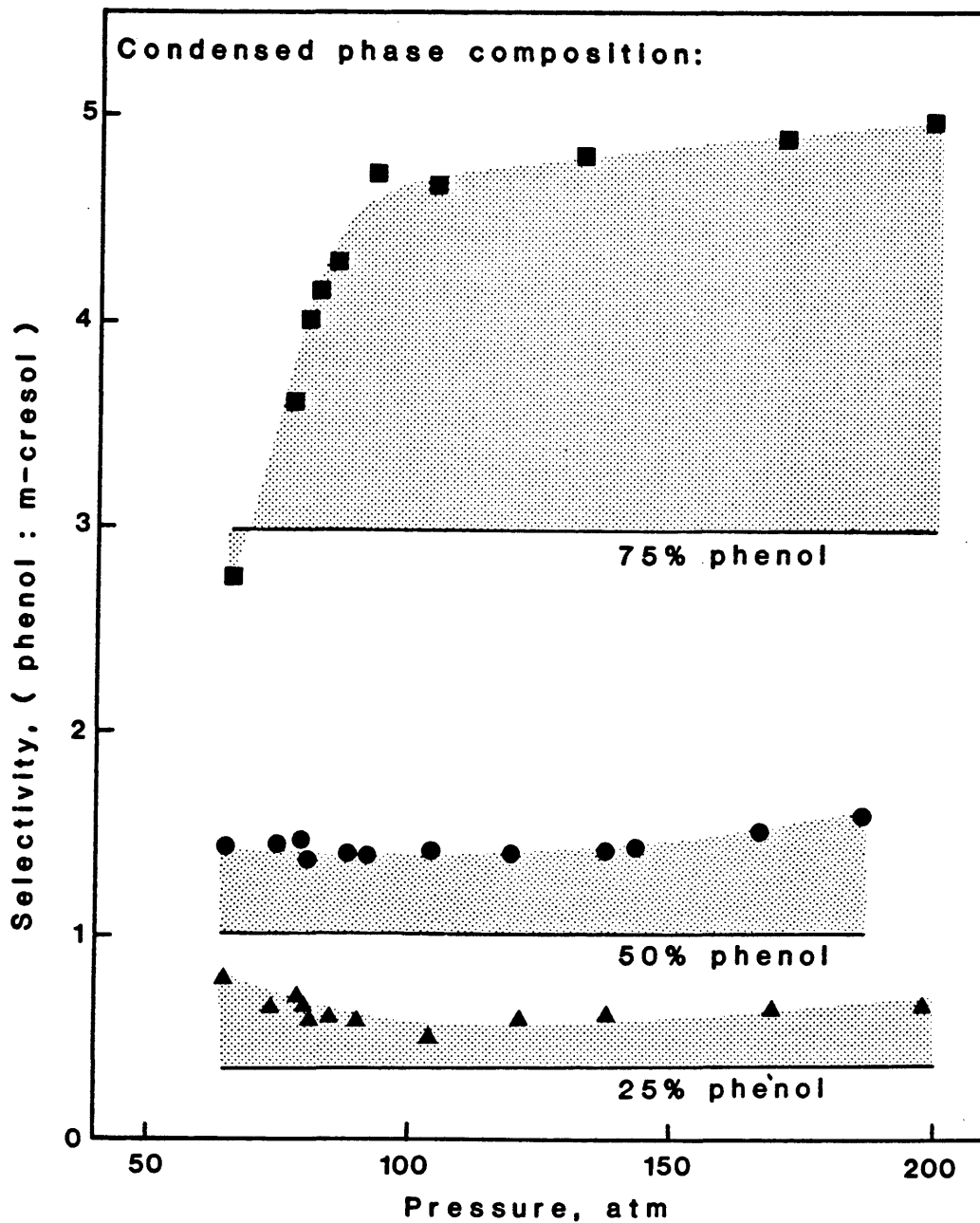
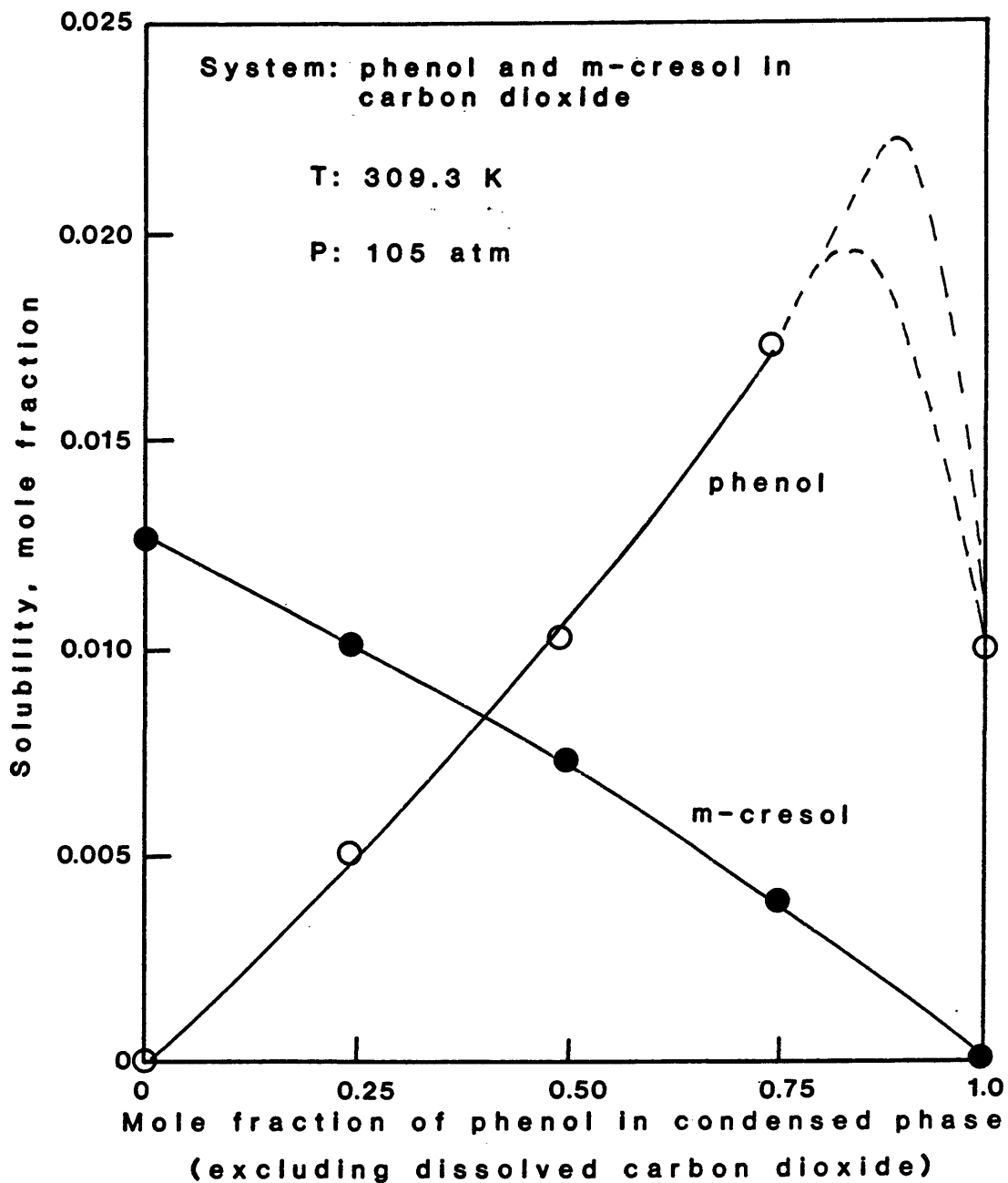




Figure 28. Experimental solubilities for phenol and m-cresol mixtures in supercritical carbon dioxide at 309.3 K and 105 atm



Attempts were made to locate and quantify the magnitude of the predicted maxima in Figure 28, but several problems were encountered during the experiments. The procedure of melting and mixing the condensed phase prior to loading did not work for mixtures containing more than 85 mole % phenol. Even though the mixtures were liquid at 309 K and atmospheric pressure, a system pressure above 80 atm resulted in the formation of an additional solid phase (a three phase system). The crystallization was indicated by a sudden increase in system temperature (up to 2 degrees change), and the subsequent cessation of the recirculation flow.

A different procedure was devised to avoid the above problem. The mixture of phenol and m-cresol was melted and allowed to crystallize in a mortar, and later pulverized with a pestle. Enough glass wool was placed inside the equilibrium cell to cover the ring sparger. The crystals were loaded into the cell and the subsequent steps described in the EXPERIMENTAL PROCEDURE section were followed. The system was pressurized above 85 atm before heating it to the desired temperature of 309 K. This step allowed the solid phase to settle above the glass wool, while the liquid phase flowed down to the bottom of the cell. Experimental runs were conducted for condensed phase compositions of 85 and 90

mole % phenol. The results suggested that the maxima is located between condensed phase compositions of 75 and 85 mole % phenol. However, the data for the above two runs were not reported in this study because it was considered that more tests should be conducted to validate the abovementioned procedure.

#### Effect of entrainers

Figure 29 shows that there was no significant effect by adding either water or acetone to the ternary system at 309 K. The entrainers were mixed with the liquid phase (50 mole % phenol) at the start of each experiment. The amount added (less than 4 g) was such that the entrainer concentration in the dense gas phase would be less than 5 mole % (assuming complete evaporation) throughout the pressure range studied.

#### Effect of system temperature

Figure 30 compares the solubilities of m-cresol and phenol (condensed phase: 50 mole % phenol) at 309 and 318 K. The expected region of retrograde solubility is attributed to dependence of the solvent density on temperature. There is not a significant difference in solubilities at pressures between 140 and 200 atm.

Figure 29. Comparison of experimental solubilities of phenol and m-cresol in supercritical carbon dioxide at 309.3 K, with acetone or water as entrainers. Condensed phase: 50 mole % phenol and 50 mole % m-cresol, excluding dissolved carbon dioxide

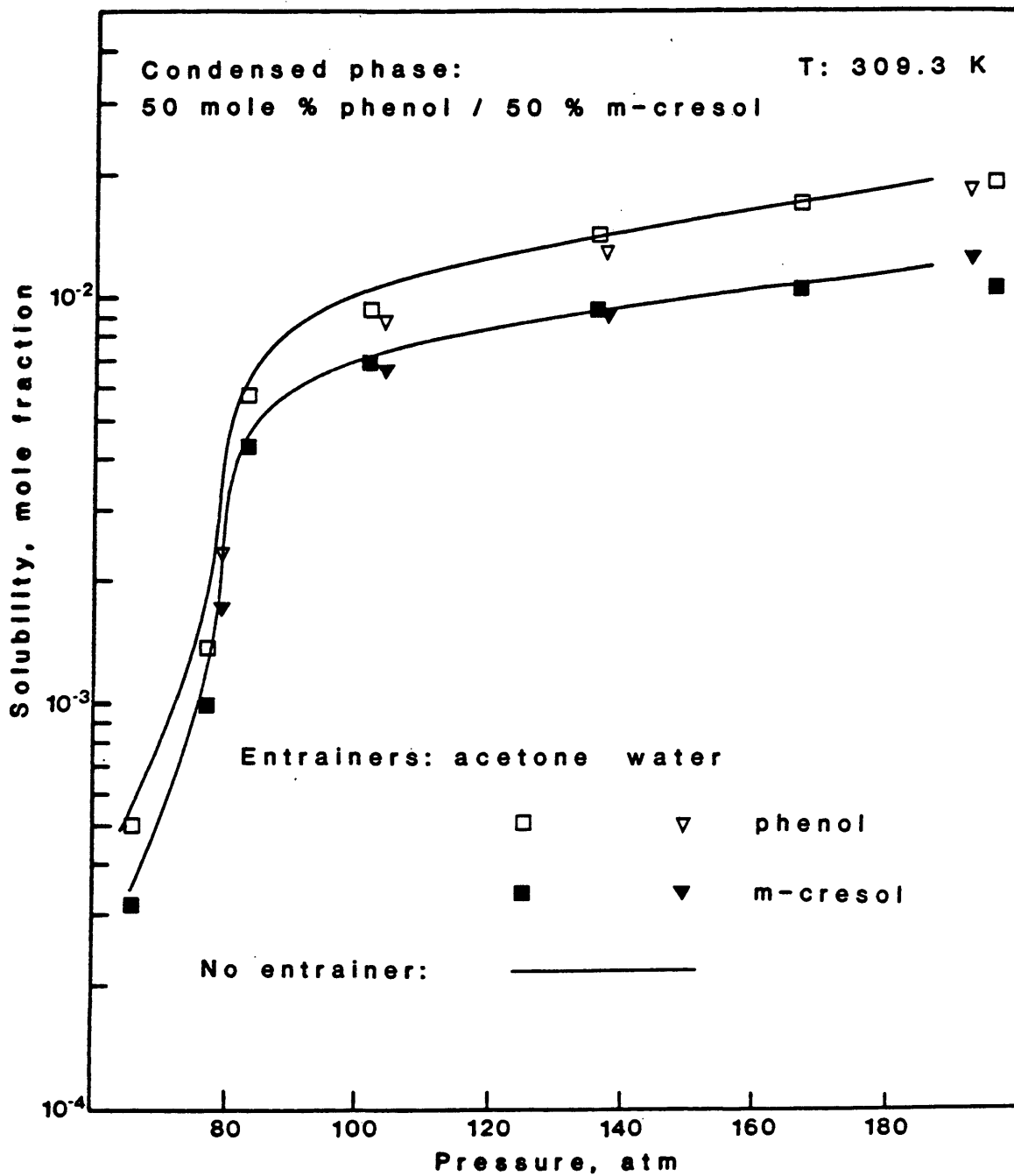
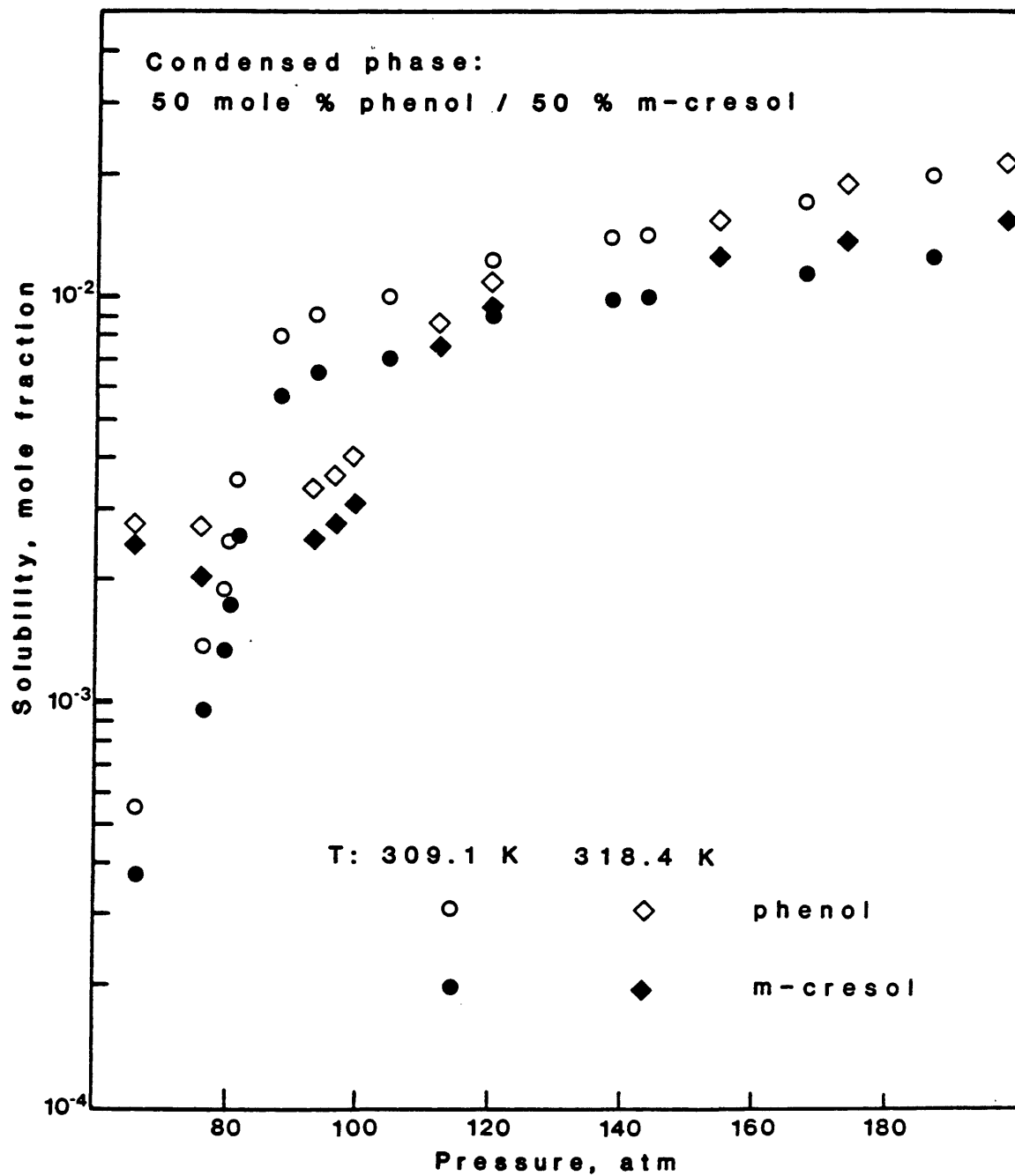
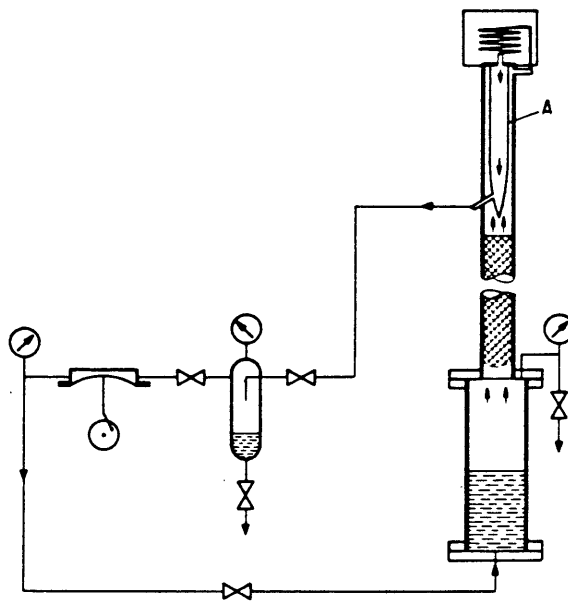


Figure 30. Comparison of experimental solubilities of phenol and m-cresol in supercritical carbon dioxide at 309.1 and 318.4 K. Condensed phase: 50 mole % phenol and 50 mole % m-cresol, excluding dissolved carbon dioxide



The above results suggest the possibility of applying the fractional distraction technique described by Zosel (1980). Figure 31 shows the schematic diagram for the apparatus. A column and heated finger may be added to the existing experimental equipment to test the feasibility of the technique. The equipment may be operated at a pressure within the retrograde region. Condensation on the tip of the finger would generate a reflux stream, thereby taking advantage of the increase in the solubility of phenol in the presence of m-cresol.

Figure 31. Schematic diagram of an apparatus for fractional distraction. A: variable temperature finger. (Zosel, 1978)



## CONCLUSIONS

The following conclusions were drawn from this study:

1. An experimental apparatus was successfully tested to measure the solubilities of pure organic compounds and mixtures in supercritical fluids. The equipment is ideal to study the critical region, where the solvent density is very sensitive to pressure and temperature fluctuations.
2. The experimental technique offers a quick screening method to evaluate the solvent properties of different fluids, or the potential application of supercritical fluid extraction to solid or liquid mixtures. The chromatographic analysis provides the relative solubilities of the solutes in terms of peak area %.
3. The solubility of phenol in supercritical carbon dioxide is enhanced with respect to the pure phenol-carbon dioxide system, by the addition of m-cresol at condensed phase compositions of 50 to 75 mole % phenol (excluding dissolved carbon dioxide). This enhancement reaches a maximum at a condensed phase composition between 75 and 100 mole % phenol.
4. The observed inflection point in a plot of enhancement factor as a function of reduced density is due to the



convergence to negative infinity of the partial molar volume of the solute in SCF as the critical point of the SCF is approached.

5. No significant effect was observed by adding either water or acetone to an equimolar condensed phase mixture of phenol and m-cresol in supercritical carbon dioxide at 309 K.

## RECOMMENDATIONS

## 1. Experimental apparatus

The addition of a Jerguson gage will help monitor any phase changes that might take place during the experimental runs. The Jerguson gage can be placed in parallel to the Autoclave pressure vessel, or could be used to replace the autoclave vessel altogether.

Further tests with a different gas chromatograph column or a multi-column system should be conducted to improve the peak shape of carbon dioxide. The 5 m methyl silicone column provides good separation between phenol, m-cresol and naphthalene; but carbon dioxide is eluted as a solvent peak, which is the major contribution for the uncertainty of the GC analysis.

## 2. Future studies

Experimental runs should be conducted for condensed phase compositions between 75 and 100 mole % phenol (phenol, m-cresol and carbon dioxide system) to determine the extent and conditions at which the maximum solubility difference between phenol and m-cresol will occur.

The experimental data obtained in this study should be used in the correlation for ternary systems proposed by DeBeer (1985). The use of theoretical correlations will

provide a stronger basis for further experimental work.

Experimental runs with other supercritical fluids such as ammonia or nitrogen might prove interesting. Furthermore, the use of mixed solvents and entrainers have been shown by other researchers to enhance the solubilities and selectivities over those of pure supercritical fluids.

## REFERENCES CITED

- Brunner, G. and S. Peter, "On the solubility of glycerides and fatty acids in compressed gases in the presence of an entrainer". *Sep. Sci. Technol.*, 17: 199-214 (1982).
- Brunner, G. and S. Peter, "State of the art extraction with compressed gases (gas extraction)". *Ger. Chem. Eng.* 5: 181-195 (1982).
- Brunner, G., "Selectivity of supercritical compounds and entrainers with respect to model substances". *Fluid Phase Equil.*, 10: 289-298 (1983).
- Chang, H. and D.G. Morrell, "Solubilities of Methoxy-1-tetralone and methyl nitrobenzoate isomers and their mixtures in supercritical carbon dioxide". *J. Chem. Eng. Data*, 30: 74-78 (1985).
- Clonts, K.E. and R.A. McKetta, "Cresols and Cresylic Acids", in J.J. McKetta and W.A. Cunningham, eds., Encyclopedia of Chemical Processing and Design, 13: 212-227, Marcel Dekker, Inc., New York, 1981.
- DeBeer, S.W., "The prediction of solubility differences between phenol and the isomers of cresol with an augmented Van Der Waals equation of state", M. Sc. thesis. Colorado School of Mines, Chemical Engineering and Petroleum Refining Dept., Golden, Colorado (1985).
- Dorau, W., H.W. Kremer, and H. Knapp, "An apparatus for the investigation of low-temperature, high-pressure, vapor-liquid and vapor-liquid-liquid equilibria". *Fluid Phase Equilib.*, 11: 83-89 (1983).
- Ely, J.F., and J.K. Baker, "A review of supercritical fluid extraction". NBS Technical Note 1070 (1983).
- Gopal, J.S., G.D. Holder, and E. Kosal, "Solubility of solid and liquid mixtures in supercritical carbon dioxide". *Ind. Eng. Chem. Process Des. Dev.*, 24: 697-701 (1985).
- Holman, J.P., Experimental Methods for Engineers, McGraw-Hill, New York (1971).

- I.U.P.A.C, International Thermodynamic Tables of the fluid state: carbon dioxide. Edited by Angus, S., B. Armstrong, and K.M. de Reuck, Pergamon Press (1973).
- Joshi, D.K., and J.M. Prausnitz, "Supercritical fluid extraction with mixed solvents". *AIChE Journal*, 30: 522-525 (1984).
- King, M.B., and T.R. Bott, "Problems associated with the development of gas extraction and similar processes". *Sep. Sci. Technol.*, 17: 119-150 (1982).
- Kline, S.J., and F.A. McClintock, "Describing Uncertainties in Single-sample Experiments". *Mech Eng*, pg 3 (1953).
- Konrad, R., I. Swaid, and G.M. Schneider, "High-pressure phase studies on fluid mixtures of low-volatile organic substances with supercritical carbon dioxide". *Fluid Phase Equilib.*, 10: 307-314 (1983).
- Krukonis, V.J., and R.T. Kurnik, "Solubility of solid aromatic isomers in carbon dioxide". *J. Chem. Eng. Data*, 30: 247-249 (1985).
- Kurnik, R.T., and R.C. Reid, "Solubility of solid mixtures in supercritical fluids". *Fluid Phase Equilib.*, 8: 93-105 (1982).
- McNeil, D., "Cresols" in A. Standen, ed., Kirk-Othmer Encyclopedia of Chemical Technology, 6: 434-444, 2nd ed., Interscience Publishers, a division of John Wiley & Sons, Inc., New York, 1965.
- Monge, A., and J.M. Prausnitz, "An experimental technique for determining solubilities of complex liquid mixtures in dense gases". *Ind. Eng. Chem. Fundam.*, 22: 505-506 (1983).
- Morris, W.O., "The perturbed-soft-chain theory equation of state and vapor-liquid equilibria in mixtures containing carbon dioxide, toluene, and 1-methyl naphthalene". M.Sc. thesis. The Johns Hopkins University, Chemical Engineering Dept., Baltimore, Maryland (1984).
- Perry, R.H. and C.H. Chilton, Chemical Engineers' Handbook, 5th ed., McGraw-Hill Book Co, NY (1973).

- Panagiotopoulos, A.Z., and R.C. Reid, "High-pressure phase equilibria in ternary fluid mixtures with a supercritical component". Paper presented in Symposium on chemistry and processing of supercritical fluids at Chicago, IL, September 8-13, 1985. ACS, Division of Fuel Chemistry. 30(3): 46-56 (1985).
- Prausnitz, J.M., Molecular Thermodynamics of Fluid-Phase Equilibria, Prentice-Hall, NJ (1969).
- Radosz, M., "Variable-volume circulation apparatus for measuring high-pressure fluid-phase equilibria". Ber. Bunsenges. Phys. Chem., 88: 859-862 (1984).
- Schmitt, W.J., and R.C. Reid, "The influence of the solvent gas on solubility and selectivity in supercritical extraction". Paper presented at the annual meeting of the AIChE, San Francisco, CA, Nov. 25-30, 1984.
- Smith, R.D., and H.R. Udseth, "Direct mass spectrometric analysis of supercritical fluid extraction products". Sep. Sci. Technol., 18: 245-252 (1983).
- Stahl, E., W. Schilz, E. Schutz, and E. Willing, "A quick method for the microanalytical evaluation of the dissolving power of supercritical gases". Angew. Chem. Int. Ed. Engl., 17: 731-738 (1978).
- Sunol, A.K., "Supercritical extraction of coal", Ph.D. Dissertation, Virginia Polytechnic Institute and State University, 1982.
- Sunol, A.K., B. Hagh and S. Chen, "Entrainer selection in supercritical extraction" in J.M.L. Penninger, M. Radosz, M.A. McHugh and V.J. Krukoni, eds., Supercritical Fluid Technology, pp 451 - 464, Elsevier Science Publishers B.V., Amsterdam, 1985.
- Swaid, I., D. Nickel, and G.M. Schneider, "NIR-Spectroscopic investigations on phase behaviour of low-volatile organic substances in supercritical carbon dioxide". Fluid Phase Equilib., 21: 95-112 (1985).
- Tiffin, D.L., G. Guzman, K.D. Lurks and J.P. Kohn, "Phase equilibria behavior of the ternary systems carbon dioxide, trans-decalin, n-eicosane and carbon dioxide, trans-decalin methyl-naphthalene. J. Chem. Data, 23: 203-206, 1978.

- Tsekhanskaya, Y.V., M.B. Iomtev, and E.V. Mushkina, "Solubility of diphenylamine and naphthalene in carbon dioxide under pressure". Russ. J. Phys. Chem. (Engl. Transl.), 36: 1177-1181 (1962).
- Tsekhanskaya, Y.V., M.B. Iomtev, and E.V. Mushkina, "Solubility of naphthalene in ethylene and carbon dioxide under pressure". Russ. J. Phys. Chem. (Engl. Transl.), 38: 1173-1176 (1964).
- Van Alsten, J.G., and C.A. Eckert, "Mixed supercritical solvents for selective solubility enhancement". Paper presented in the Symposium on chemistry and processing supercritical fluids at Chicago, IL, on Sep. 8-13, 1985. ACS, Division of Fuel Chemistry, 30(3): 13-15.
- Van Leer, R.A., and M.E. Paulaitis, "Solubilities of phenol and chlorinated phenols in supercritical carbon dioxide". J. Chem. Eng. Data, 25: 257-259 (1980).
- Van Wasen, U., and G.M. Schneider, "Partial molar volumes of naphthalene and fluorene at infinite dilution in carbon dioxide near its critical point". J. Phys. Chem., 84: 229-230 (1980).
- Wise, W.S., "Solvent extraction of coal". Chemistry and Industry (London), July 18, 1970.
- Zosel, K., "Separation with supercritical gases: practical applications". Angew. Chem. Int. Ed. Engl., 17: 702-709 (1978).

APPENDIX A  
GAS CHROMATOGRAPH CALIBRATION DATA



Table A-1. Pure component calibration equations

RANGE	b	c	d	e
CARBON DIOXIDE				
3	-9.898 x 10 <sup>-6</sup>	2.1515 x 10 <sup>-12</sup>	0	0
5	-2.175 x 10 <sup>-5</sup>	1.4564 x 10 <sup>-11</sup>	0	0
7	0	2.8688 x 10 <sup>-11</sup>	6.3638 x 10 <sup>-19</sup>	0
PHENOL				
3	1.929 x 10 <sup>-10</sup>	4.2880 x 10 <sup>-14</sup>	0	0
5	1.716 x 10 <sup>-9</sup>	1.6411 x 10 <sup>-13</sup>	0	0
7	0	6.2665 x 10 <sup>-13</sup>	1.7577 x 10 <sup>-19</sup>	0
m-CRESOL				
3	-1.186 x 10 <sup>-10</sup>	4.0633 x 10 <sup>-14</sup>	0	0
5	1.007 x 10 <sup>-9</sup>	1.4323 x 10 <sup>-13</sup>	0	0
7	0	5.8117 x 10 <sup>-13</sup>	-8.5300 x 10 <sup>-20</sup>	4.8395 x 10 <sup>-25</sup>
NAPHTHALENE				
3	-1.146 x 10 <sup>-10</sup>	3.3809 x 10 <sup>-14</sup>	0	0
5	1.763 x 10 <sup>-10</sup>	1.2929 x 10 <sup>-13</sup>	0	0
7	0	4.4769 x 10 <sup>-13</sup>	3.0507 x 10 <sup>-19</sup>	7.6818 x 10 <sup>-25</sup>

Note:  $M = b + (c * A) + (d * A^2) + (e * A^3)$

where A is the peak area, and M is the number of moles

Figure A-1. Calibration curve for carbon dioxide, TCD range 3

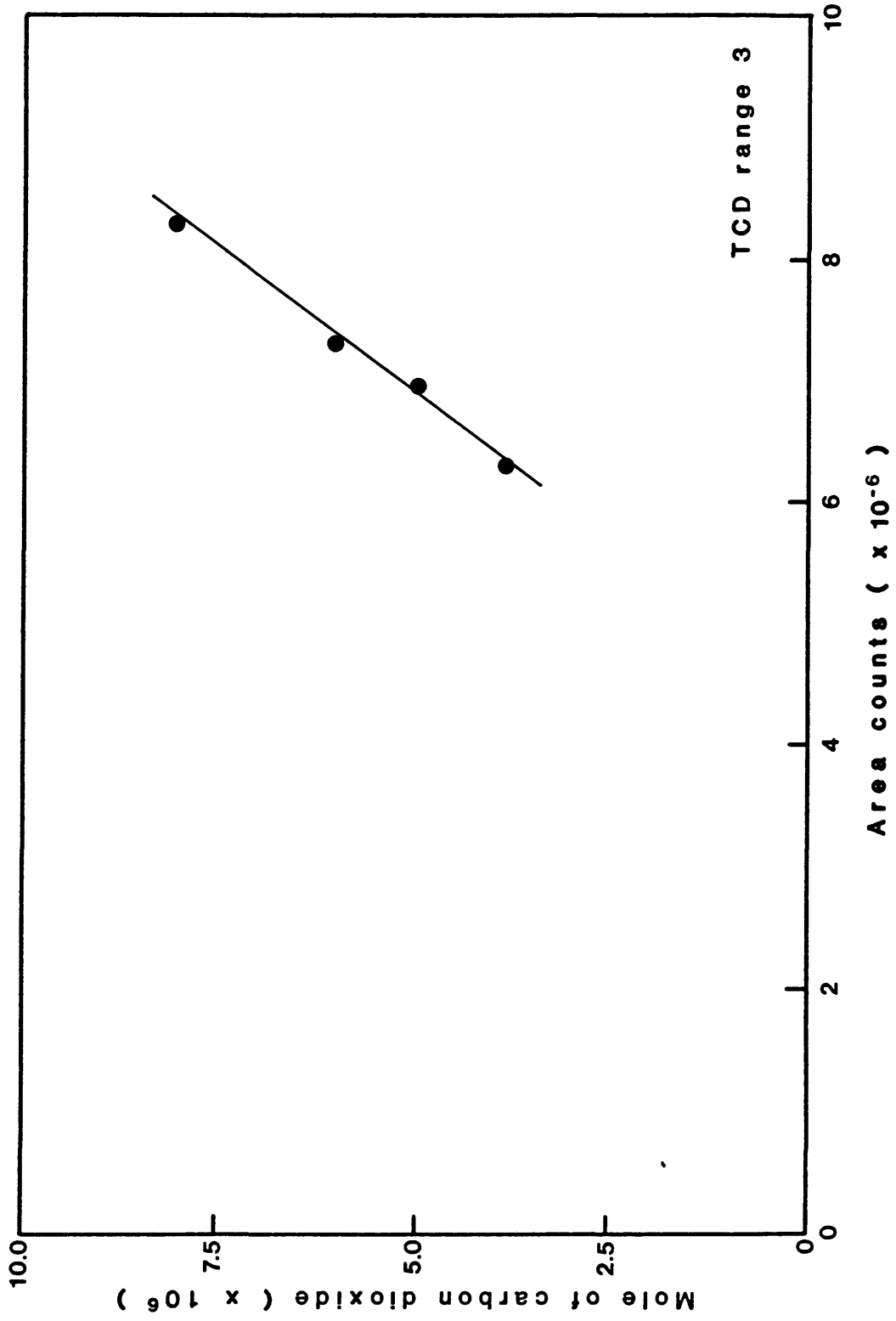


Figure A-2. Calibration curves for phenol, m-cresol and naphthalene, TCD range 3

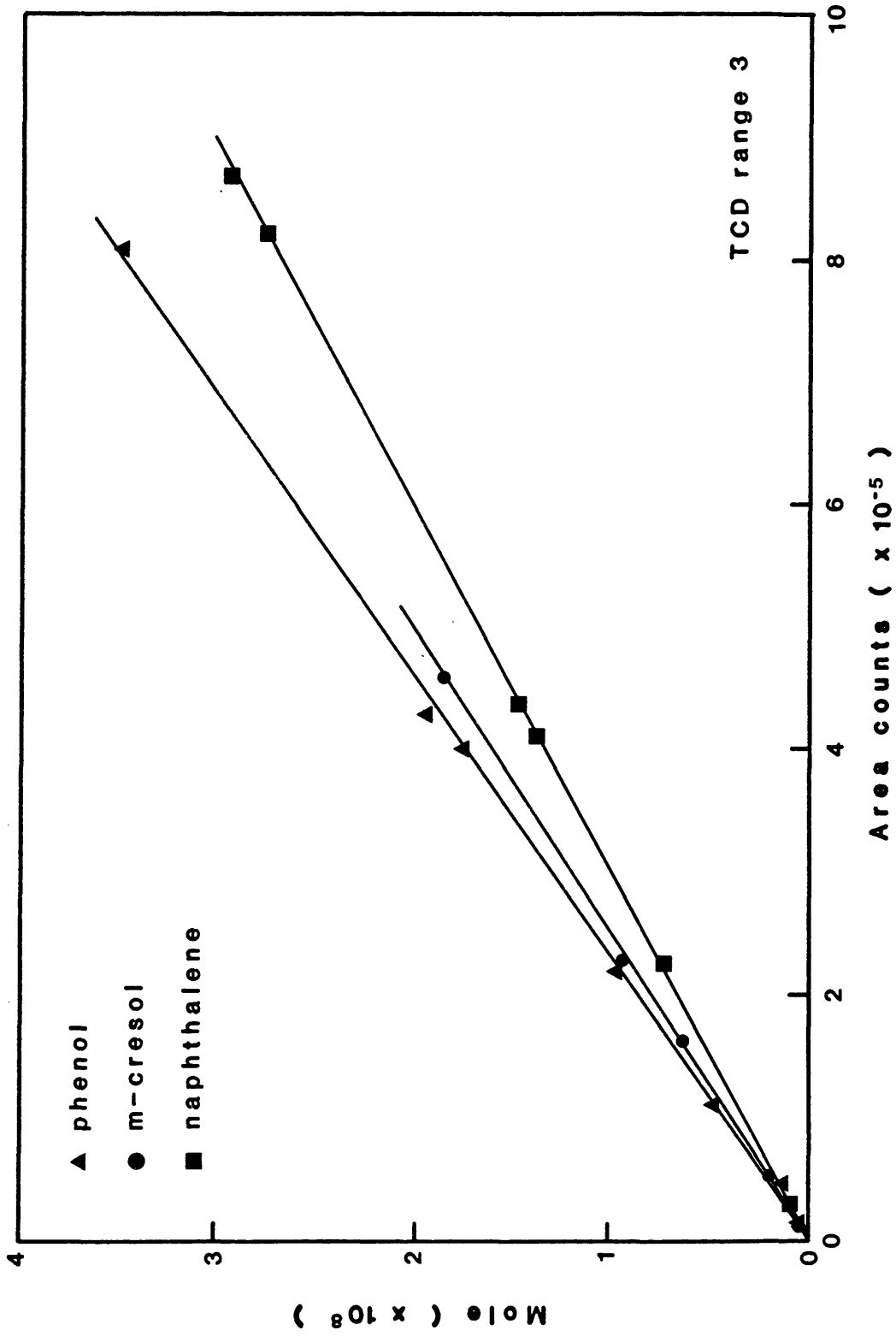


Figure A-3. Calibration curve for carbon dioxide, TCD range 5

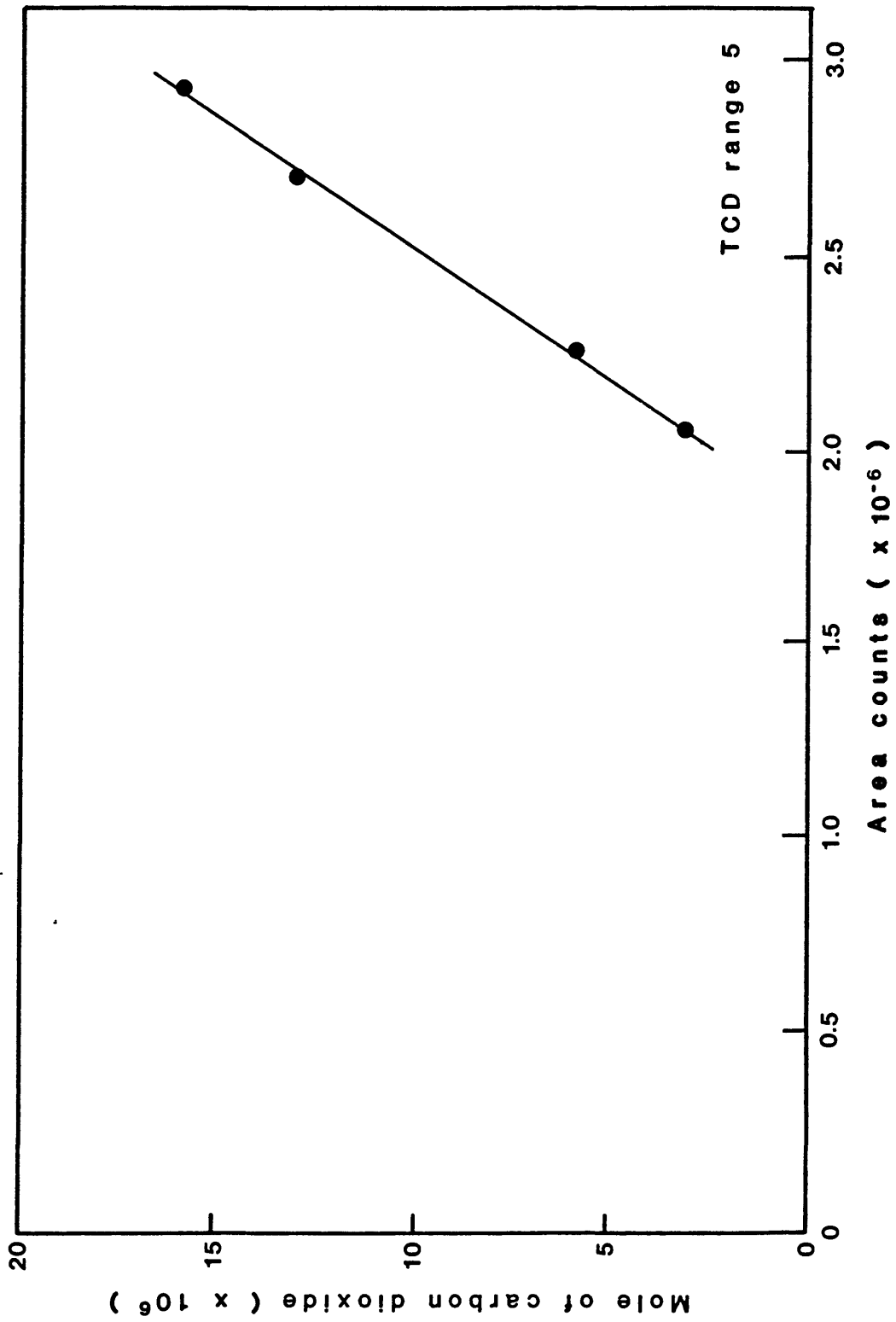


Figure A-4. Calibration curves for phenol, m-cresol and naphthalene, TCD range 5

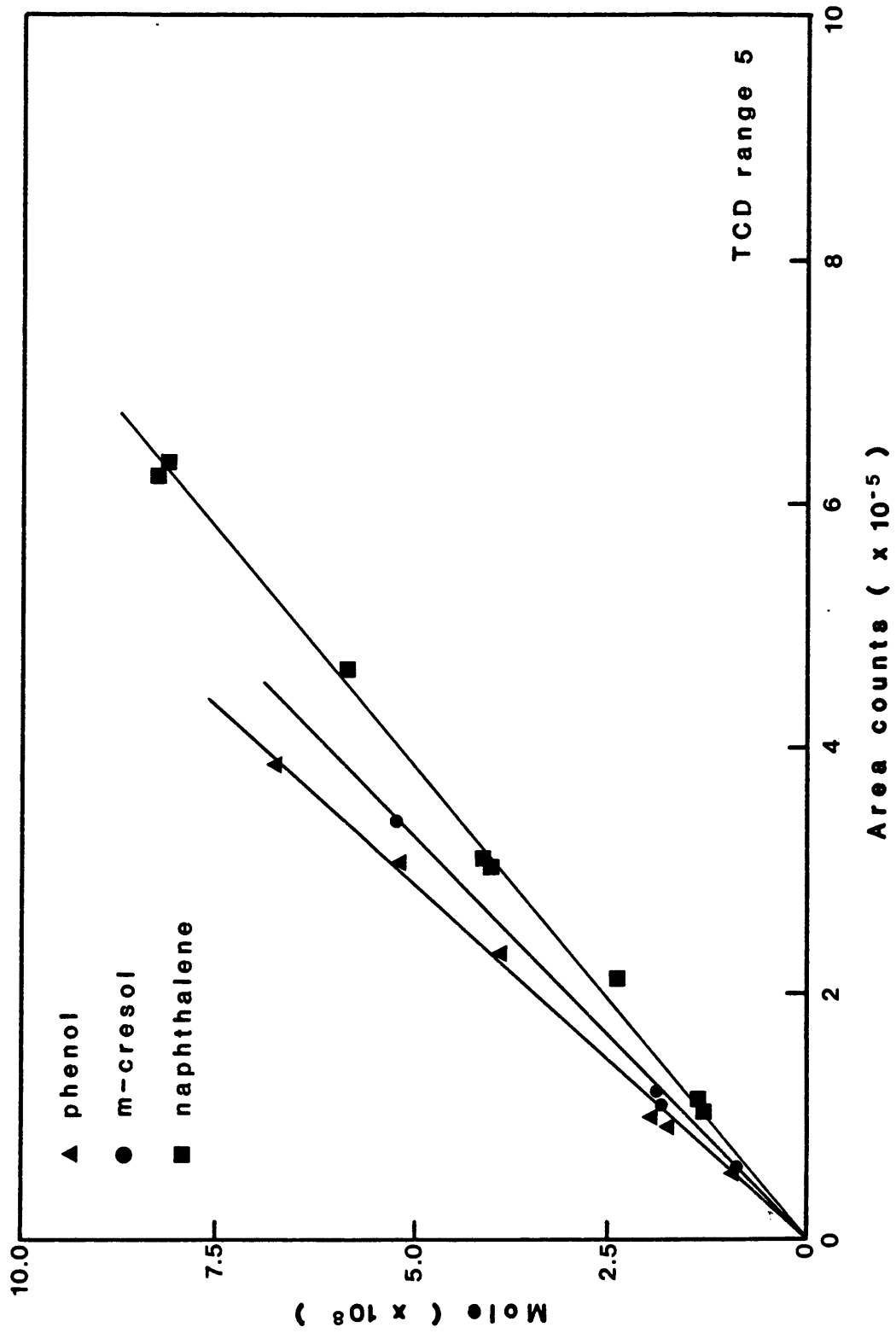


Figure A-5. Calibration curve for carbon dioxide, TCD range 7

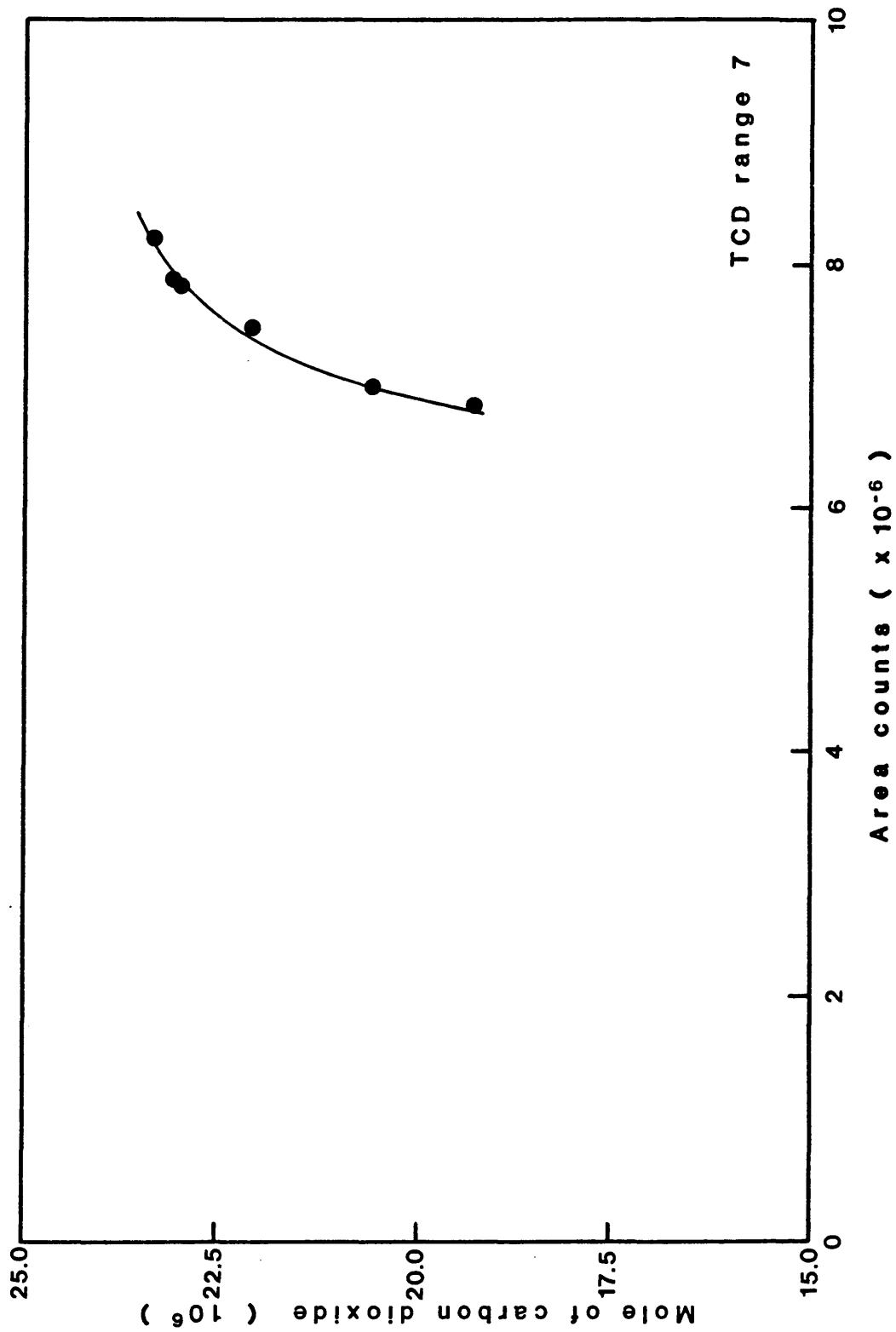


Figure A-6. Calibration curve for phenol, TCD range 7

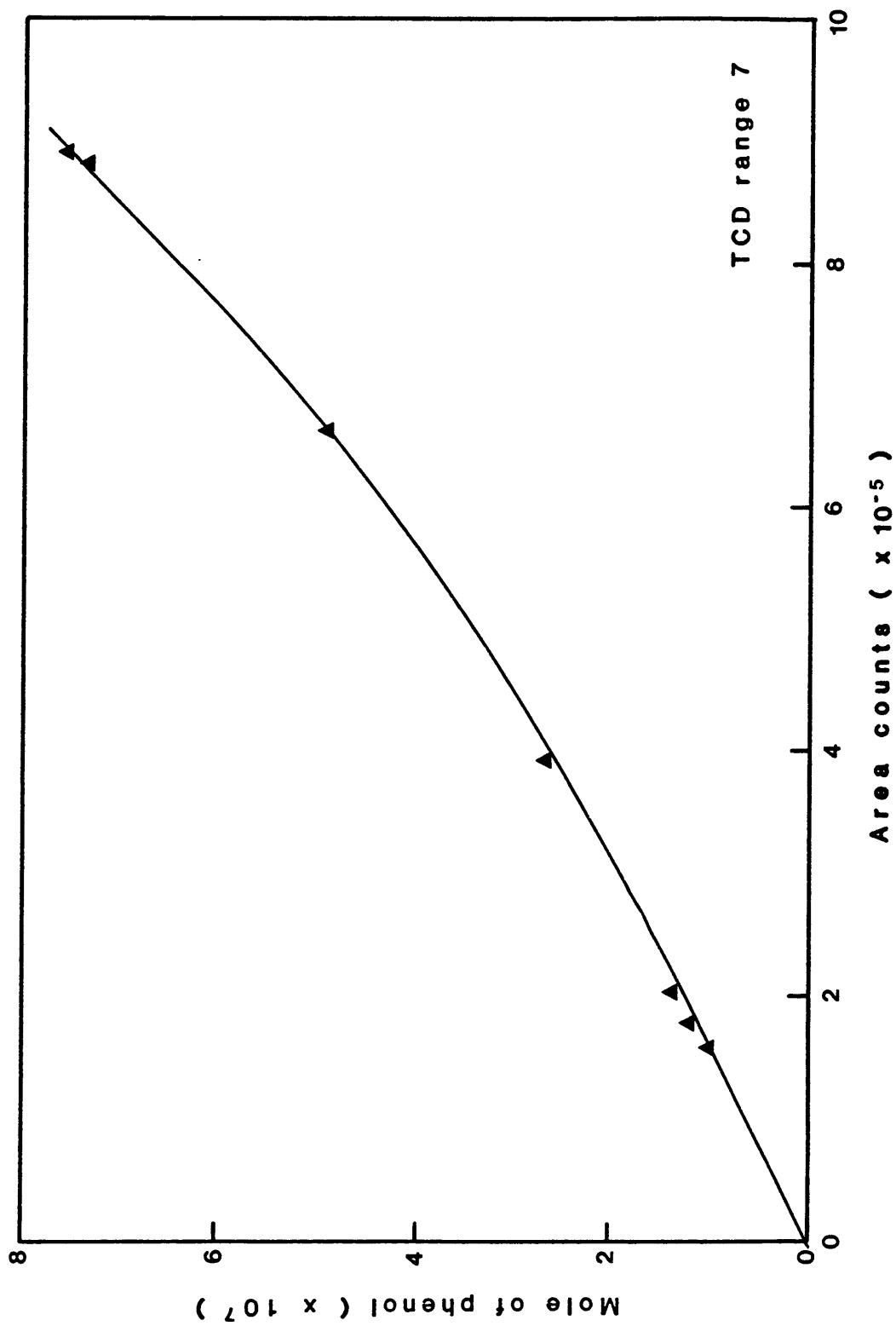


Figure A-7. Calibration curve for m-cresol, TCD range 7

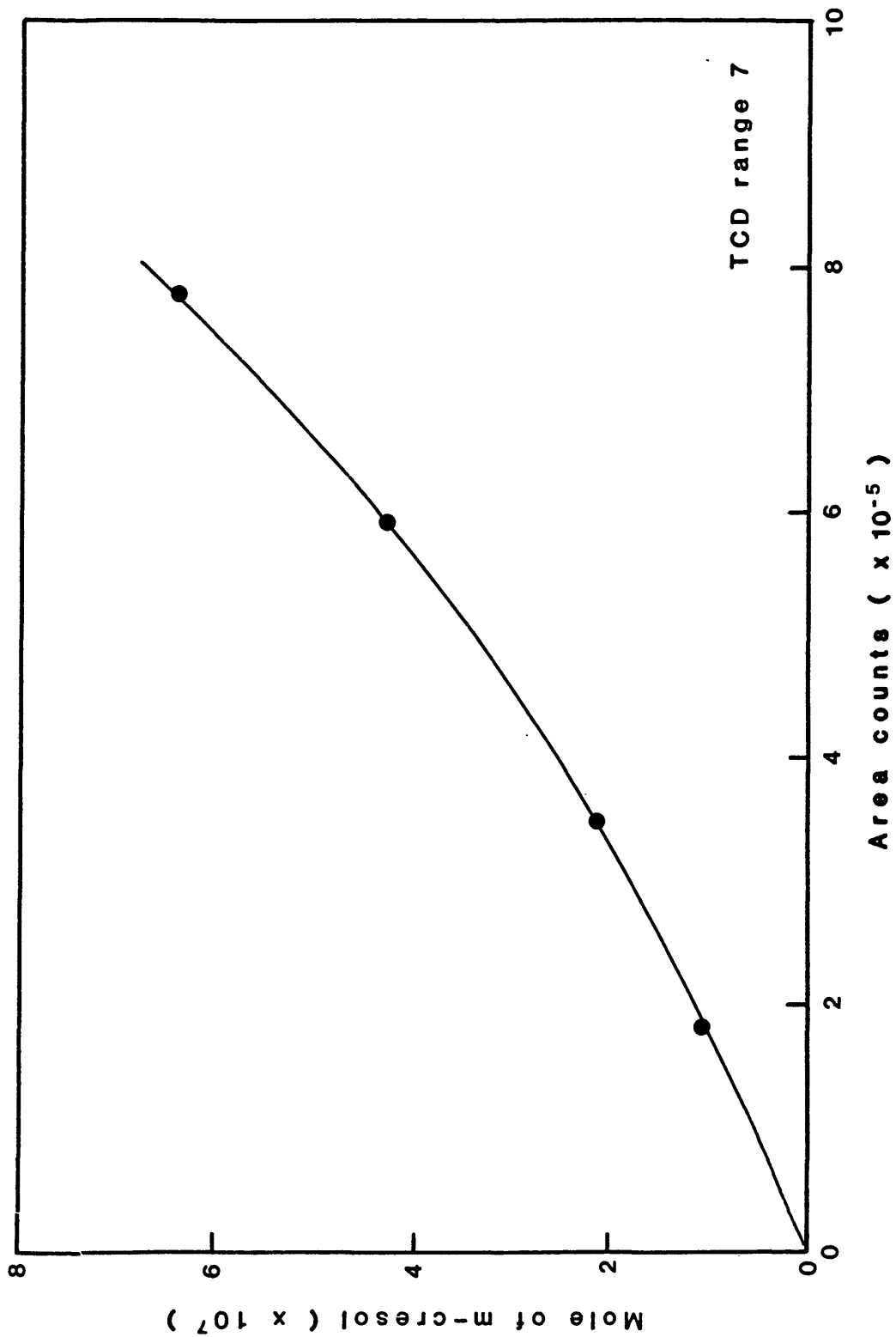
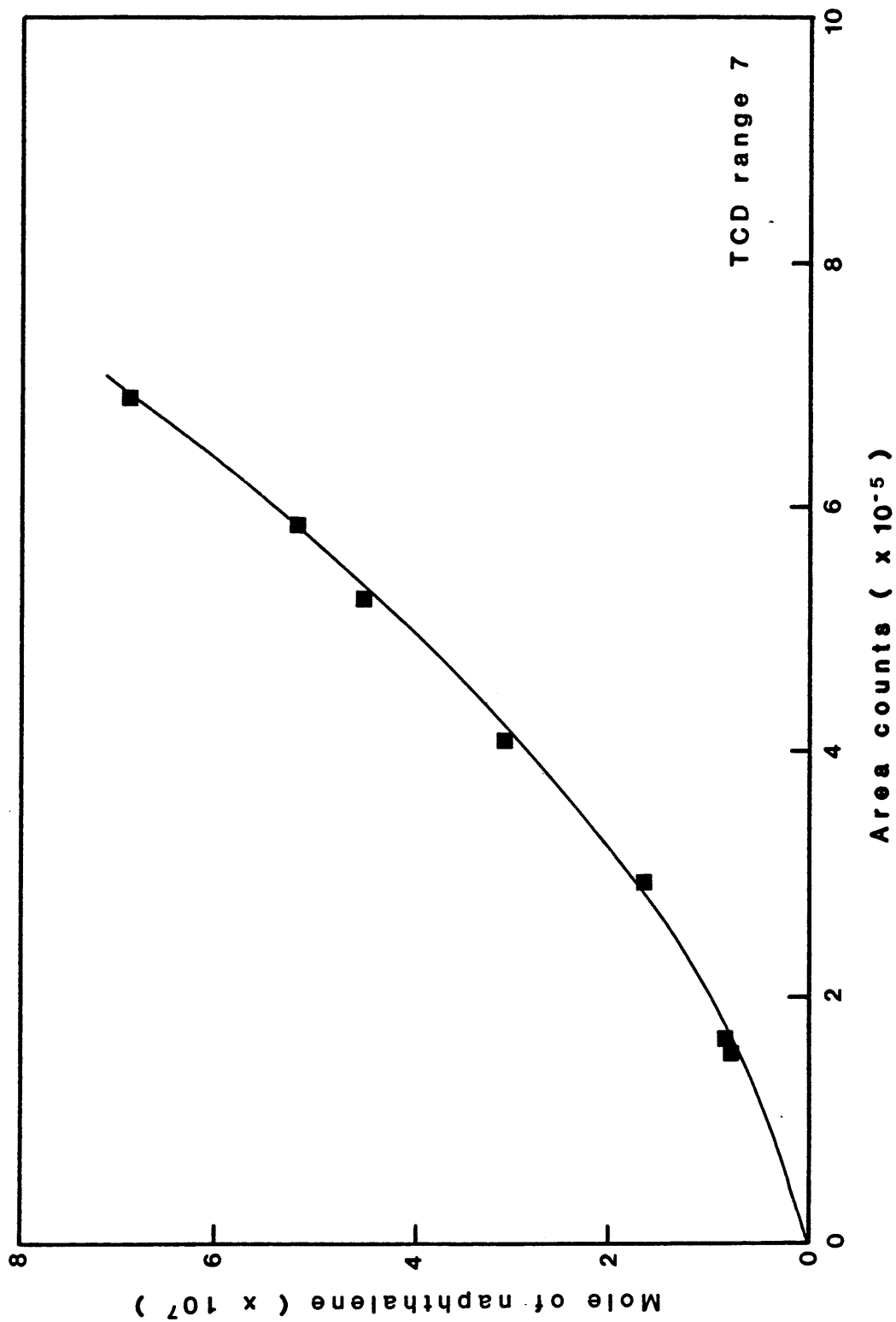




Figure A-8. Calibration curve for naphthalene, TCD range 7



APPENDIX B  
EXPERIMENTAL DATA

Table B-1. Experimental solubilities of naphthalene (peak area %) in supercritical carbon dioxide at 313.3 K. Condensed phase (solid): 100 % naphthalene.

First run		Second run	
Pressure (atm)	Naphthalene (Area %)	Pressure (atm)	Naphthalene (Area %)
23	0.38	25	0.33
29	0.40	35	0.31
35	0.38	48	0.31
47	0.29	61	0.36
52	0.31	66	0.50
62	0.53	74	1.0
70	0.90	82	11.
76	2.0	85	15.4
		92	20.0
		96	22.5
99	20.5	103	23.2
103	21.5	116	24.7
115	24.0	138	26.4
136	27.2	169	27.4
		199	29.4

Table B-2. Experimental mole fraction of naphthalene in supercritical carbon dioxide at 318.2 K. Condensed phase (solid): 100 % naphthalene.

Pressure (atm)	Mole Fraction	Reduced Density	Enhancement Factor
First Run			
66.2	0.000698		
69.9	0.000790		
73.6	0.000974		
76.2	0.00104		
79.2	0.00125		
84.5	0.00183		
86.2	0.00259		
89.5	0.00291		
93.7	0.00440		
104.0	0.00958		
Second Run			
69.3	0.000847	0.396	60
80.0	0.001559	0.540	130
83.4	0.002327	0.612	210
87.7	0.002627	0.717	250
90.0	0.003964	0.795	380
93.9	0.005563	0.871	560
97.1	0.008611	0.970	890
99.7	0.01026	1.04	1090
104.5	0.01250	1.11	1390
110.8	0.01441	1.23	1700
120.0	0.01668	1.41	2130
136.7	0.01929	1.53	2810
165.7	0.02281	1.65	4020
198.5	0.02672	1.74	5650

Table B-3. Mole fractions of naphthalene in supercritical carbon dioxide at 318 K measured by other researchers

Chang and Morrell (1985)		Tsekhanskaya, et al. (1964)	
Pressure (atm)	Mole Fraction	Pressure (atm)	Mole Fraction
82	0.0009	62.0	0.00047
102	0.0089	72.0	0.00048
137	0.0198	77.0	0.00067
170	0.0223	81.0	0.00078
204	0.0243	84.5	0.00110
272	0.0252	87.0	0.00130
		91.0	0.00210
		94.5	0.00430
		96.5	0.00510
		98.0	0.00610
		100	0.00690
		105	0.00970
		108	0.0113
		118	0.0142
		125	0.0154
		140	0.0183
		153	0.0197
		200	0.0245
		275	0.0285
		310	0.0294

Table B-4. Experimental mole fractions of phenol in supercritical carbon dioxide at 309.3 K. Condensed phase (solid): 100 % phenol.

Pressure (atm)	Mole Fraction	Reduced Density	Enhancement Factor
71.8	0.001407	0.516	110
77.7	0.002274	0.706	190
79.6	0.003079	0.839	320
81.0	0.006572	1.00	570
86.2	0.007524	1.31	690
96.0	0.01024	1.45	1050
114.3	0.01474	1.59	1800

Table B-5. Experimental mole fractions of phenol in supercritical carbon dioxide at 309 K (Van Leer and Paulaitis, 1980)

Pressure (atm)	Mole Fraction
78.25	0.003488
79.86	0.007314
85.40	0.009581
95.50	0.01127
104.44	0.01243
109.53	0.01280
117.58	0.01367
121.99	0.01390
131.05	0.01486
144.42	0.01502
153.67	0.01589
159.39	0.01604
161.30	0.01636
169.50	0.01590
180.22	0.01671
180.59	0.01651
191.37	0.01670
193.83	0.01686
204.88	0.01755
210.94	0.01788
213.09	0.01793
218.84	0.01822
231.13	0.01834
246.17	0.01816

Table B-6. Experimental mole fractions of m-cresol in supercritical carbon dioxide at 309.2 K. Condensed phase (liquid): 100 % m-cresol.

Pressure (atm)	Mole Fraction	Reduced Density	Enhancement Factor
69.3	0.000517	0.394	90
74.2	0.001424	0.575	280
78.9	0.003248	0.781	680
80.2	0.005643	0.922	1210
82.0	0.007817	1.11	1710
85.7	0.009661	1.30	2210
94.1	0.01178	1.42	2960
107.0	0.01371	1.54	3910
120.0	0.01636	1.63	5240
148.7	0.01991	1.73	7900
178.4	0.01832	1.80	8720
196.5	0.02200	1.84	11500



Table B-7. Experimental mole fractions of phenol and m-cresol mixtures in supercritical carbon dioxide at 309.4 K. Condensed phase (liquid): 25 mole % phenol and 75 mole % m-cresol.

Pressure (atm)	Mole Fraction		Reduced Density	Enhancement Factor	
	phenol	m-cresol		phenol	m-cresol
79.2	0.001287	0.001827	0.800	110	390
80.4	0.001964	0.002935	0.928	170	630
81.5	0.002223	0.003881	1.06	190	840
85.2	0.003341	0.005621	1.28	300	1280
91.0	0.004043	0.007057	1.41	390	1710
104.2	0.004947	0.01010	1.52	550	2810
121.5	0.007116	0.01241	1.63	920	4020
138.3	0.007991	0.01385	1.75	1180	5110
169.2	0.009533	0.01525	1.78	1720	6880
197.7	0.01085	0.01658	1.84	2290	8740

Table B-8. Experimental mole fractions of phenol and m-cresol mixtures in supercritical carbon dioxide at 309.3 K. Condensed phase (liquid): 50 mole % phenol and 50 mole % m-cresol.

Pressure (atm)	Mole Fraction		Reduced Density	Enhancement Factor	
	phenol	m-cresol		phenol	m-cresol
	First Run				
65.1	0.000538	0.000378	0.405	40	70
75.4	0.001364	0.000960	0.611	110	190
78.8	0.001954	0.001339	0.770	160	280
80.6	0.003622	0.002696	0.952	310	580
92.3	0.009284	0.006733	1.39	920	1660
103.8	0.01013	0.007163	1.52	1120	1980
119.6	0.01280	0.009031	1.62	1640	2880
143.4	0.01471	0.01025	1.71	2250	3920
	Second Run				
79.6	0.002653	0.001812	0.839	230	380
87.2	0.008374	0.005981	1.34	780	1390
137.9	0.01483	0.01042	1.70	2190	3830
167.4	0.01816	0.01202	1.78	3250	5370
186.9	0.02083	0.01318	1.82	4160	6570

Table B-9. Experimental mole fractions of phenol and m-cresol mixtures in supercritical carbon dioxide at 309.3 K. Condensed phase (liquid): 75 mole % phenol and 25 mole % m-cresol.

Pressure (atm)	Mole Fraction		Reduced Density	Enhancement Factor	
	phenol	m-cresol		phenol	m-cresol
65.9	0.001254	0.000458	0.416	90	80
77.0	0.001944	0.000541	0.668	160	110
79.6	0.003370	0.000843	0.839	290	180
81.8	0.005954	0.001435	1.09	520	310
85.2	0.008226	0.001924	1.28	750	440
92.7	0.01309	0.002774	1.39	1300	690
104.7	0.01695	0.003634	1.53	1900	1020
132.5	0.02135	0.004430	1.65	3020	1570
170.8	0.02880	0.005894	1.79	5260	2680
198.4	0.03238	0.006524	1.84	6860	3450

Table B-10. Effect of entrainers on the experimental mole fractions of phenol and m-cresol mixtures in supercritical carbon dioxide at 309.3 K. Condensed phase (liquid; 150 g): 50 mole % phenol and 50 mole % m-cresol.

Pressure (atm)	Mole Fraction phenol	Mole Fraction m-cresol	Reduced Density	Enhancement Factor phenol	Enhancement Factor m-cresol
64.6	0.000504	0.000326	0.398	35	55
76.6	0.001383	0.000985	0.656	110	200
82.8	0.005844	0.004319	1.17	520	950
101.7	0.009554	0.006974	1.51	1040	1890
136.6	0.01459	0.009537	1.69	2130	3470
167.5	0.01736	0.01060	1.78	3110	4740
196.8	0.01943	0.01071	1.84	4090	5620
Entrainer: 4.0 g acetone					
79.0	0.002366	0.001720	0.780	200	360
103.9	0.008978	0.006670	1.52	1000	1850
137.6	0.01310	0.009155	1.68	1930	3360
193.1	0.01877	0.01265	1.83	3870	6520
Entrainer: 3.0 g water					

Table B-11. Experimental mole fractions of phenol and m-cresol mixtures in supercritical carbon dioxide at 318.4 K. Condensed phase (liquid): 50 mole % phenol and 50 mole % m-cresol.

Pressure (atm)	Mole Fraction		Reduced Density	Enhancement Factor	
	phenol	m-cresol		phenol	m-cresol
66.0	0.002620	0.002333	0.363	90	200
76.4	0.002576	0.001927	0.484	100	190
93.0	0.003272	0.002411	0.847	160	290
96.6	0.003521	0.002691	0.953	180	340
99.5	0.003954	0.003051	1.04	210	400
112.3	0.008526	0.007266	1.26	500	1060
120.2	0.01065	0.009115	1.41	670	1430
153.3	0.01512	0.01212	1.60	1220	2420
174.3	0.01891	0.01372	1.68	1740	3110
197.1	0.02121	0.01524	1.74	2200	3910

APPENDIX C

PRESSURE DEPENDENCE OF ENHANCEMENT FACTOR

Given that the enhancement factor is inversely proportional to the vapor-phase fugacity coefficient:

$$\left(\frac{\partial E}{\partial P}\right)_T \propto \frac{\partial}{\partial P} \left(\frac{1}{\phi_2}\right)_T = -\frac{1}{\phi_2^2} \left(\frac{\partial \phi_2}{\partial P}\right)_T \quad (C-1)$$

the fugacity coefficient may be expressed in the following terms:

$$\ln \phi_2 = \frac{1}{RT} \int_0^P \left(\bar{V}_2 - \frac{RT}{P}\right) dP \quad (C-2)$$

where  $\bar{V}_2$  is the partial molar volume of solute in SCF.

Taking the partial derivative of equation (C-2) with respect to pressure:

$$\left(\frac{\partial (\ln \phi_2)}{\partial P}\right)_T = \frac{1}{\phi_2} \left(\frac{\partial \phi_2}{\partial P}\right)_T = \frac{1}{RT} \left(\bar{V}_2 - \frac{RT}{P}\right) \quad (C-3)$$

Substitution of equation (C-3) into equation (C-1) yields:

$$\left(\frac{\partial E}{\partial P}\right)_T \propto -\frac{1}{\phi_2} \left[\frac{1}{RT} \left(\bar{V}_2 - \frac{RT}{P}\right)\right] \quad (C-4)$$

Taking the partial derivative of equation (C-4) with respect to pressure:

$$\left(\frac{\partial^2 E}{\partial P^2}\right)_T \propto \frac{\partial}{\partial P} \left[ -\frac{1}{\phi_2} \left( \frac{1}{RT} \left( \nabla_2 - \frac{RT}{P} \right) \right) \right]_T$$

$$\propto \frac{\partial}{\partial P} \left( \frac{1}{\phi_2 P} - \frac{\nabla_2}{\phi_2 RT} \right)_T$$

$$\propto -\frac{1}{(\phi_2 P)^2} \frac{\partial}{\partial P} (\phi_2 P)_T - \frac{\partial}{\partial P} \left( \frac{\nabla_2}{\phi_2 RT} \right)_T$$

$$\propto -\frac{1}{(\phi_2 P)^2} \left[ P \left( \frac{\partial \phi_2}{\partial P} \right)_T + \phi_2 \right]$$

$$- \frac{1}{(\phi_2 RT)^2} \left[ \phi_2 RT \left( \frac{\partial \nabla_2}{\partial P} \right)_T - RT \nabla_2 \left( \frac{\partial \phi_2}{\partial P} \right)_T \right]$$



$$\left(\frac{\partial^2 E}{\partial P^2}\right)_T \propto \frac{1}{\varnothing_2^2} \left(\frac{\partial \varnothing_2}{\partial P}\right)_T \left[\frac{\nabla_2}{RT} - \frac{1}{P}\right] - \frac{1}{\varnothing_2 P} - \frac{1}{\varnothing_2 RT} \left(\frac{\partial \nabla_2}{\partial P}\right)_T \quad (C-5)$$

Substitute equation (C-3) into equation (C-5):

$$\begin{aligned} \left(\frac{\partial^2 E}{\partial P^2}\right)_T &\propto \frac{1}{\varnothing_2^2} \left(\frac{\nabla_2}{RT} - \frac{1}{P}\right)^2 - \frac{1}{\varnothing_2 P} - \frac{1}{\varnothing_2 RT} \left(\frac{\partial \nabla_2}{\partial P}\right)_T \\ &\propto \frac{1}{\varnothing_2^2} \left[ \left(\frac{\nabla_2}{RT} - \frac{1}{P}\right)^2 - \frac{1}{P} - \frac{1}{RT} \left(\frac{\partial \nabla_2}{\partial P}\right)_T \right] \end{aligned} \quad (C-6)$$

at the critical point and infinite dilution

$$\left(\frac{\partial \nabla_2}{\partial P}\right)_T \rightarrow 0 \quad \text{and} \quad \nabla_2 \rightarrow -\infty$$

$$\left(\frac{\partial^2 E}{\partial P^2}\right)_T \propto \frac{1}{\varnothing_2^2} \left[ \left(\frac{\nabla_2}{RT} - \frac{1}{P}\right)^2 - \frac{1}{P} \right] \quad (C-7)$$

$$\left(\frac{\partial^2 E}{\partial P^2}\right)_T \propto \frac{\left[\left(\frac{V_2}{RT} - \frac{1}{P}\right)^2 - \frac{1}{P}\right]}{\exp\left[\frac{1}{RT} \int_0^P \left(V_2 - \frac{RT}{P}\right) dP\right]} \quad (\text{C-8})$$

$$\lim_{V_2 \rightarrow -\infty} \left(\frac{\partial^2 E}{\partial P^2}\right)_T \quad \text{does not exist.}$$

Therefore, there is an inflection point at the critical point.

APPENDIX D  
UNCERTAINTY ANALYSIS

The uncertainty analysis of the solubility of a solute in supercritical carbon dioxide is based on a propagation of errors estimate.

This method is described by Holman (1971) and Kline and McClintock (1953), and it is based on a careful specification of the uncertainties in the primary experimental measurements, which are: temperature ( $\pm 0.2$  °C, thermocouple); pressure ( $\pm 3$  psia, transducer); the peak area counts reported by the integrator ( $\pm 2.5\%$  of the absolute value), weight ( $\pm 0.1$  mg, analytical balance) and volume ( $\pm 0.005$  ul, microliter syringe).

If  $R$  is the result computed from a series of experimental measurements ( $X_1, X_2, X_3, \dots$ ), so that

$$R = R(X_1, X_2, X_3, \dots) \quad (D-1)$$

and  $w_1, w_2, \dots$  are the uncertainties of the experimental measurements, then the uncertainty of the result,  $w$ , is given as (Kline and McClintock, 1953):

$$w = \left[ \left( \frac{\partial R}{\partial X_1} w_1 \right)^2 + \left( \frac{\partial R}{\partial X_2} w_2 \right)^2 + \dots \right]^{\frac{1}{2}} \quad (D-2)$$

The above relation is used to estimate the uncertainty of each computation leading to the final result, i.e. the mole fraction of the solute in supercritical carbon dioxide.

Table D-1 lists the chain of uncertainties which lead to an estimated solubility error of  $\pm 10\%$ . This estimated value was based on a three component system in the critical region.

Table D-1. Tabulated uncertainties

Source of uncertainty	Uncertainty (%)
Density of carbon dioxide	$\pm 7$
Volume delivered by HPLC valve	$\pm 4$
Detector response factor for carbon dioxide	$\pm 8$
Composition of the solute calibration standard	$\pm 0.1$
Density of the solute calibration standard	$\pm 1$
Detector response factor for the solute	$\pm 3$
MOLE FRACTION OF SOLUTE IN SCF	$\pm 10$